PERFORMANCE-BASED APPROACH TO EVALUATE ALKALI-SILICA REACTION POTENTIAL OF AGGREGATE AND CONCRETE USING DILATOMETER METHOD

A Dissertation

by

CHANG SEON SHON

Submitted to the Office of Graduate Studies of
Texas A&M University
in partial fulfillment of the requirements for the degree of

DOCTOR OF PHILOSOPHY

May 2008

Major Subject: Civil Engineering

PERFORMANCE-BASED APPROACH TO EVALUATE ALKALI-SILICA REACTION POTENTIAL OF AGGREGATE AND CONCRETE USING DILATOMETER METHOD

A Dissertation

by

CHANG SEON SHON

Submitted to the Office of Graduate Studies of
Texas A&M University
in partial fulfillment of the requirements for the degree of

DOCTOR OF PHILOSOPHY

Approved by:

Chair of Committee,	Dan G. Zollinger
Committee Members,	Charles J. Glover
	Dallas N. Little
	David Trejo
Head of Department,	David V. Rosowsky

May 2008

Major Subject: Civil Engineering

ABSTRACT

Performance-based Approach to Evaluate Alkali-Silica Reaction Potential of Aggregate and Concrete Using Dilatometer Method. (May 2008)

Chang Seon Shon, B.S., Taegu University;

M.S., Pusan National University

Chair of Advisory Committee: Dr. Dan G. Zollinger

The undesirable expansion of concrete because of a reaction between alkalis and certain type of reactive siliceous aggregates, known as alkali-silica reactivity (ASR), continues to be a major problem across the entire world. The renewed interest to minimize distress resulting from ASR has emphasized the need to develop predictable modeling of concrete ASR behavior under field conditions. Current test methods are either incapable or need long testing periods in which to only offer rather limited predictive estimates of ASR behavior in a narrow and impractical band of field conditions. Therefore, an attempt has been made to formulate a robust performance approach based upon basic properties of aggregate and concrete ASR materials derived from dilatometry and a kinetic-based mathematical expressions for ASR behavior.

Because ASR is largely an alkali as well as a thermally activated process, the use of rate theory (an Arrhenius relationship between temperature and the alkali solution concentration) on the dilatometer time-expansion relationship, provides a fundamental aggregate ASR material property known as “activation energy.” Activation energy is an indicator of aggregate reactivity which is a function of alkalinity, particle size, crystallinity, calcium concentration, and others. The studied concrete ASR material properties represent a combined effects of mixture related properties (e.g., water-cementitious ratio, porosity, presence of supplementary cementitious materials, etc.) and maturity. Therefore, the proposed performance-based approach provides a direct accountability for a variety of factors that affect ASR, such as aggregate reactivity (activation energy), temperature, moisture, calcium concentration, solution alkalinity, and water-cementitious material ratio.

Based on the experimental results, the following conclusion can be drawn concerning the performance-based approach to evaluate ASR potential of aggregate and concrete using dilatometer method; (i) the concept of activation energy can be used to represent the reactivity of aggregate subjected to ASR, (ii) the activation energy depends on the reactivity of aggregate and phenomenological alkalinity of test solution, and (iii) The proposed performance-based model provides a means to predict ASR expansion development in concrete.

DEDICATION

To my parents, Jang-Woon Shon and Jung-Ja Kim, and my wife, Min-Young Lee.

ACKNOWLEDGMENTS

The author wishes to express his great appreciation to his advisor, Dr. Dan G. Zollinger, for his guidance and continuous encouragement during the course of this work. Special thanks are extended to Dr. Dallas N. Little, Dr. David Trejo, and Dr. Charles J. Glover for their useful suggestions and for serving as advisory committee members.

The author would also like to thank Dr. Anal K. Mukhopadhyay for his helpful advice and abundant discussions. Grateful thanks are extended to Dr. Don Saylak for his support and encouragement.

Finally, this research was supported in part by grants from the Innovative Pavement Research Foundation (IPRF) and 2004 Education Foundation Fellowship from Portland Cement Association (PCA). The author is grateful for their support.

TABLE OF CONTENTS

TABLE OF CONTENTS (Continued)

TABLE OF CONTENTS (Continued)

TABLE OF CONTENTS (Continued)

Page

LIST OF FIGURES

LIST OF FIGURES (Continued)

LIST OF FIGURES (Continued)

LIST OF FIGURES (Continued)

LIST OF FIGURES (Continued)

LIST OF TABLES

LIST OF NOTATION

The following abbreviations are commonly used throughout this dissertation:

1N NaOH solution	1 normality of sodium hydroxide solution
AASHTO	American Association of State Highway and Transportation Officials
ASR	Alkali-Silica Reaction
ASTM	American Society for Testing and Materials
DRUW	Dry rodded unit weight
E_a	Apparent Activation Energy
EDX	Energy dispersive x-ray analysis
ESEM	Environmental Scanning Electron Microscope
NM rhyolite	New Mexico rhyolite
SCMs	Supplementary Cementitious Materials
w/c	Water to cement ratio
w/cm	Water to cementitious material ratio
XRD	X-ray diffraction

CHAPTER I

INTRODUCTION

BACKGROUND

Alkali-silica reaction (ASR) is a chemical reaction that can induce expansion and severe cracking in concrete structures and pavements. A deleterious chemical reaction between certain reactive forms of siliceous minerals in coarse or fine aggregates and OH^-, Na^+, K^+, and Ca^{2+} ions in the concrete pore solution produces a gel around the reacting aggregate particles and cement pastes (Chatterji and Thaulow 2000; Thomas 2001). When this alkali-silica gel is exposed to moisture, it imbibes water and expands. It is widely believed that when the expansive force exceeds the tensile strength of the concrete, cracks radiate from fissures in the aggregate particles into the surrounding cement paste. Formation of ASR gel in cracks causes more expansive pressure and distress. Once cracking has initiated, greater amounts of moisture penetrate the concrete, continuing to feed ASR growth (Mindess et al. 2003).

Since the ASR-related problems were first identified in the early 1940s (Stanton 1940, 1943; Stanton et al. 1942), extensive research worldwide has been carried out on ASR. One of the main areas of research that has been recently addressed is developing a quick and reliable test method to assess the potential ASR of an aggregate and concrete combination. Consequently, other tests that have been informative but perhaps of only qualitative value are listed as:

- American Society for Testing and Materials (ASTM) C 227 Potential Alkali Reactivity of Cement-Aggregate Combinations (Mortar-Bar Method)
- ASTM C 289 Potential Alkali Reactivity of Aggregates (Chemical Method)
- ASTM C 295 Petrographic Examination of Aggregate for Concrete

---

This dissertation follows the style and format of the *Journal of Materials in Civil Engineering*.

• ASTM C 441 Effectiveness of Mineral Admixture or Ground Blast-Furnace Slag in Preventing Excessive Expansion of Concrete Due to the Alkali-Silica Reaction
• ASTM C 1260 Potential Alkali Reactivity of Aggregate (Mortar-Bar Method)
• ASTM C 1293 Determination of Length Change of Concrete due to Alkali-silica Reaction.

Despite of a wealth of data that exists on ASR of aggregate and concrete based on the above test methods, doubts remain as to whether these tests to predict ASR potential (i) are realistic under field conditions and (ii) are able to address how different combination of concrete materials and exposure conditions interact to affect ASR behavior. For example, the ASTM C 1260 test has been the most commonly used method because its test results can be obtained within as little as 16 days. Recently, the C 1293 test has been suggested to be the most effective test in predicting the field performance of an aggregate source (Folliard et al. 2002). A free linear expansion at 14-day for mortar bar (the C 1260) or 1-year for concrete prism (the C 1293) has been assigned as an expansion criterion to evaluate the ASR potential. Experience with these tests has clearly indicated that the expansion history rather than a single value of expansion would be the appropriate criteria to assess ASR potential. Certainly, a unifying theory is needed to better tie the features that manifest in the foregoing list of ASR related tests to ASR performance. The best way to address this lies in the determination of basic ASR material characteristics that are representative of the expansion history (time-expansion relationship) and then combine those properties through a kinetic-type mathematical formulation to predict concrete behavior matching field observations.

RESEARCH SIGNIFICANCE AND SCOPE

The aim of this study is to develop a new rapid test method for predicting alkali-silica reactivity of aggregate and concrete. The concept of a new rapid test method is based on a performance-based testing protocol by combining laboratory measured material properties and exposure conditions through a kinetic-based mathematical formulation for predicting concrete ASR performance under field conditions. The performance-based procedure to assess expansion due to ASR is based on the formulation of a test parameter that is based

upon the actual expansion obtained by an apparatus referred to as a dilatometer. The expansion is produced by ASR gel when reactive siliceous aggregate reacts with alkali over time. Major topics covered in this dissertation are summarized as the following:

- A critical review of the existing test methods – (i) to properly address the need of a performance-based approach, (ii) to review the existing information pertaining to the application of kinetic-type modeling approach for better interpretation of the existing test methods (e.g., the C 1260).
- Measuring ASR activation energy (calculated based on the time-expansion relationship as a function of temperature) as an aggregate material property for the selective aggregates by the dilatometer
- Dilatometer concrete testing – to measure basic concrete material properties based on concrete ASR expansion characteristics
- Predicting concrete ultimate expansion through a performance-based kinetic-type model
- Analyzing the C 1293 and C 1260 data for the tested aggregates through the proposed performance-based model to draw a comparative assessment between the dilatometer and C 1293/1260 test results.

STRUCTURE OF DISSERTATION

This dissertation consists of seven chapters, each with specific objectives. The first chapter provides background information, the research significance, the scope of this research, and finally the overall structure of the dissertation. In following paragraphs, a brief description of each of the chapter is provided, highlighting the main ideas presented.

The second chapter of this dissertation provides a basic overview of ASR, including primary factors influencing ASR, mechanisms of ASR, current test methods for assessing ASR, and methods of mitigating ASR. The main objective of this chapter is to provide the reader with sufficient technical background on ASR, which is essential in understanding why a new test method needs to be developed to assessing ASR potential of aggregate and concrete.

Chapter III provides a general discussion of the methodology developed in this dissertation to evaluate the ASR potential of aggregate and concrete. A comprehensive review of the proposed performance-based model is presented, including discussions on how to determine each model parameter and how to use the model parameters in predicting the expansion due to ASR.

The fourth chapter presents materials and experimental details, providing information on the characteristics and properties of the materials used in this research. Also presented are the details of testing equipment and procedures used for sample preparation and calculation of expansion.

The fifth chapter outlines the first series of exploratory experiments used to evaluate the concept of activation energy (E_a). The experiments were mainly based on the determination of ASR of minerals and aggregates and the direct measurement strain produced by the expansive ASR products. A testing apparatus called a dilatometer was used to measure this strain. The concept of the E_a was verified using experimental results.

An experiment devoted to characterizing the combined material effect on the ASR potential of aggregate and concrete is presented in Chapter VI. The highlights of this chapter include how key material properties and factors are accounted for relative to their overall contribution to the ASR process when different temperatures, aggregates, and alkalinities of test solution are used. Additionally, a model, aimed at predicting ultimate expansion of concrete due to ASR through a performance-based kinetic-type approach, is presented. Experimental factors include normality of test solution (1N and 0.5N NaOH solution), different aggregate type (siliceous gravel and New Mexico rhyolite), calcium hydroxide ($Ca(OH)_2$), and lithium compound ($LiNO_3$).

The sixth chapter also introduces and assesses the suitability of the new performance-based model for assessing ASR potential of aggregate and concrete is evaluated by comparing the concrete parameters from the new test method to those from existing test methods.

Finally, a summary of the major findings and an overview of the research are summarized in Chapter VII. In addition, recommendations for future research are suggested in Chapter VII.

CHAPTER II

LITERATURE REVIEW

Since ASR-related problems were first identified in the early 1940s, broad research has been carried out on ASR. Main areas of research have addressed better understanding of the mechanisms of ASR leading to the development of test methods to assess the potential alkali-reactivity of aggregates, development of specifications for preventing ASR in new concrete, and management guidelines for existing ASR-induced damaged concrete structure.

This chapter provides an overview of the fundamentals of ASR in concrete, starting with the well-documented fundamentals of ASR and continues with the mechanistic treatment of the ASR process. The primary factors influencing ASR are summarized, followed by discussions on current theories of the ASR mechanism and test methods for assessing ASR towards the development of a new approach to characterize ASR performance.

PRIMARY FACTORS INFLUENCING ALKALI-SILICA REACTION (ASR)

The mechanisms governing ASR and expansion are quite complex. It is widely accepted that three essential conditions necessary for ASR-induced damage in concrete structures (Fig. 2-1) are (i) sufficient availability of alkalis (Na and/or K), (ii) reactive form of silica or silicate in the aggregate, and (iii) sufficient moisture (not less than 80% RH). The optimum combination of conditions (i) and (ii) is essential to initiate ASR whereas condition (iii) is essential to make ASR expansive (i.e., deleterious).

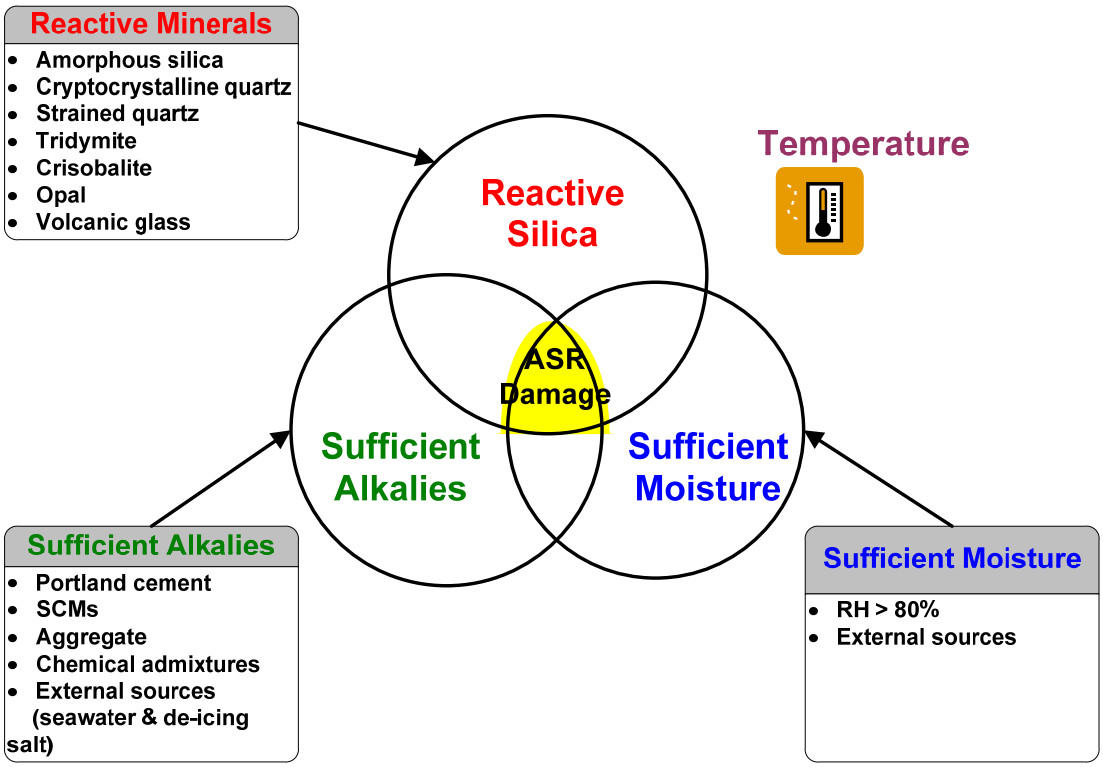

Fig. 2–1. Three essential components for ASR-induced damage in concrete

Sufficient Alkalis

In chemistry, an alkali is a basic, ionic salt of an alkali metal or alkaline earth metal element. The periodic table shows the position of the alkalis, i.e., second to seventh elements in group I and II (Fig. 2-2). Alkalis are known for being bases when dissolved in water and their pH values are above 7. The alkali compounds (e.g., alkali salts) easily dissolve in water and produce alkali hydroxides: lithium hydroxide, sodium hydroxide, potassium hydroxide and so on.

Concrete consists of innumerable pores that are filled with solution containing alkalis (Na^+, K^+, and Ca^{2+}) and hydroxyl (OH^-) ions. The alkalinity (hydroxyl ion concentration) of the pore solution is primarily influenced by the sodium and potassium alkali metals in the cement. Other sources, such as supplementary cementitious materials (SCMs), aggregate, chemical admixture, seawater, and de-icing solution can also contribute additional alkalis other than cement alkalis and modify the pH of pore solution.

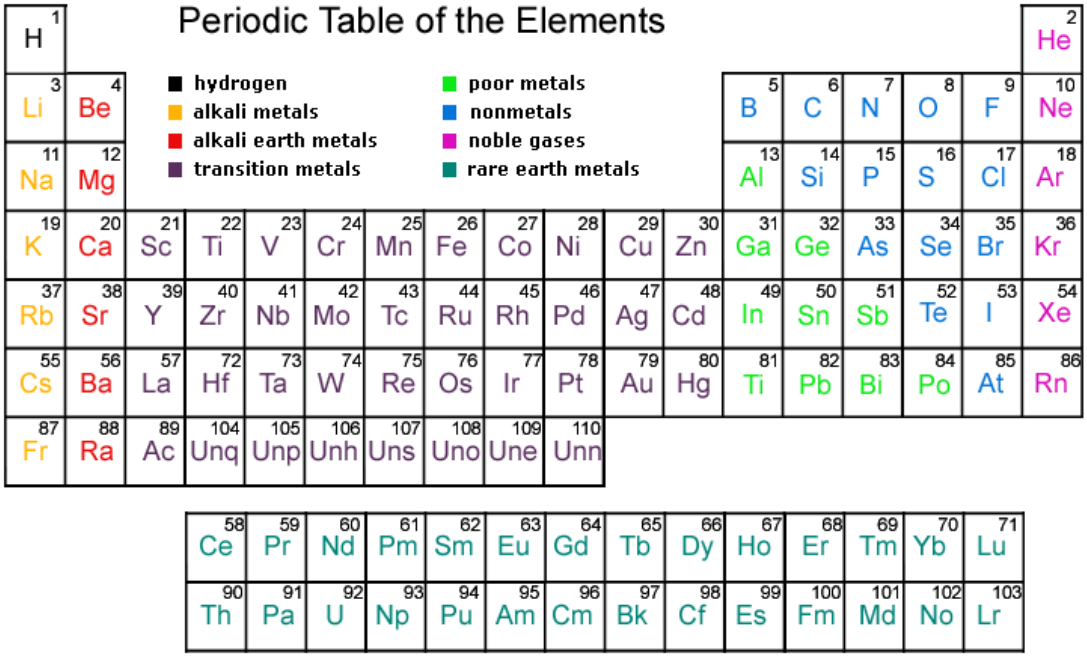

Fig. 2-2. The Periodic Table showing the position of alkalis (McCutchen's web site)

For ASR, the alkali content of concrete must be determined in the summation of alkalis contributed from the above sources:

$$[Alkalis]_{concrete} = \sum([a]_{cement} + [a]_{SCMs} + [a]_{aggregates} + [a]_{external\ sources}) \quad (2-1)$$

where,

$[Alkalis]_{concrete}$ = alkali content of concrete (kg/m^3)

$[a]_{cement}$ = [% $Na_2O_{equivalent}$ x cement content] / 100

$[a]_{SCMs}$ = [%$Na_2O_{equivalent}$ x SCMs content / 100]

$[a]_{aggregate}$ = $[a]_{fine\ aggregate} + [a]_{coarse\ aggregate}$

$[a]_{external\ sources}$ = $[a]_{seawater} + [a]_{de-icing\ salts} + [a]_{sulphate-bearing\ groundwater}$, and

$[a]$ = amount alkalis.

The alkalis present in the portland cement are represented by the equivalent sodium oxide content. This value is calculated through a summation of the sodium oxide (Na_2O) and potassium oxide (K_2O):

$$Na_2O_e = Na_2O + 0.658K_2O \quad (2-2)$$

where, Na_2O_e is the total sodium oxide equivalent in percent; Na_2O is the sodium oxide content in percent; K_2O is the potassium oxide content in percent; and 0.658= the weight ratio of Na_2O to K_2O.

According to the ASTM C 150, a cement having a Na_2O_e of less than 0.6 percent is generally considered as a low-alkali cement. However, it is reported that even this value may be high when used with reactive aggregate. Although a combination of low alkali cement ($\leq$ 0.6 percent) and a potentially reactive aggregate is considered to be safe (i.e., no deleterious expansion due to ASR), it should be noted that this approach using low alkali cement does not control alkali content of the concrete mixture to prevent ASR-induced damage because this value assumes that the contribution of alkali from other sources is small. The contribution to the total active alkali content of the concrete from the aggregate in the mixture or even external sources (e.g., de-icing salts) has resulted in the occurrence of ASR with low alkali cement as reported by several researchers (Nixon and Sims 1992 and Folliard et al. 2002).

In general, SCMs such as fly ash, ground granulated blastfurnace slag (GGBS), and condensed silica fume are all used to reduce abnormal expansion caused by ASR. The mechanisms are not well understood, but it is agreed that the reactive silica in SCMs combines with the cement alkalis (that is, NaOH and KOH) more readily than the silica in aggregate. Therefore, alkalis are rapidly consumed and the level of hydroxyl ions is reduced to a level at which aggregates react very slowly or not at all (Carrasquillo and Farbiaz 1988; Diamond and Penko 1992). Furthermore, this reaction results in the formation of alkali-calcium-silicate-hydrates which is non-expansive, unlike the water absorbing expansive gels produced by ASR. However, not all SCMs increase ASR resistance. Some SCMs can be a source of alkalis. Diamond (1981) reported that Class F fly ash is more effective in controlling ASR than Class C fly ash. Shehata et al. (1999;

2000) and Shon et al. (2003; 2004) supported that Class C fly ashes are less effective than Class F fly ashes in controlling ASR because Class C fly ashes tend to make their alkalis more readily available.

Some aggregates themselves may be a potential source of alkalis. For example, sea-dredged aggregates would be obvious source of sodium chloride. Poulsen et al. (2000) reported potential problems with release of alkalis from feldspar. Stark and Bhatty (1986) and Thomas et al. (1992) reported that certain aggregates can release alkalis equivalent to 10 percent of the portland cement content under extreme conditions, thereby increasing the alkali content of the mixture. Furthermore, when recycled concrete coarse aggregates are used, careful monitoring would also be required because they contain alkalis originated from cement hydration. Typically, alkalis are released when the aggregate's lattice structure begins to break down during ASR. These alkalis later provide an additional source for further ASR expansion.

Nixon et al. (1987) and Hobbs (1988) described a variety of external sources for alkalis introduced into concrete. Sources of external alkalis include road de-icing salts, seawater, and industrial alkalis. Addition of sodium chloride to cement paste rapidly converts to alkali hydroxide, which increases the hydroxyl ion concentration. Therefore, this exacerbates the threat of ASR. Oberholster (1992) reported that studies using seawater spray on large concrete blocks exhibited twice the expansion when compared with tap water spray. Chatterji (1989a, 1989b) stated that the presence of sodium chloride (NaCl) contributed to the following process:

$$\text{reactive silica} + 2Na^{+} + 2Cl^{-} + Ca^{2+} + 2OH^{-} + aq. =$$
$$\text{solid alkali-silica hydroxyl complex} + Ca^{2+} + 2Cl^{-} + aq. \qquad (2-3)$$

where, *aq.* is the aqueous solution.

The smaller Na^{+} ions and OH^{-} ions from salts penetrate the reactive aggregate and breakdown the Si-O-Si bonds. This reaction opens up the reactive grains for further attack by more Na^{+} ions and OH^{-} ions.

Sufficient Moisture

Moisture is an essential ingredient for ASR. Moisture plays mainly two roles in this reaction. These roles are as follows:

- is a transport medium for the ionic species involved in ASR
- is a supplier for the ASR gel swelling (water is included in the ASR gel)

The minimum humidity is generally present in concrete because of the sufficient residual water after complete hydration. This internal humidity plays a role in any dissolution, reaction, and formation of amorphous gel and precipitates as it brings into contact the involved reactants in the ASR mechanism. With moderate internal humidity, the diffusion of reactants and reaction products would be limited to the connected network of pores around the reactive aggregate particles, thus, the reaction is limited principally to the aggregate-cement paste interface (Dent Glaser and Kataoka 1981). If the internal humidity is increased, however, the dissolved silica may diffuse away from the reactive aggregate particles and the subsequent reaction in solution forming amorphous gel or precipitates may then take place anywhere in the concrete (Steffens et al. 2003). Therefore, a higher water to cement ratio (w/c) of concrete could lead to higher expansion in ASR due to (i) higher porosity / permeability, (ii) higher ionic mobility and more reaction, and (iii) greater availability of free (capillary) water to make the gel more expansive. If sufficient moisture is available, the ASR gel will imbibe water that causes expansion within the concrete, ultimately leading to tensile stresses and cracking.

It is generally accepted that a minimum relative humidity (RH) of 80 percent is required to cause ASR, although there are various opinions on the minimum relative humidity value for ASR damage. Vivian (1981), Olafsson (1986), Kurihara and Katawaki (1989), and Larive et al. (2000) observed that ASR expansion is directly correlated with water mass variations from test results of mortar samples affected by ASR. The higher the water mass gain, the more expansion.

Tomosawa et al. (1989) and Pedneault (1996) reported that concrete maintained in an environment with less than 80 percent relative humidity did not undergo significant expansion (Fig. 2-3). Folliard et al. (2002) reported that even concrete containing a

reactive aggregate and high alkali content can be protected against ASR expansion by limiting access of water to the reaction site.

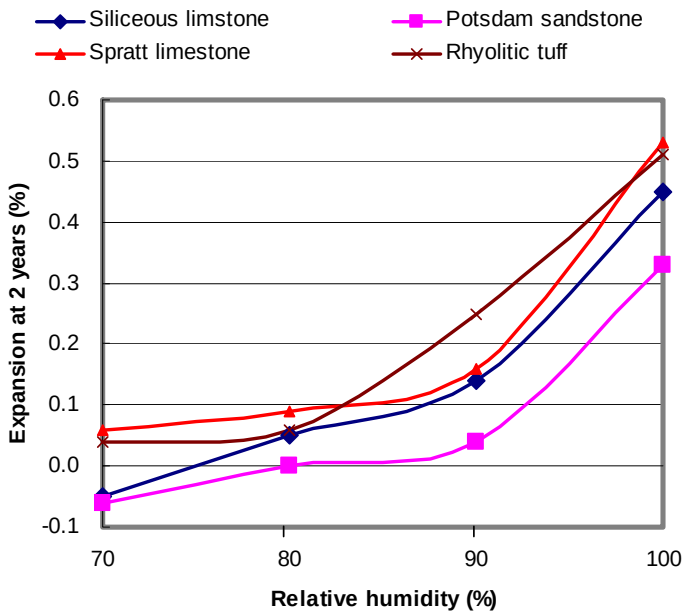

Fig. 2–3. Effect of relative humidity on expansion using ASTM C 1293

Reactive Silica

Many of the coarse and fine aggregates used in concrete mixtures consist of siliceous components, i.e., different forms of silica mineral. For example, quartz and chalcedony are crystalline forms of silica while opal is an amorphous form of silica mineral. Nonetheless, not all forms of silica can be ASR reactive. For example, well-crystallized quartz is not considered susceptible to ASR whereas opal is very reactive. The basic structure of silicates involves a framework of silicon-oxygen tetrahedral. Each oxygen atom is shared between two silicon atoms, where each silicon atom is bonded to four oxygen atoms (siloxane bridge). The tetrahedral can be present singly or can form doubles, rings, chains, bands, sheets, or frameworks (Fig. 2-4). A regular (ordered) arrangement of the basic Si-O tetrahedron creates a crystalline structure (e.g., quartz) whereas an irregular (disordered)

arrangement of the tetrahedron creates poorly crystalline (e.g., chalcedony shown in Fig. 2-5) to amorphous structure (e.g., opal) depending on the degree of irregularity.

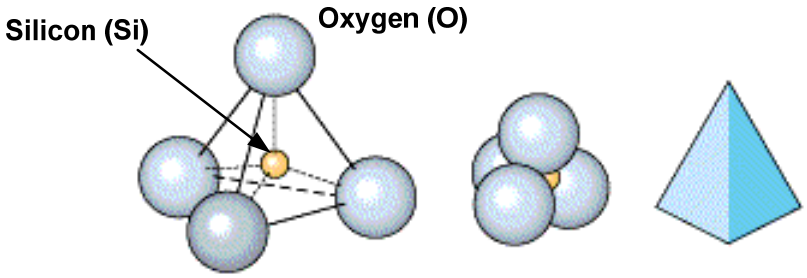

Fig. 2–4. A silica tetrahedral structure

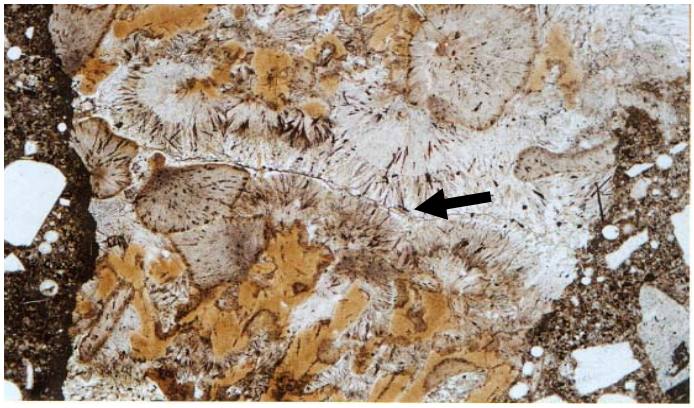

Fig. 2–5. Photomicrograph of a very fine grained (cryptocrystalline) chalcedony aggregate in concrete. Note the characteristic acicular crystals of chalcedony shown by the arrow.

Reactive siliceous aggregate in concrete is necessary for ASR to occur. The term reactive aggregate is defined as the aggregate that trends to breakdown under exposure to the highly alkaline pore solution in concrete whcih subsequently reacts with the alkali hydroxide (sodium and potassium) to form ASR gel.

With parameters such as alkali content and moisture content being constant, the degree of reactivity of siliceous aggregates mainly depends on the degree of the disordered crystal structures, grain size of the reactive particle, and the proportion of these reactive phases within the reactive aggregate. This is because of the more disordered the structure the greater the surface area available for reaction. Amorphous, crypto-crystalline, and microcrystalline silica structures are particularly susceptible to ASR.

Diamond (1976), Tatematsu and Sasaki (1989), and Mehta and Monteiro (1992) have designated the nature of these reactive forms of silica and the order of reactivity of aggregate as follows: opal, crystobalite, tridymite, microcrystalline quartz, cryptocrystalline quartz, chalcedony, chert, volcanic glass, and strained quartz.

Zhang et al. (1990) and West (1991) have examined thin sections of quartz-bearing aggregate. The quartz grains usually exhibit dark or white uniform extinction (how much light intensity is lost for each object in optical microscope) behavior (Fig. 2-6). Sometimes, however, undulatory extinction (strain shadow) is seen in which an extinction band sweeps across a quartz grain due to bending of the crystal lattice by stress. Quartz exhibiting undulatory extinction is highly reactive because of its high dislocation density (Fig. 2-7).

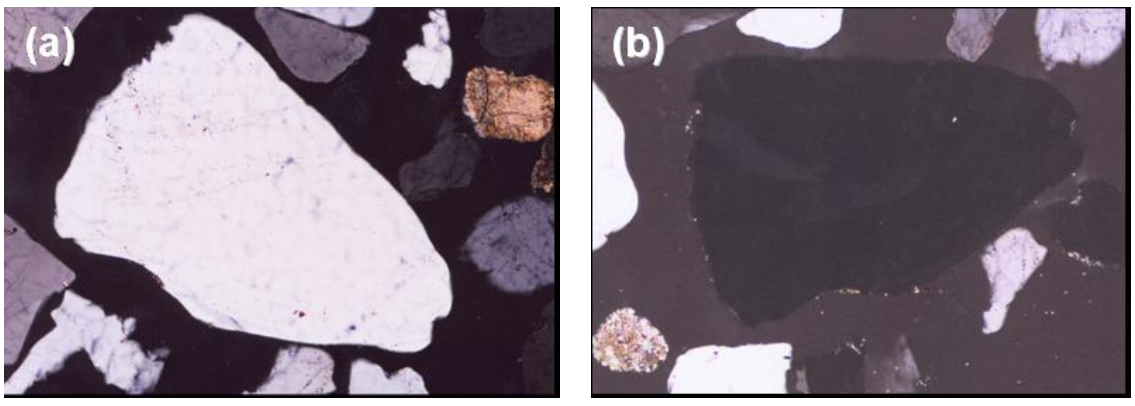

Fig. 2–6. Non-reactive quartz. The entire quartz grain is either uniformly bright (a) or totally dark (b) under cross-polarized light when the microscope stage is rotated 360°.

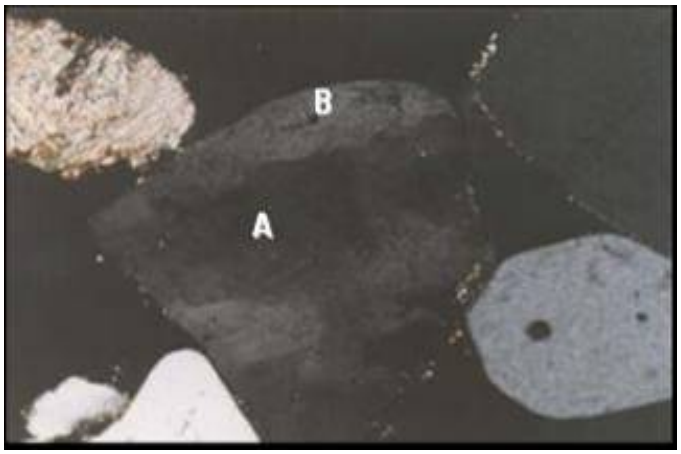

Fig. 2–7. Reactive or strained quartz exhibiting dark (A) and light bands (B) within a single grain

Environmental Effects

The major environmental effects on ASR are those of moisture content and temperature variations and exposure to soluble salts which penetrate into the concrete. Concrete can be exposed to slow cycles of temperature and moisture content changes due to seasonal climatic variations and this can have major effects on ASR cracking. The widespread use of deicing salts on pavements can be responsible for much deterioration. The interaction between such environmental effects and ASR is as yet not well understood.

One of the three requirements for expansive ASR to occur in concrete is sufficient moisture for absorption by gel reaction products. The moisture condition of concrete under which ASR and its associated distress that may or may not develop appears to be best defined in terms of RH of the concrete in question. Expansive ASR occurs when RH values of concrete exceed about 80 percent referenced to 21 to 25 $^{\circ}$C. Research data show that RH values higher than 80 percent are able to sustain expansive ASR in most of the pavement below the top surface layer, even in the summer in a hot desert climate (SHRP-C-342, 1993). Data also show that humidity conditions are sufficiently moist to support expansive ASR in much of the concrete in pavements and structures for at least part of each year in most of the continental United Sates. Wetting and drying cycles can enhance the ASR in the following way:

- Drying concentrates alkali hydroxides in the pore solutions and increases the pH and the solubility of silica. Local concentration of alkalis may increase due to wetting and drying and can cause ASR even with low alkali cement if reactive aggregate present.
- Rewetting dilutes the solutions, but permits swelling of gels formed by the concentrated gels.
- These gels can affect local stresses

Many experiments have established that higher temperature accelerates the reaction although the ultimate expansion is not necessarily greater in the long term. It is reported that concrete slabs submitted to natural outdoor conditions (i.e., natural wetting and drying cycles and heating and cooling cycles) present more expansion than the laboratory samples maintained under constant humidity and temperature conditions. Moderately elevated temperatures can be effective in drying concrete sufficiently to prevent expansive ASR.

At elevated temperatures reactions rates and expansion rates are high but decline with time (Fig. 2-8). At low temperatures the rates are slower but total expansion may eventually reach or exceed that at higher temperatures.

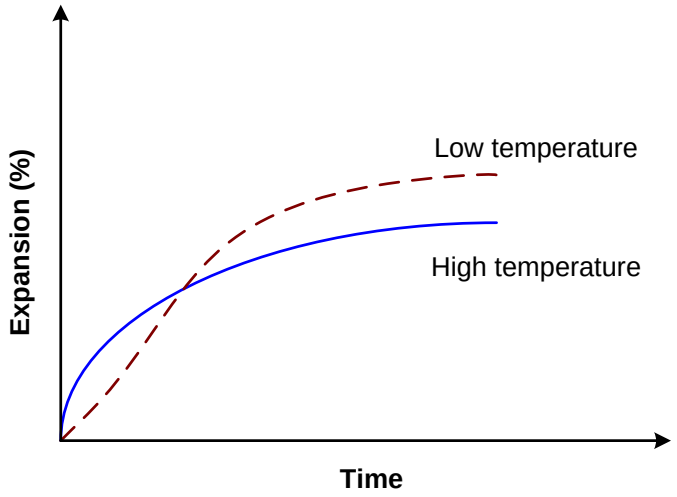

Fig. 2–8. Influence of temperature on ASR expansion

Hobbs (1992) found that the reaction occurred seven times faster for specimens stored at 38°C than for those stored externally at an average temperature of 9 °C. The rate was four times faster than for samples stored at 20 °C. The reaction generally tends to mature and cease in about twenty years but longer periods may be expected in colder climates and shorter in hot climate.

MECHANISM OF ALKALI-SILICA REACTION

Broadly, the ASR mechanism can be divided into two parts: (i) the actual chemical reaction and (ii) expansion arising from the chemical reaction. Each of these reactions will be described more thoroughly, including the current proposed mechanism for expansion. The mechanism of ASR is not fully understood, but alkali attack of reactive siliceous aggregates may be described by three distinct reactions:

- Dissolution of silica in the aggregate by hydroxyl attack
- Charge equilibrium by alkali cations (K^+ or Na^+) in pore solution
- Combination of calcium hydroxide [$Ca(OH)_2$]

Dissolution of Silica

The alkali-silica attack in concrete is initiated by the dissolution of reactive siliceous mineral present in the aggregate. For example, the structure of quartz involves a framework of silicon-oxygen tetrahedral. Each oxygen atom is shared between two silicon atoms, which each silicon is bonded to four oxygen atoms (siloxane bridge). If the framework is poorly-crystallized (Fig. 2-9 (a)), hydroxyl (OH^-) ions penetrate into the structure, and then some of the siloxane bridge (≡Si−O−Si≡) are ruptured. This penetration results in the formation of silanol (Si−OH) bonds (Fig. 2-9 (b)).

$$\equiv Si–O–Si\equiv + 2OH^- \rightarrow 2\equiv Si–O^- + H_2O \qquad (2-4)$$

As additional hydroxyl ions penetrate into the structure, a continuous acid-base dissolution occurs between the hydroxyl ions abundant in the pore solution of concrete and existing silanol groups or silanol groups produced by the hydroxyl penetration.

$$\equiv Si–OH + OH^- \rightarrow \equiv Si–O^- + H_2O \qquad (2–5)$$

The hydroxyl ions rupture the ≡Si−O−Si≡ bonds, loosing siloxane bridge and producing Si−O^- species. The dissolution of silica from the aggregate is the initial step in the ASR and the amount of solubility of silica is increased in strongly alkaline environments. The amount of dissolution is governed by the pH of the pore solution, concentration of alkali cations (e.g., Na^+, K^+) and calcium (Ca^{2+}) in the pore solution, temperature, and the particle size of the silica.

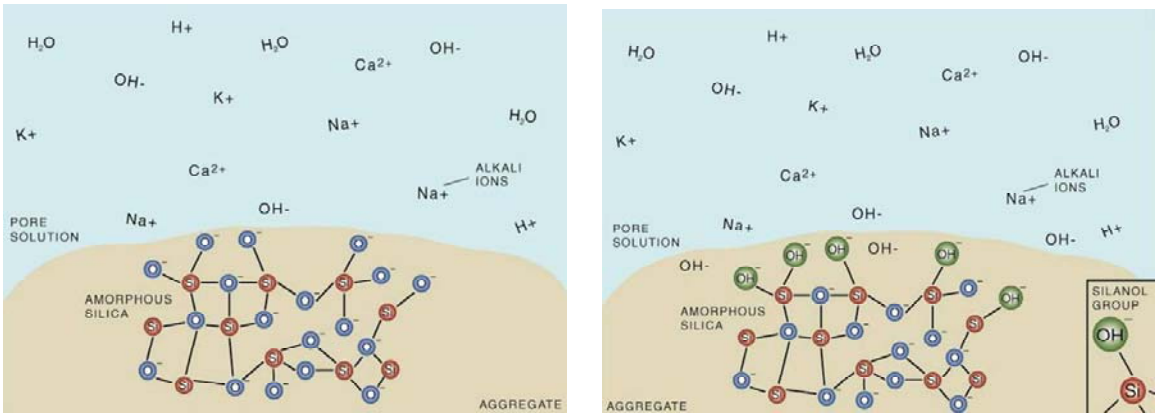

(a) amorphous siliceous aggregate (b) OH^- ions penetration into aggregate

Fig. 2–9. Mechanism of alkali-silica reaction: dissolution of silica (Collins et al. 2003)

Charge Equilibrium by Alkali Cations in Pore Solution

Dent Glasser and Kataoka (1981; 1982) illustrated the dissolution of silica from reactive aggregates and the role of alkali cations. To maintain charge equilibrium, the formation of negatively charged Si−O^- species from the aggregate attracts positively charged ions (e.g., Na^+, K^+) from the pore solution (Fig. 2-10(a)). The driving force of alkali ions that diffuse into the aggregate grain is dependent on concentration of alkali hydroxides. Provided that

sufficient amounts of alkali hydroxides are available, more siloxane bridges are broken as more hydroxyl ions penetrate. With further breaking of the siloxane bridges, the alkali cations such as Na^+ and K^+ abundant in the pore solution are attached to $Si{-}O^-$ species and become incorporated into the alkali-silica reaction gel (Fig. 2-10(b)). It is the disruption of the siloxane bridges that ultimately weakens the structure.

$$\equiv Si{-}O^- + Na^+ + H_2O \rightarrow \equiv Si{-}O{-}Na + H_2O \qquad (2{-}6)$$

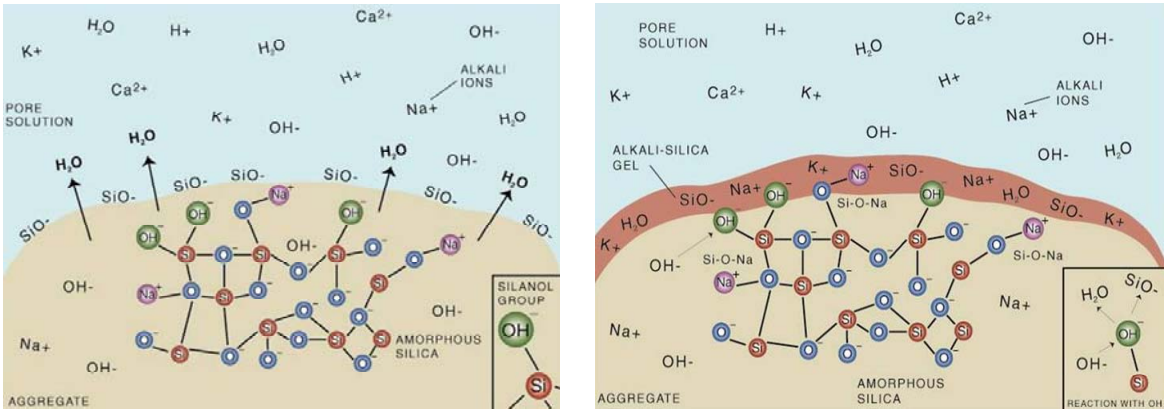

(a) Formation of $Si{-}O^-$ species (b) Formation of ASR gel

Fig. 2–10. Mechanism of alkali-silica reaction: formation of $Si{-}O^-$ and ASR gel

Combination of Calcium Hydroxide [$Ca(OH)_2$]

Classic theories describing ASR in concrete generally do not consider calcium in the primary role of reaction and expansion. The mechanism of expansion proposed by McGowan and Vivian (1952) does not consider calcium to influence the chemistry of ASR or the mechanisms of expansion. In her study on the structure of ASR gels, Dent Glasser (1979) proposed that the alkali-silica gel acts as a semi-permeable membrane, but does not consider calcium as a contributory factor.

However, a number of workers have suggested that the presence of $Ca(OH)_2$ is required for ASR induced damage. Hanson (1994) postulated that $Ca(OH)_2$ is not involved in the initial reaction process (i.e., no mechanistic involvement), but helps to sustain

further ASR by regenerating alkalis through cation exchange with alkalis in the reaction product. Wang and Gillott (1991) support this view with their work. They found that $Ca(OH)_2$ maintains a high concentration of OH^- ions (buffering the pore solution), but there is also an ion exchange between the Ca^{2+} ions in the pore solution and the Na^+ and K^+ ions in the alkali-silica gel. The exchange of the Ca^{2+} ions results in a non-expansive gel and the newly released alkali ions cause further reaction.

Powers and Steinour (1955) observed that the reaction with highly reactive opal particles could be safe or unsafe depending on the relative amounts of calcium and alkalis in the reaction products. High calcium content gels do not swell and form safely at the particle surface as long as Ca^{2+} can penetrate to the reaction sites. Gels with low calcium content (Ca^{2+} concentrations are too low to form non-swelling gels) are swelling gels. For a non-expansive reaction, some of the silica must diffuse out through the reacted layer as H_2O, Ca^{2+}, Na^+, K^+ diffuse inward to the reaction zone. However, in contrast to this view, other researchers feel that the role of calcium hydroxide is more involved than previously thought. It was suggested that the presence of $Ca(OH)_2$ and its availability for reaction is required for the formation of potentially destructive expansive gel (Conrow 1952; Hester and Smith 1953; Chatterji, 1979, 1989a, 1989b; Chatterji et al. 1987; Thomas et al. 1991; Thomas 1994; Bleszynski and Thomas 1998; Chatterji and Thaulow 2000; Thomas 2001).

Chatterji (1979) showed that the removal of $Ca(OH)_2$ from mortar bars containing opaline silica prevented expansion when immersed in a saturated host solution of NaCl at 50 °C. Additional mortar bars cast with very low cement contents similarly showed no expansion due to insufficient amounts of $Ca(OH)_2$ in the mixes. Silica gel was observed to precipitate on the surface on these low-cement specimens. A theory describing a mechanism of expansion that addresses the contribution of calcium was proposed by Chatterji (1989a, 1989b). He showed that gels containing considerable calcium did not assure no deleterious reaction because the products impeded the escape of dissolved silica from the reaction sites. Although the escape of silica has been clearly recognized by Powers and Steinour, Chatterji concluded that in ASR reactions accelerated by salt solutions, the limitation or removal of $Ca(OH)_2$.can prevent deleterious ASR.

In 1981, Struble performed studies on opal in model pore solutions in the presence and absence of calcium. She demonstrated that in the absence of cement hydration

products, significant quantities of silica (≥ 2M) could remain in solution rich with alkali hydroxides without the formation of alkali-silica gel. In comparison, pore solutions extracted from mortars containing OPC and the reactive opal revealed silica concentrations 2000 times lower (< 0.001M), together with the formation of gel. Based on this study, Diamond (1989) suggested that, in the absence of calcium, silica is soluble in alkali hydroxide solution and does not form an alkali-silicate gel.

Kilgour (1988) supports these findings. She found that low-calcium fly ashes exposed to alkali hydroxide solution in the absence of calcium lose 20% of their soluble mass in 6-months (silica being the principal soluble phase). The addition of calcium hydroxide to the solution caused an increase in mass of silica due to the formation of a reaction product similar to ASR gel.

Thomas et al. (1991) found evidence of ASR reaction (presence of gel) in fly ash concretes without any associated expansion or cracking. Gels of similar composition (Ca/Si = 0.30) were found in OPC control specimens without fly ash, but only in the interior of reacting aggregate particles. Gel found filling the cracks in the cement matrix and air voids of the OPC concrete had a composition much higher in calcium (Ca/Si = 0.90). It was postulated that initially a gel low in calcium was formed by a reaction between the cement alkalis and the reactive silica. This low-calcium fluid-like gel dispersed into the surrounding cement paste where a cation exchange took place between the alkalis in the gel and calcium from the paste causing the gel to become more viscous. The continued imbibition of pore water caused the now high-calcium gel to swell, as it does not readily disperse into the cement paste. The swelling of the gel caused internal tensile stresses to develop leading to cracking of the paste. In fly ash concretes, the low availability of calcium prevents the formation of high-calcium gels, and the gel remains in a fluid-like state and disperses through the concrete rather than forming internal stresses (Bleszynski et al. 2000).

Current Proposed Mechanism for Expansion

In general, ASR gel produced from chemical reactions is believed to expand by taking in water, generating an osmotic pressure on the surrounding cement paste and aggregate. While the mechanism for ASR gel expansion is not completely understood, the pressure

generated can be great enough to lead to cracking in the paste and aggregate and to expansion of the structure. A more detailed review of ASR expansion mechanism will be described below.

Powers and Steinour's Theory

Hansen (1944) and McGowan and Vivian (1952) proposed similar but distinctive theories: osmotic pressure theory and mechanical expansion theory, respectively. Upon a comprehensive review, Powers and Steniour (1995) proposed a compromise between these two theories. They were of the opinion that the nature of the ASR product depends upon its structure: a structure that is very similar to that of CSH formed from hydration of cement. In such a reaction, the environment is initially rich in Ca^{2+} (derived from calcium hydroxide) causing a high calcium to alkali ratio, and the alkali-silica gel is quickly converted to CSH (a rigid structure based on Ca–O layers). This has been termed a non-expansive reaction product. Conversely with ASR, Ca^{2+} is not as abundant in the pore solution and the cement paste cannot supply calcium fast enough to allow this gel to transform into C–S–H. A low calcium to alkali ratio gel results and is termed as an expansive reaction product. The ASR product has the ability to imbibe water and swell. The stress due to gel swelling causes expansion and cracking of the concrete.

In the cases of some aggregates that are amorphous and porous, such as opal, this lack of available Ca^{2+} is increased as the formation of alkali-silica gel occurs within the particles, and not on the surface. This results in the production of large outflows of gel from the reaction site. In instances of surface reactions, the initial attack of alkali and calcium hydroxides results in the formation of a layer surrounding the silica grain consisting of non-expansive lime-alkali-silica complex. This layer separating the non-reacted silica from the pore solution rich in alkalis and calcium hydroxides allows the diffusion of additional alkali and calcium ions (if not already consumed in the initial reaction). The relative amount of alkalis to calcium controls the expansive nature of resulting gel. Research by Pike and Hubbard (1957) supports this hypothesis.

However, Struble and Diamond (1981a, 1981b) challenged Powers and Steinour's description of this expansive mechanism as an oversimplified explanation. In their study of synthetic sodium-silicate gels and lime-sodium-silicate gels of varying composition,

they found no consistent relationship between the composition of synthetic gels and either the free expansion or swelling pressure. No significant effect on the free expansion or free swelling pressure was detected due to the presence of calcium in the gels. An interesting observation as to the state of the gel after testing was that the gels containing calcium remained solid, whereas the sodium-silicate gels were fluid in nature.

Chatterji's Theory

The mechanism of ASR expansion proposed by Chatterii et al. (1986, 1989) is summarized as follows:

Step 1: When placed in a solution with a pH of 7 or greater, hydroxyl ions penetrate reactive siliceous particles, in amounts increasing with solution pH and ionic strength. At a constant solution pH and ionic strength, the absorption of OH^- decreases with the increasing size of the associated hydrated cation (OH^- absorption decreases in the series K^+, Na^+, Li^+, Ca^{2+}).

Step 2: In a pore solution with mixed ionic species (e.g. $Ca(OH)_2$ and NaCl), both of the cations will penetrate into the reactive silica grain following the penetrating OH^- ions, however, more of the smaller hydrated cations will do so than the larger ones (in this example, hydrated Na^+).

Step 3: Penetrating OH^- ions attack siloxane bonds according the following equation:

$$Si–O–Si + OH^- = Si–OH + Si–O^- \qquad (2-7)$$

The reactive silica grain is further opened up to attack by this reaction. Silica ions are liberated from their original sites enabling them to diffuse out of the reactive grains.

Step 4: The rate of silica diffusing out of reacting grains is controlled by Ca^{2+} in the immediate vicinity. A higher Ca^{2+} ion concentration lowers silica diffusion.

Step 5: Calcium hydroxide plays three roles in alkali-silica reaction:

- $Ca(OH)_2$ accelerates the penetration of Na^+, Ca^{2+}, OH^-, and H_2O molecules into a reactive grain,
- $Ca(OH)_2$ promotes the preferential penetration of Na^+, OH^-, and H_2O molecules into a reactive grain in the presence of NaCl solutions,
- $Ca(OH)_2$ impedes the diffusion of silicate ions away from the grain.

Step 6: When the net amount of materials (Na^+, K^+, Ca^{2+}, OH^-, and H_2O) entering a reactive silica grain exceeds the amount of materials leaving (SiO_2^{2-}), expansion occurs.

Chatterji's theory draws upon diffuse double layer (DDL) phenomena to explain ionic mass transport, and the effect of ion-ion interactions on ionic diffusion.

Diffuse Double Layers (DDL) Theory

In 1999, a third theory was proposed citing electrostatic repulsion between DDLs as responsible for generating expansive forces (Rodrigues et al. 1999). Diffuse double layers are recognized phenomena in surface-solvent interactions. An exchange of electrical charges occurs when two dissimilar materials come into contact. In a cementitious system, cement hydration products are negatively charged (Chatterji and Kawamura 1992). Increasing negative surface charges are also observed with silica grains, and even more so with alkali-silica gel (Bolt 1957; Rodrigues et al. 1999). Due to their negatively charged states, cations are attracted, and positively charged electrical double layers are formed. Two layers defined as the Gouy-Chapman layer or the Stern layer has a collective thickness of a few nanometers that can be calculated from the ionic strength of the pore solution electrolyte.

Movement of Ions

ASR involves the movement of ions to reactive grains, and a subsequent accumulation of ions at the surfaces of grains and within these grains. Electron-probe microanalyses of ASR reaction products showed that the alkali ion concentration could reach up to 50 percent, whereas the concentrations in the cement paste were 1 to 2 percent (Knudsen and

Thaulow 1975). Similarly, calcium ions migrating inside reactive silica grains have yielded ASR gels with a CaO concentration of 15 to 20 percent (Chatterji et al. 1986; Regourd-Moranville 1989). There are normally very low concentrations (0.001-0.003 N) of calcium in concrete pore solutions (Diamond 1983). It is not obvious that this low calcium ion concentration is sufficient to explain the 20 percent CaO content of the ASR product. The following considerations clarify the situation: As reactive silica grains have greater negative charges due to the inonization of ≡Si−OH groups on individual reactive grains, a negative potential draws the positive cations towards the reaction sites forming a DDL (an electrical double layer forms round each reactive grain). These cations then penetrate into the silica grains and participate in the reaction. The contribution of these ions is responsible for a high CaO content in ASR products.

To explain contradictions between pore solution analyses and physio-chemical processes observed in portland cement pastes, Chatterji and Kawamura (1992) and Chatterji (2005) proposed an alternate mechanism of ionic mass transport. They suggested that cations, preferentially concentrated in the diffuse double layers surrounding negatively charged grains in a cementitious system could be transported through overlapping double layers. Fig. 2-11 shows a schematic representation of ion distribution in DDL. Diffusion studies provided support of this double layer transport by predicting previously unexplained observations in salt diffusion through cement pastes. From the proposed model by Chatterji, one would expect anions (Cl^- and OH^-) to diffuse through the bulk solution, whereas cations (Na^+, K^+, and Ca^{2+}) would diffuse through the double layers where their concentrations are higher. Calcium ions were shown to co-diffuse with sodium ions through a paste sample in the same ratio as that calculated to be in the double layer. Furthermore, the upstream and downstream cells, both initially free of calcium, showed equal concentrations of calcium diffusing from the sample. Chloride ions balanced the charge in the forward direction, whereas in the reverse direction, balance was achieved by the hydroxyl ions. Consequently, Fig. 2-11 shows that within the double layer the concentration of positive ions exceeds that of the negative ions, and the composition of the double layer solution, which is in contact with the grain, is different from that of the bulk solution.

Chatterji and Kawamura stated that there is a preferential accumulation of calcium ions over alkali ions in the double layer due to calcium's double valence, and suggested that this may explain a number of observations:

- The rapid growth of large portlandite crystals in hardened cement paste.
- High calcium concentrations found in ASR reaction products could be a consequence of the calcium-rich double layer surrounding reacting particles.
- The formation and maintenance of a highly concentrated solution of alkali ions (as found in the double layers) and subsequent diffusion of alkalis into reactive grains explains the mechanism for the continued migration of alkalis from the comparatively dilute pore solution to the concentrated environments found inside reactive grains.

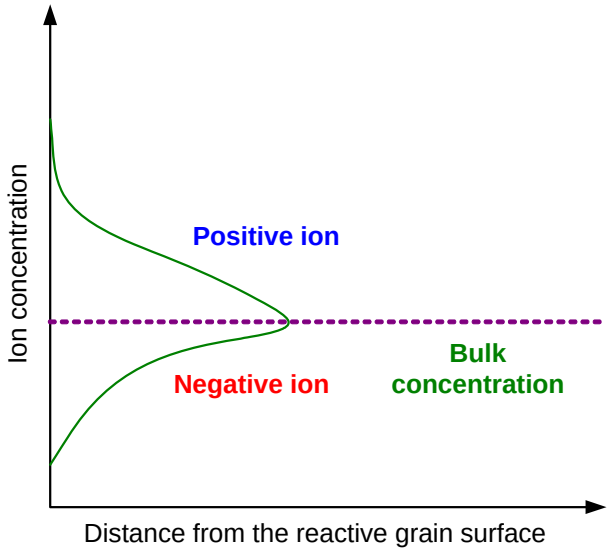

Fig. 2–11. A schematic representation of ion distribution around negatively charged silica grain (Chatterji 2005)

Effect of Ionic Strength

It has been shown that the rate of ASR reaction and expansion increases with increasing ionic strength of the host/pore solution (Chatterji et al., 1987). Diamond (1989) explained the arrest of alkali-silica reaction in portland concrete in the absence of alkali ions. A dense layer of calcium-silicate hydrates forms on the surface of reactive grain particles from the reaction of Ca^{2+} and OH^-. Further reaction will proceed only if the large hydrated Ca^{2+} ions diffuse to the reactive site through the dense CSH layer. Alkali-silica reaction is virtually stopped.

Chatterji and Thaulow (2000) suggested that in such a situation, the ionic strength of the pore solution is relatively low resulting in a low surface charge density on the silica particles and a very slow rate of dissolution of the silica grains (cleaving of the Si−O−Si bonds). Due to the low negative charge on the grain surfaces, a low calcium concentration results in DDL.

In such an alkali-free system, the pore solution's ionic strength will only increase by the presence of alkali ions; available only by the hydration of cement containing alkalis, or ingress from an exterior source. An increase in ionic strength (due to the addition of alkalis) yields a corresponding increase in the surface charge density of silica grains, and thus also an increase in the rate of cleaving the Si-O-Si bonds and dissolution of the silica. The chemistry of the double layers is also affected by the increasing ionic strength. Diamond (1989) showed that the diffusion of silicate ions is very low as long as the Ca^{2+}/Na^+ ratio in the DDLs is high. The Ca^{2+}/Na^+ ratio decreases (with the addition of alkalis and increasing ionic strength) causing the calcium-silicate hydrate layer to be less dense as there is less calcium available. Permeability to water molecules and other ions are increased. The lower calcium content in the double layer allows some silicate ions to diffuse out of the reactive grain. Expansion occurs when the rate of ingress of ions exceeds the amount of silicate ions diffusing out of the reactive grain.

Effect of Anion Species

It has been observed that higher ASR expansions levels have been produced with alkali chloride solutions as compared to alkali hydroxide solutions. Producing even greater

expansions yet are alkali nitrate solutions. One would expect that NaOH solution would produce the highest expansion, as hydroxyl ions are needed for reaction to occur.

A highly concentrated alkali hydroxide solution will suppress the solubility of $Ca(OH)_2$ in the pore solution, resulting in low calcium contents in the DDLs. Silicate ions freed by the ASR will diffuse away from the silica grains; the relative amounts of calcium in the vicinity controlling this rate of diffusion. When other host solutions, such as alkali chloride or alkali nitrate, are used, higher calcium to alkali ratios result in the DDLs (Chatterji and Thaulow, 2000). The greater calcium contents impede the transport of silicate ions away from the reaction site, and greater expansion levels result.

In conclusion, ASR mechanism proposed by many researchers summarizes that the ASR is a multistage process. The first step is the chemical reaction between reactive silica in the aggregate with the alkali present in concrete to produce alkali-silica gel. The second step is the expansion of the alkali-silica gel when it comes in contact with moisture. The proposed mechanisms are comprehensive. It is rooted in the topochemical silica dissolution and the through-solution diffusion mechanism based on chemistry and physics. In spite of much research on ASR, there is still discordance between mechanism models, test methods for assessing ASR, and application under actual field performance.

TEST METHODS FOR ASSESSING ASR

Despite a wealth of data that exists on alkali reactivity of aggregates from different sources, doubts remain as to whether current tests used to assess ASR potential are realistic under field conditions. This section provides an overview of test methods that have been used either on an experimental basis or in practice world wide for determining potential for ASR expansion in concrete.

Standard Testing Techniques

Fig. 2-12 shows several of the most commonly used standard test methods to assess ASR. Basically, current test methods are classified into three categories: aggregate testing, cement-aggregate combination testing, and gel identification testing.

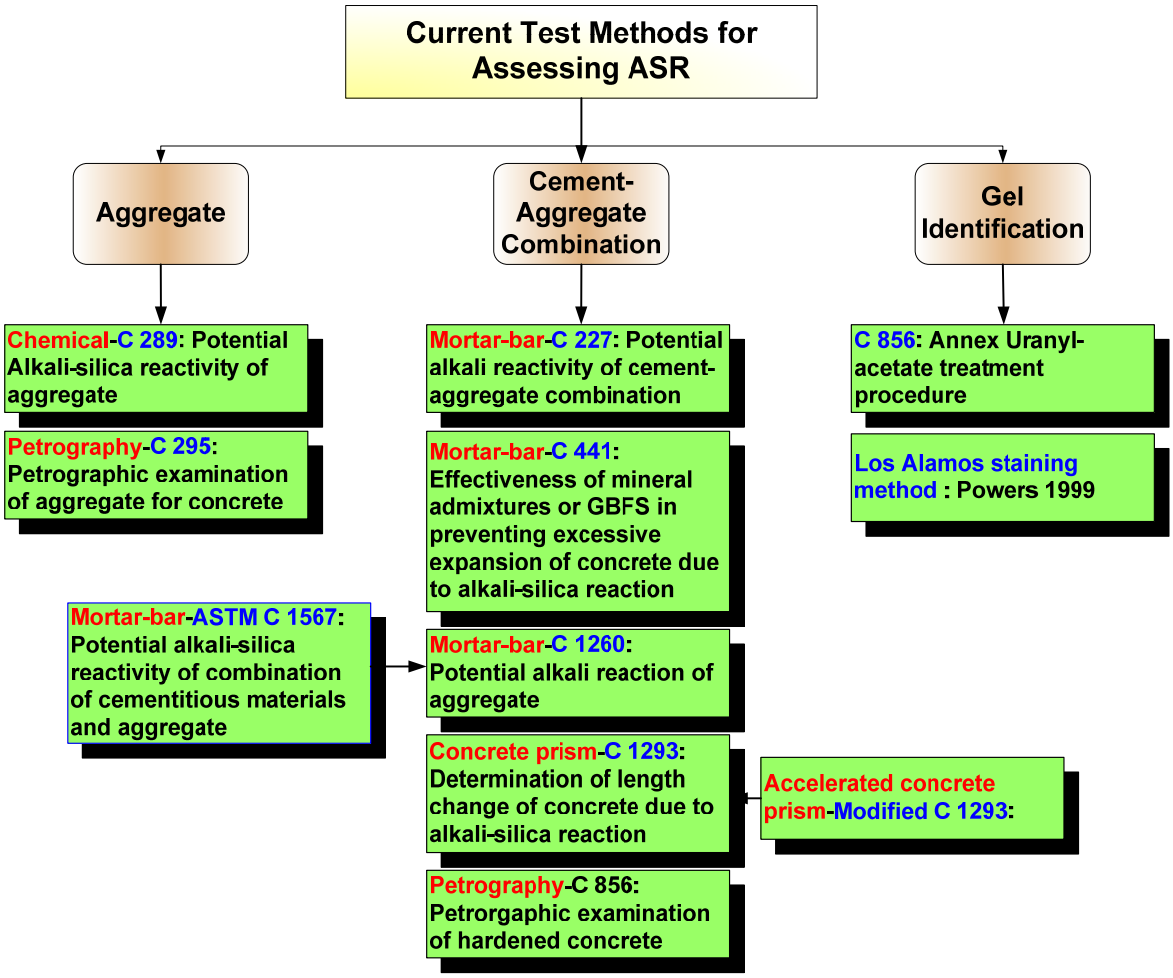

Fig. 2–12. Current test methods for assessing ASR

Aggregate Testing

Swamy in 1992 reviewed the various tests used to identify alkali-reactive aggregates and their potential for deleterious expansion in concrete. It was noted that although laboratory testing is the surest way to assess and evaluate the potential reactivity of aggregates prior to their use in concrete, testing can often be difficult, complex, confusing, time-consuming and even inconclusive.

Strunge and Chatterji (1991) used a chemical method to detect alkali-silica reactivity of sand. In this method, the sand is digested in a mixture of $Ca(OH)_2$ and KCl for 24 hours. The OH^- concentration is determined from titration. The difference in OH^-

concentration between control and tested samples is used as a measure of alkali-silica reactivity. Strunge and Chatterji found reproducibility of the method fairly high.

The original ASTM C 289 decision chart was developed based on highly reactive siliceous aggregates. However, the increased application of this chemical method led to the conclusion that the original chart was not universally applicable (Turriziani 1986). Vivian (1981) suggested that aggregate producing dissolved silica in excess of 100 millimoles per liter according to ASTM C 289 test method should contain sufficient amounts of reactive material to produce expansion in concrete. Thaulow and Olafsson (1983) also found this value useful for predicting potential alkali reactivity of some Scandinavian sands. Brandt and Oberholster (1983) suggested that increasing the test duration from three to seven days gives more representative values. Certain mineral phases are known to cause interference, which underestimates the amount of dissolved silica. This leads to a false diagnosis of aggregate reactivity, i.e., a reactive aggregate may pass by this test. Furthermore, crushing and sieving of the aggregate sample produces new exposed surfaces which alter the reactivity of the aggregate. Therefore, evaluation of aggregate reactivity by this test method needs additional information such as petrography and chemical composition of aggregates being tested.

The German Committee for Reinforced Concrete developed a test method (1986) to evaluate the potential reactivity of opal and flint. In this method, specified quantities of 1 to 2 and to 2 to 4 mm aggregate size fractions are immersed in 1N NaOH solution at 90°C for one hour. The fractions are then washed, dried and weighed. The loss in mass, called soluble alkalis is taken as a measure of the potential reactivity of the aggregate. Similar to most of the other chemical tests for ASR, this dissolution test essentially measures reactivity of an aggregate in an alkaline environment. It does not indicate how deleterious or expansive an aggregate would be in a concrete structure. This method does not take into account the potential reactivity of materials less than 1 millimeter.

An osmotic cell was developed by Verbeck and Gramlich in 1955 to study the mechanism of expansion resulting from ASR and to identify factors that determine whether an expansive reaction will occur (Stark 1983). The osmotic cell used in this test consists of two chambers; each filled with 1N NaOH solution (Fig. 2-13).

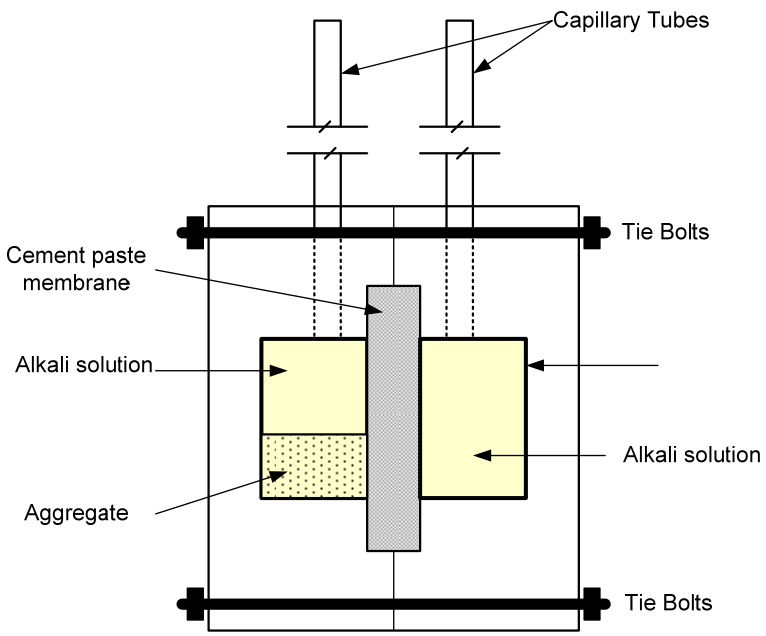

Fig. 2–13. A schematic diagram of the osmotic cell

The chambers are separated by a cement paste membrane at a water-cement ratio of 0.55. A representative specimen of the aggregate to be tested is placed in the reaction chamber. When ASR occurs the solution flows from the reservoir chamber (left to right), thus creating a positive flow through the cement paste membrane. The differential in height in the vertical capillary tubes attached to the top of each chamber indicates the reactivity of the aggregate. For example, positive flow rates of 1.5 to 2 mm per day indicate an aggregate with the potential for deleterious alkali reactivity in concrete, whereas a reverse flow corresponds to non-reactive aggregates. A testing period of 30 to 40 days is generally recommended to be sufficient when testing 12 g of aggregate sample, while two to three days are normally sufficient for highly reactive aggregates. Results (Schmitt and Stark 1989) indicate that the technique is promising as a rapid method for determining the deleterious reactivity of aggregates.

Knudsen (1987) developed another quick chemical test based on the principle that a reactive sand in a concentrated alkali solution will experience volume contraction, or chemical shrinkage, as a result of silica dissolution. This method is a current test method used in Denmark and the precision of this test method has been evaluated through a multi-

laboratory test program. Based on the recommendations of the Basic Concrete Specification of Building Structures, a limit of 0.30 mL of chemical shrinkage per kg of sand has been set for acceptance of sands to be used in concrete exposed to moderate and aggressive environments (Knudsen 1992).

Cement-Aggregate Combination Testing

According to Grattan-Bellew (1997), the major requirement of accelerated test methods for evaluating potential reactivity of aggregates is that they should be able to correctly predict the potential reactivity in over 95 percent of the cases. Owing to the complexity and variability in composition and grain size of aggregates, it is highly unlikely that a single test method will be able to evaluate all types of aggregates. Another major requirement of accelerated test methods is that inter-laboratory coefficient of variation should be low, preferably less than 12 percent.

The literature indicates that the accelerated mortar bar method should be used with caution when rejecting aggregates. Many innocuous aggregates that perform well in the field, do not pass this test. Nevertheless, the accelerated mortar bar test still remains a standard for assessing aggregate ASR potential.

In 1992, the Pennsylvania Department of Transportation (PennDOT) initiated a program to test all their approved aggregate sources for ASR potential using the rapid mortar bar test, known as ASTM C 1260 method (Thompson 2000). Although the program ended in 1993, PennDOT has continues to evaluate new aggregate sources for ASR potential using this method. The department also performed a joint experiment with the Northeast Cement Shippers Association (NECSA) using a modified form of the rapid mortar bar method to assess the amounts of Class F fly ash and slag required to combat ASR with highly reactive aggregates. It was found that rapid mortar bar test could be used to evaluate the effect of fly ash and slag on suppressing ASR expansion and detect the deleterious behavior of aggregate due to ASR.

Marks (1994) reported ASTM C 1260 results from tests on Iowa sands obtained from 30 different sources. Marks identified many sands as reactive, while only two were innocuous. He concluded that more research was needed on this test method because pavement performance history has shown very little deterioration due to alkali-silica

reaction. Six of the sands were evaluated by the Canadian Prism Test. None were identified as reactive by this test method.

Hossain and Zubery's research (1995) consisted of testing larger concrete beams, 75 mm x 100 mm x 400 mm, as per ASTM C 1260 method. The variables evaluated included the percentage of limestone aggregate, source of fine aggregates, and percent and source of Class C fly ash. This limited study indicated that C 1260 method has the potential to detect the deleterious behavior of aggregates due to ASR.

Canadian researchers (Berube et al. 1995) claim to have successfully evaluated the effectiveness of SCMs in suppressing expansion due to ASR using both ASTM C 1260 and CSA A 23 methods. According to authors, these methods are effective because the alkalis in the pore solution decrease in the presence of SCMs when the bars are immersed in 1N NaOH solution at 80°C. Mortar bars made with different SCMs were tested in normal conditions, in water and in air at 100 percent RH. Their results indicated that in the presence of SCMs, the alkali decrease in the pore solution. Additionally, the alkali equilibrium between the pore solution and the NaOH immersion solution is not achieved in the presence of SCM at the end of the testing period of 14 days.

The experimental program of Glauz et al. (1996) on the evaluation of ASR mitigation using mineral admixtures included aggregates from various sources, cement with different alkali contents, fly ashes, silica fume and natural pozzolans. The mixtures which were evaluated using the ASTM C 227 method indicated that the chemical makeup of mineral admixtures, alkali content of cement, and replacement rates of cement by mineral admixtures influence the test results.

Duchesne and Berube (1994) investigated the two ASTM methods that are used to determine the amount of alkalis released by various SCMs available for ASR. ASTM C 114, which measures water soluble alkalis, gives only the amount of rapidly soluble alkalis in the form of alkali salts (sulfates and chlorides), whereas the modified and standard C 311 give values between 40 and 100 percent of total alkalis. In most cases, both methods clearly overestimated the percentage of available alkalis from SCMs. Duchesne and Berube explained this as due to a large proportion of alkalis trapped in secondary hydrates released with water washing at the end of the tests. Results of pore solution analysis suggest that more alkalis are trapped in secondary hydrates than released from SCMs in the

pore solution. These results agree with expansion tests on concretes made with the same SCM and two very reactive aggregates. Duchesne and Berube (1994) claim pore solution extraction method to be the best to evaluate the balance between the alkalis released by SCM in the pore solution and those trapped in reaction hydrates.

The use of the mortar bar expansion test in a 1N NaOH solution at 80 °C as a means of assessing the effectiveness of fly ash and silica fume against alkali silica reaction was investigated using fused quartz as reactive aggregate (Bera et al. 1994). Long term ASTM C 227 test results were used for comparison. The NaOH test provided reasonable results on the minimum contents of fly ash and silica fume needed to prevent deleterious expansion in mortars containing fused quartz. The researchers noted that a consistent relationship develops between the expansion of mortar bars and Na^+ ion concentration in the pore solution after 14 days of immersion of specimens in NaOH solution. They concluded that neither of these test methods provides a direct correlation between the performance of fly ashes and total and available alkali contents.

The Association Francaise de Normalization (AFNOR) adopted a mortar bar test method known as AFNOR P 18-585 (1990). In this method, a cement with an alkali content equal to or greater than 0.75 percent Na_2O_e is used and the total alkali content of the mortar mixture is raised to 1.25 percent Na_2O_e by adding NaOH to the mixture water. Mortar bars measuring 25 x 25 x 285 mm are used in this test. The bars are stored above water in a sealed steel container such that there is no wicking action. This container is then stored above water inside a larger insulated container in which the temperature is maintained at 38 °C by heating the bottom water. These containers have been designed to eliminate temperature gradients which can affect the overall humidity inside the storage containers. There is no doubt that this specification regarding the storage condition will be beneficial in overcoming some of the problems encountered in the ASTM C 227 test procedure.

In another method proposed by the Cement and Concrete Association, England (Hobbs 1986) three bars measuring 25 x 25 x 250 mm are cast using an aggregate to cement ratio of 3:1 at a w/c of 0.40, and a cement with an alkali content of 1.0 percent Na_2O_e. The bars are moist cured for 24 hours, then demolded and individually wrapped with a damp tissue and placed in plastic sleeves. The expansion limit is set at 0.05 percent

after six months. This method could overcome many of the problems related to the influence of w/c, alkali content and storage conditions in the ASTM C 227 procedure.

In the Danish accelerated mortar bar test method (Chatterji 1978), mortar bars measuring 40 x 40 x 160 mm in size are prepared with the cement : aggregate : water ratio of 1 : 2 : 0.50. After an initial 24-hour curing period the bars are immersed in water for 28 days then stored in saturated NaCI solution at 50 °C, and the expansion measured at weekly intervals. The proposed limit for deleterious aggregates is set at 0.10 percent after 20 weeks. The method obtained a good correlation for a number of Scandinavian sands using ASTM C 227 and ASTM C 289 methods. Chatterji et al. (1987) showed that in the long term, mortar bars tested according to this method may expand more than the companion bars immersed in a 1N NaOH solution at 50 °C, although there is a much slower onset of expansion in the short term. The same trend occurs at 30 °C. The total expansion is attributed not only to ASR, but also to the formation of calcium chloroaluminate hydrate. Moreover, this method takes five months to complete, which is not significantly faster than some of the other test methods. In Canada, the CSA concrete prism method which does not take much longer than ASTM C 227, is preferred.

In the South African NBRI mortar bar test method (Oberholster and Davies 1986), and Canadian test method CAN/CSA A23.2-25A (1992), the test bars are prepared as the same as ASTM C 227 method. After 24 hours of initial moist curing in molds, the bars are placed in sealed containers filled with water at 23 °C, then transferred to 80 °C. The zero reading is taken the next day, and the bars are transferred to a 1N NaOH solution at 80 °C, and measured every day for 14 days. The CSA A23 proposes using a fixed W/C of 0.50 for coarse aggregates and 0.44 for uncrushed natural sands. The cement type and alkali content were found to have a negligible effect on expansion, provided no SCMs were used.

In the Canadian test procedure proposed by Fournier et al. (1991) the mortar bars are made in accordance with ASTM C 227, but at a constant W/C of 0.50 or 0.44 for uncrushed natural sands and an alkali content 3.5 percent Na_2O_e. The bars are then moist cured for 48 hours at 23 °C, 24 hours in their molds and 24 hours in a moist cabinet. The bars are placed in an autoclave for five hours at 130 °C. The effectiveness in recognizing the potential reactivity of reactive aggregates or the innocuous character of non-reactive

aggregates was generally better with this autoclave test than with the accelerated mortar bar tests.

The type of container significantly affects the ASTM C 227 method, that is, whether wicking occurs inside the storage container or not. The variation in the alkali content of cements may also be a factor to be considered. The mortar bar test does not specify any w/c, as water is added to reach the specified flow. Based on these observations, it is not surprising that several modifications to the test procedure have been proposed by different researchers and agencies over the years.

Davies and Oberholster (1987), Grattan-Bellew (1989), and Fournier and Berube (1991) observed that expansion of mortar bars increased as a function of W/C, but the cement type and alkali content did not appear to have a significant effect on expansion, provided the cement contained no SCMs. Therefore, the proposed ASTM C 9 – P 214 and CAN/CSA A23.2 – 25A specify a fixed w/c of 0.50 for coarse aggregates and 0.44 for uncrushed natural sands.

Shayan et al. (1988) suggested pre-curing for three days in a fog room and a mortar bar expansion limit criterion of 0.10 percent at 10 days for non reactive aggregates. Hooton and Rogers (1989) after testing 61 Canadian aggregates of known reactivity suggested that expansion limit criteria of 0.15% at 14 days and 0.33% at 28 days were effective in distinguishing expansive from non-deleterious aggregates. The 28-day expansion value was found to be particularly effective in recognizing some marginally reactive aggregates that continued to expand rapidly after 14 days.

Roy et al. (1997) prepared concrete prisms with crushed aggregate, non-reactive sand, cement with added alkali content and water in proportion of 1:1:1:0.5. The prisms were demolded after 24 hours, cured in water at room temperature for another 24 hours, then boiled at constant pressure and temperature of 111 °C in an autoclave for two hours, cooled to room temperature and examined for the presence of cracks and changes in ultrasonic pulse velocity as well as dynamic Young's modulus. Conditions for a suspect aggregate to be innocuous could be established from these measurements. Researchers found results obtained by this method agreed with those obtained by the other ASTM methods in practice, that is, C 295, C 289 and C 1260.

Gel Identification Testing

Tests to determine the potential reactivity of aggregates were previously considered in the 1940s. Stanton et al. (1942; 1943) developed the gel pat test method for assessing potential ASR. In this test method the selected aggregate particles are cast in a pat of neat cement (a small mass shaped by patting cement). After a convenient moist curing period one surface of the pat is wrapped until the particles are exposed. The pat is then immersed with a polished face up in a container filled with a lime-saturated alkali hydroxide solution. When using opal aggregates and testing at room temperature, the method has been found to be produce a significant amount of gel in only five days. For testing other reactive aggregates, increasing the temperature to 54 °C produced similar quantities of gel within 16 to 17 hours.

Jones and Tarleton (1958) applied a similar technique to test aggregates. They, however, emphasized that the reactivity shown in this test is not necessarily an indication that the aggregate will be expansively reactive in concrete. Hobbs (1986) described this method applicable to reactive silica that is too finely distributed to be observed under a petrographic microscope. It is claimed that the test represents a quicker and more reliable way to detect small amounts of opal in aggregate samples. Although it often allows differentiating between non-reactive and reactive particles, this method remains qualitative and can be used only as a complementary tool for assessing the potential alkali reactivity of aggregates. It does not, like C 1260, indicate how deleterious the material might be in a concrete structure.

A modified gel pat test was developed by Fournier and Berube (1993) in which polished concrete slices were immersed in a normal solution at 38 °C for 56 days. A rating system called the gel pat test rating (GPTR) was developed to quantify the amount of gel formed on the polished section. The method was applied to 65 carbonate aggregates from Quebec province in Canada. Fairly good correlations were obtained between the GPTR and results of various other test methods that are currently in practice.

In a later test, Sergi (1994) embedded steel plates in concrete prisms made from a potentially reactive siliceous aggregate with alkali content just below the threshold level required to induce significant expansion due to ASR. The steel plates were subjected to electrical current passed either potentiostatically or galvanostatically. Significant

expansion, development of ASR products, alkali metal concentration and cracking of concrete around the steel cathodes were noted in those samples where potentiostatic polarization was applied. Very little expansion was detected for the prisms in which only cathodic polarization was applied, even when the total charge passed was equivalent to that for the potentiostatically controlled specimens. Rasheeduzzafar (1993) subjected steel plate embedded mortar specimens made with reactive crushed Pyrex glass and high alkali cement to 215 and 1076 mA/m^2 (20 and 100 mA/ft^2) to cathodic protection (CP) current at the steel surface. He observed that CP current advanced the time of cracking by up to 60 percent compared to specimens cracking that were not subjected to any electrical current.

Other Test Methods

A series of mortar bar tests was conducted by Hearne et al. (1992) using compression wave velocity measurements. In addition to length and weight measurements, two different compression wave velocity measurements were made over a 1-year period. The cycle velocity measurement was more repeatable than ultrasonic pulse velocity measurement. However, both were found to be good laboratory indicators for monitoring progress of alkali-silica reaction in concrete. Pulse and cycle velocities were noted to be inversely related to expansion.

Rogers and Hooton (1989) developed a technique for determining the water soluble alkali content to help in assessing the likely cause of concrete deterioration and to assess to some extent the potential for future distress. In this method a 2 kg concrete test sample is crushed so that it passes through 200 mesh sieve (< 75 μm). A sub sample weighing 1 gram is then immersed in 100 mL distilled water, boiled for 10 minutes and allowed to stand overnight at room temperature. The suspension is then filtered and the volume adjusted to 100mL by adding more distilled water. Flame photometry is then used to determine the Na and K contents in solution. The values are expressed as kg/m^3 of concrete. Fournier (1997), however, cautions that since the alkali content varies between different components within a single concrete structure, more than one determination should be made at different depths.

Some of the proposed test methods for evaluating potential ASR involve steam curing or boiling water or alkaline solutions. Samples of mortar or concrete are tested

under relatively high pressure and temperature conditions. The test method proposed by Tang and coauthors (1983a; 1983b) requires only two days. In this method the aggregate is reduced in size by crushing, grinding and sieving to 150 to 700 μm. Small mortar bars, 10 x 10 x 40 mm in size, are made with a cement/ aggregate/ water ratio of 10 : 1 : 3. The total alkali content of the mixture is raised to 1.5 percent Na_2O_e. The bars are first cured for 24 hours at 20 °C and 100 percent RH, steam cured for four hours then immersed in a 10 percent KOH solution for six hours at 150 °C in a autoclave. Expansion in excess of 0.10 to 0.15 percent corresponds to potentially deleterious aggregates. This test has failed in detecting a number of reactive aggregates. In addition, an aggregate identified as reactive in this autoclave test might not necessarily react deleteriously in concrete. The test has been applied to a limited number of aggregates and further testing is required to confirm the limit criteria to be used with other types of aggregates.

Criaud et al (1990; 1992a; and 1992b) tested a number of reactive and sound aggregates from different sources using a slightly modified version of Tang's autoclave test method. The Criaud test method is known as a micro bar method. A 160 to 630 μm aggregate fraction is used. Portland cement is used to prepare three mixtures with different cement to aggregate ratios of 2:1, 5:1 and 10:1. Each mixture is prepared with a 0.30 w/c and a total alkali content of 1.5 percent $Na2O_e$. The curing and testing procedures are similar to those in Tang's method. The authors claim that the method provides a reliable evaluation of the potential ASR of aggregate. The reliability of the method seems to improve by performing the test at three cement/aggregate ratios, slowly expanding materials being more effectively detected at lower cement/aggregate ratios. A slightly modified version of this method has been found to be affective in evaluating the effectiveness of supplementary cementing materials to control ASR.

Nishibayashi et al. (1987) proposed another method in which the mortar bars are prepared at 40 x 40 x 160 mm in size using a cement/aggregate/water ratio of 1:2.25: 0.25. The total alkali content of the mixture is the same as that of the previous Criaud method. The autoclave treatment is carried out under 0.15 MPa at 120 °C for four to five hours. The final reading is taken at room temperature. The expansion values obtained after five hours in autoclave were similar to those obtained after 20 weeks in ASTM C227 method.

So far the test has been applied to a limited number of Japanese aggregates and further testing is necessary.

In another Japanese method proposed by Tamura and co-workers (1984), the mortar bars are made at an alkali content of 2.25 percent in with a cement/aggregate/water ratio of 4 : 2 : 1. After curing the bars exactly the same way as in the other methods, they are then placed in boiling water in an autoclave for two hours. After cooling at 20 °C the bars are examined for cracks. The propagation of ultrasonic waves through the bars and the dynamic elasticity are also measured. The samples are considered reactive when cracks are observed; the Young modulus decreases by 15 percent or more, and the acoustic waves are slowed down by 5 percent or more. Again the test has only been applied to a limited number of Japanese aggregates.

Despite a wealth of data that exists on alkali reactivity of aggregates from different sources, doubts remain as to whether the current tests used to predict ASR are realistic under field conditions. A number of accelerated test methods for determining potential reactivity of aggregate have been developed over the past 15 years. In general, accelerated tests are performed under high temperature and high alkalinity or autoclaved conditions. These methods and their limitation are summarized in Table 2-1.

Table 2-1. Available Standard Tests for Assessing ASR

Type of test	Test name	Purpose / Material properties	Test method	Test duration	Comments
Aggregate	ASTM C 289: Potential alkali reactivity of aggregate	To determine amount of dissolved silica and alkalinity; related to aggregate reactivity	Sample reacted with alkaline solution at 80°C (176°F)	24 hours	· Quick results · Helpful for initial screening of aggregate · Poor reliability · Fail in case of slow reacting aggregate
	ASTM C 294: Constituents of natural mineral aggregate	To give descriptive nomenclature for the more common or important natural minerals-an aid in determining their performance	Visual identification	Short duration-as long as it takes to visually examine the sample	· Used to characterize naturally-occurring minerals that makeup common aggregate sources
	ASTM C 295: Petrographic examination of aggregate for concrete	To identify potentially reactive components (but not all) in aggregate	Visual and microscopic examination of prepared samples- sieve analysis, microscopy, scratch or acid tests	Short duration	· Used in conjunction with other laboratory tests · Reliability of examination is dependent on experience and skill of individual petrographer
Cement-aggregate combination	ASTM C 227: Potential alkali reactivity of cement-aggregate combinations	To test the susceptibility of cement-aggregate combinations to expansive reactions involving alkalis; related to the rate of reaction at specific conditions	Mortar bars stored over water at 38.7ºC (100ºF)	Varies: first measurement at 14 days, then 1, 2, 3, 4, 6, 9, and 12 months	· Carbonate aggregate may not produce significant expansion · Long test duration · Excessive leaching of alkalis from specimens
	ASTM C 342: Potential volume change of cement-aggregate combination	To determine the potential ASR expansion of cement-aggregate combination; related to the rate of reaction at specific conditions	Mortar bars stored in water at 23ºC (73.4ºF)	52 weeks	· Primarily used for aggregate from Oklahoma, Kansas, Nebraska, and Iowa

Table 2-1. (Cont'd)

Type of test	Test name	Purpose / Material properties	Test method	Test duration	Comments
Cement-aggregate combination	ASTM C 441: Effectiveness of mineral admixture or ground blast-furnace slag in preventing excessive expansion of concrete due to the alkali-silica reaction	To assess effectiveness of supplementary cementitious materials (SCMs) in controlling expansion form ASR	Mortar bars-using Pyrex glass as aggregate- stored over water at 38.7ºC (100ºF) & high relative humidity	12 months; every 6 months after that as necessary	· Pyrex containing alkalis may be released during the test · Highly reactive artificial aggregate may not represent natural aggregate
	ASTM C 856: Petrographic examination of hardened concrete	To outline petrographic examination procedures for hardened concrete	Visual and microscopic examination of prepared samples	Short duration- includes preparation of samples and visual and microscope examination	· Useful in determining conditions or performance · Specimens can be examined with stereomicroscope, polarizing microscopes, and scanning electron microscope · Reliability of examination is dependent on experience and skill of individual petrographer
	ASTM C 1260: Potential alkali r eactivity of aggregate	To test the potential for deleterio us alkali-silica reaction of aggre gate; related to both the rate of re action and ultimate expansion at specific conditions	Mortar bars soaked in 1N NaOH at 80ºC (176ºF)	16 days	· Very fast alternative to C 227 · Useful for slowly reacting aggregate · Promise in testing lithium compounds, but the test solution must be modified · Not used to reject a given aggregate by itse lf because of severity of test condition
	ASTM C 1293: Concrete aggregate by determination of length change of concrete due to alkali-silica reaction	To determine the potential ASR expansion of cement-aggregate combinations; related to both the rate of reaction and ultimate expansion at specific conditions	Concrete prisms stored over water at 60ºC (140ºF)	3 months	· Fast alternative to C 227 · Need more data and verification

Table 2-1. (Cont'd)

Type of test	Test name	Purpose / Material properties	Test method	Test duration	Comments
Cement-aggregate combination	Accelerated concrete prism test (Modified ASTM C 1293)	To determine the potential ASR expansion of cement-aggregate combinations; related to both the rate of reaction and ultimate expansion at specific conditions	Concrete prisms stored over water at 60ºC (140ºF)	3 months	· Fast alternative to C 227 · Need more data and verification
	ASTM C 1567: Potential alkali-silica reactivity of combinations of cementitious materials and aggregate (Accelerated mortar-bar test)	To test the potential for deleterious alkali silica reaction of cementitious materials and aggregate combinations in mortar bars; related to both the rate of reaction and ultimate expansion at specific conditions	Mortar bars soaked in 1N NaOH at 80ºC (176ºF)	16 days	· Evaluate mortar bar in the presence of different chemical solutions
Gel Identification	ASTM C 856 (AASHTO T 229) : Annex Uranyl-Acetate Treatment Procedure	To identify products of ASR in hardened concrete	Staining of a freshly exposed concrete surface and viewing under UV light	Immediate results	· Identify small amount of ASR gel whether they cause expansion or not · Opal, a natural aggregate, and carbonated paste can glow : interpret results accordingly · Test must be supplemented by petrographic examination and physical tests to determine concrete expansion
	Los Alamos Staining Method (Power 1999)	To identify products of ASR in hardened concrete	Staining of a freshly exposed concrete surface with tow different reagents	Immediate results	

Analytical Techniques

Following the approach of Brandt and Oberholster (1983), Sorrentino et al. (1992) proposed improvement to the method by measuring the amount of silica dissolved from the aggregates as a function of time of immersion in 1N NaOH solution at 80°C. This test came to be known as the French kinetic chemical test. They suggested storing the test specimens for a minimum of 72 hours in the NaOH solution, with measurements of SiO_2 to Na_2O ratio in the solution being made at 24-hour intervals (Fig. 2-14). Based on a fairly large number of tests the researchers produced a chart showing three different degrees of reactivity corresponding to non-reactive aggregates, potentially reactive aggregates and reactive aggregates. However, this modified test is unable to detect a number of marginally to moderately reactive siliceous carbonate aggregates.

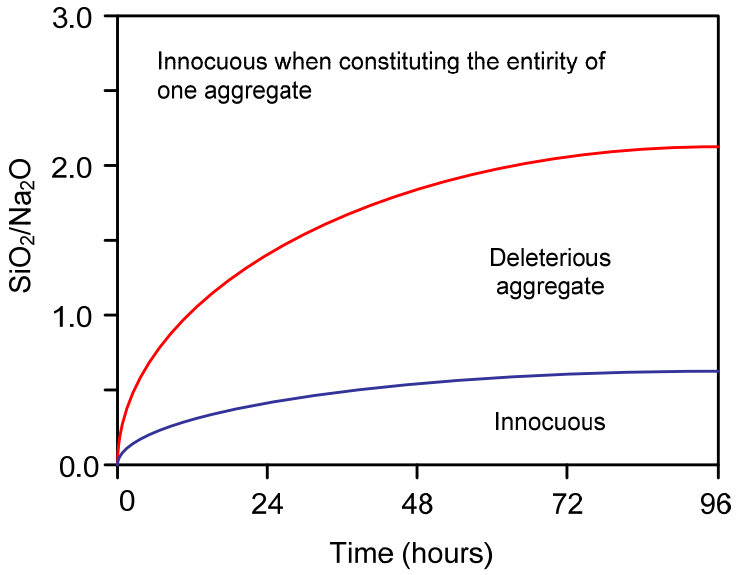

Fig. 2–14. Diagram used in the French kinetic chemical test (Sorrentino 1992)

Lane and Ozyildirim (1995), using their 336-day test results using ASTM C 227, noted that expansions of control mortars with alkali contents of 0.40 percent or less were negligible. With cements having alkali content above 0.40 percent equilibrium between cement alkali content and mortar bar expansion was reached at 56 days, when a strong

linear relationship between increasing expansion and increasing alkali content developed. A regression analysis was performed on data from the control batches.

Lane (1993) conducted tests to evaluate ASTM C 1260's effectiveness using aggregates from Virginia. He concluded that further experience with the method was necessary to determine whether suitable criteria can be established to discriminate between non-reactive and reactive aggregates containing microcrystalline or strained quartz.

Uomoto et al. (1992) presented a new kinetic model to predict the expansion behavior of mortar bars. The model incorporates factors such as size and reactivity of aggregates and alkalinity of cement. A leaching test measures the change of soluble silica content and alkali-silica ratio of reaction products over time. The results obtained are then analyzed on the basis of kinetics in order to obtain the alkali diffusion coefficients of aggregates. The expansion behavior is characterized using the diffusion coefficients and the alkali-silica ratios of the reaction products. Good agreement was obtained when comparing the observed expansion behaviors with the calculated expansion behaviors.

To improve the interpretation of the ASTM C 1260 results, two models were introduced by Johnston of the South Dakota Department of Transportation. In the first model (1994a), he modified the ASTM C 1260 method to test potential reactivity of sands used in concrete. Two different NaOH concentrations were used to explore the feasibility of using two base strengths to better predict reactivity. The first model consisted of using a polynomial fit procedure on the C 1260 expansion versus time for each of the tested aggregates and then to plot the coefficient of these curves against each other (the interpretation of test results included a best fit line (Fig. 2-15) for the expression at 3, 7, 11 and 14 days).

$$\text{Expansion (\%)} = A_2X_2 + A_1X + A_0 \qquad (2-8)$$

where, $X = \text{Time}^{1/2}$ and A_2, A1, and A_0 are coefficients

The advantage of this model was that it considered the expansion history over the full 14-day period instead of just using 14-day expansion reading. The sands could then be divided into two linear families of coefficients, one reactive and the other non-reactive.

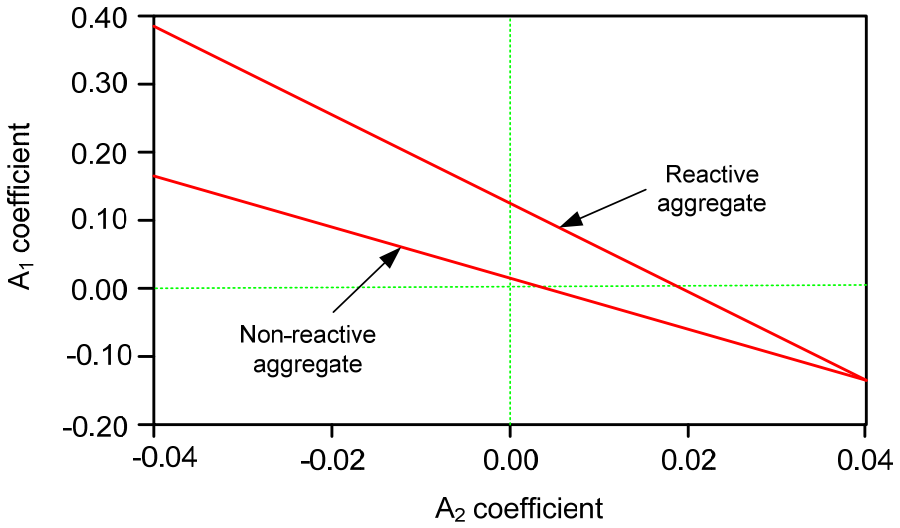

Fig. 2–15. Plot of A_1 versus A_2 for sands

However, although this model yielded some promising results, it was limited in scope because each laboratory running the C 1260 has to develop its own correlations for using the method and the days upon which expansion data are taken have to be the same for a proper comparison.

In a parallel study to evaluate the effectiveness of different ASTM test procedures at predicting alkali-silica reactivity, Johnston (1994b) evaluated ASTM C 289, C 227 and an autoclave expansion test using 31 fine aggregate sources in South Dakota. Only ASTM C 1260 was capable of reliably predicting potential ASR when results were compared to actual field performance.

The second model was a kinetic-based model applying Avrami's equation to the C 1260 expansion (2000; 2002). This equation described the nucleation and growth or phase transformation reaction kinetics:

$$\alpha = 1 + \alpha_0 - e^{-k(t-t_0)^M} \quad (2-9)$$

where, α = the degree of reaction (α cannot exceed 1); α_0 is the degree of expansion at time t_0; k is a rate constant that reflects the effects of nucleation, multidimensional growth, the geometry of reaction products, and diffusion; t_0 is the fourth day of curing; and M is an exponential term related to the form and growth of the reaction products.

Taking the double natural log of both sides of above equation results in below equation:

$$\ln\left[\ln\frac{1}{1+\alpha_0-\alpha}\right] = M \times \ln\left(t - t_0\right) + \ln k \quad (2-10)$$

where, $\ln k$ is the intercept and M is the slope of the regression line.

The value of t_0 depends on the extent of the induction period before reaction begins. A plot of the exponent M versus $\ln k$ is used for interpreting potential reactivity as shown in Fig. 2-16. Johnston concluded that aggregate with $\ln k$ greater than -6 are reactive and aggregate with $\ln k$ less than -6 are innocuous. He also concluded that this method is efficient in evaluating samples involving fly ash and other SCMs. However, the interpretation of this method is based on the test results of the C 1260 which needs to be ground to a specific size before it can be tested. Once an aggregate is ground finer, the effect of specific surface is likely to occurs, whereas this effect is non-existent under field conditions. Thus, fine grains with higher specific surface may not be a true representation of its reactivity in field concrete.

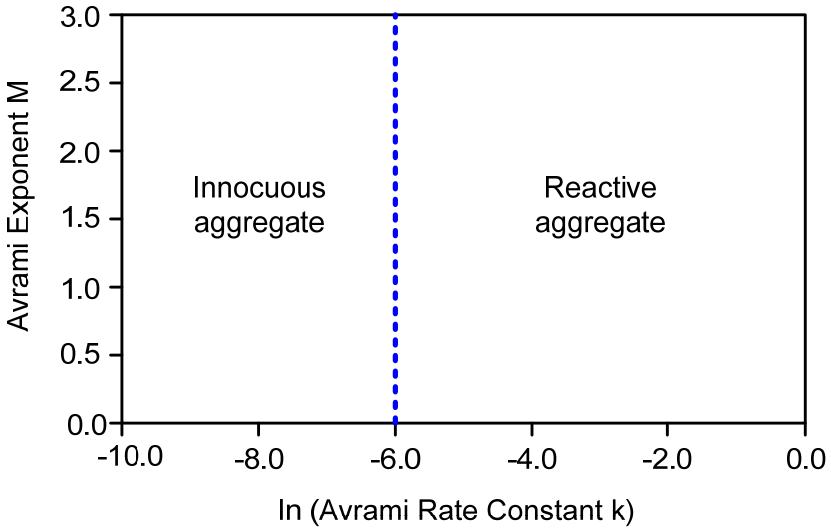

Fig. 2–16. Avrami exponent versus rate constant

This literature survey provides an overview of ASR in concrete, including primary factors influencing ASR and mechanisms of ASR, and reveals that the three most frequently used methods for assessing potential ASR are ASTM C 227, C 1260, and C 1293. Since these methods have some drawbacks, researchers and agencies all over the world have been trying to improve test procedures. Some of the new methods or modifications of existing methods have been proposed to overcome many of the problems related to the influence of w/c, alkali content, and storage conditions (alkalinity of testing solution and temperature). Different aggregate testing procedures have been adopted to evaluate the potential reactivity of aggregate and different mitigation measures that best fit their needs. Although some of these test methods have come to be accepted as "standard tests," current test procedures are largely empirical and yield test results that are applicable to a narrow band of conditions. Few have been adequately evaluated in terms of the material performance of concrete placed in the field. It is clear that there is a lack of a unified approach to address how different combinations of concrete materials may interact to affect ASR behavior. Therefore, it has become necessary to take a completely new approach, preferably one that is performance-based and provides a measure of ASR potential of concrete that is definable at realistic levels of alkali and temperature representative of actual field conditions.

CHAPTER III

APPROACH TO PROTOCOL DEVELOPMENT

BACKGROUND

As noted in Chapter II, there are some initial conditions related to alkalinity, aggregate reactivity, humidity, and temperature conditions that must be met to initiate alkali-silica reaction (ASR). By a chemical study of the ASR and from a phenomenological point of view of ASR, the basis of a performance-based approach relative to assessment of the potential for ASR is the relationship between key material properties and factors and ASR which may be a function of material combination such as alkalinity, aggregate reactivity, humidity, temperature conditions are accounted relative to their overall contribution to the ASR process. ASR potential varies according to combinations of all these factors.

$$ASR = f\left(A,\ a,\ t,\ T, \mathrm{RH}\right) \tag{3-1}$$

where, A = alkalinity; a = reactivity of aggregate; t = time; T = temperature, and RH = relative humidity

To address an combined approach, the equivalent age concept is subsequently elaborated as it incorporates the moisture and temperature history. An effective test assessment to evaluate ASR potential of aggregate and concrete ideally should account for the inherent variability associated with the primary factors affecting ASR development. The variability of these factors impacts the degree of ASR where probability of its development both explicitly and implicitly becomes a viable component of evaluating if a certain level of expansion due to ASR will or will not occur. The degree of ASR in concrete is related to any one or a combination of its constituents, or even due to reaction between its constituents in terms of combinations of the main constituents. Expansion of concrete is often taken as an indication of ASR damage as a function of certain concrete material properties and the exposure conditions, namely temperature and humidity.

$$\varepsilon_{ASR} = f\left(e,\ C\right) \tag{3-2}$$

where, ε_{ASR} = expansion of concrete due to ASR; e = exposure conditions and C = concrete material characteristics and combinations, and

$$C = f\left(c,\ ca,\ fa,\ w,\ x_1 \cdots x_n,\ soln\ pH\right) \tag{3-3}$$

where, c =cement content; ca = coarse aggregate content; fa = fine aggregate content; w = water; $x_1 \cdots x_n$ = various types of admixture contents; and $soln\ pH$ = pH of pore solution.

AFFECT OF MATERIAL CHARACTERISTICS AND COMBINATIONS ON ASR BEHAVIOR

In terms of ASR factors, Fig. 3-1 shows the effect of temperature and alkalinity on ASR expansion. Because expansion (both rate and total) increases with increasing temperature and alkalinity, it is important to understand how material characteristics and combinations, as well as exposure conditions can be manipulated to control ASR expansion to tolerable levels. Exposure conditions such as temperature and humidity are known to be important factors influencing ASR. Ludwig (1981) studied the effect of humidity and temperature on mortar bars cured for 3 years and found the critical humidity required to prevent damage through ASR to be less than 85 percent At an elevated temperature of 40 ºC, the expansion of mortar bar started earlier but reached lower values at later ages relative to the control bars at 20ºC. Therefore, increasing the temperature at early age increases the rate of chemical reaction occurring between the alkalis and reactive silica in the aggregate and as a result higher expansion takes place during the early life of the concrete, but lower at later age.

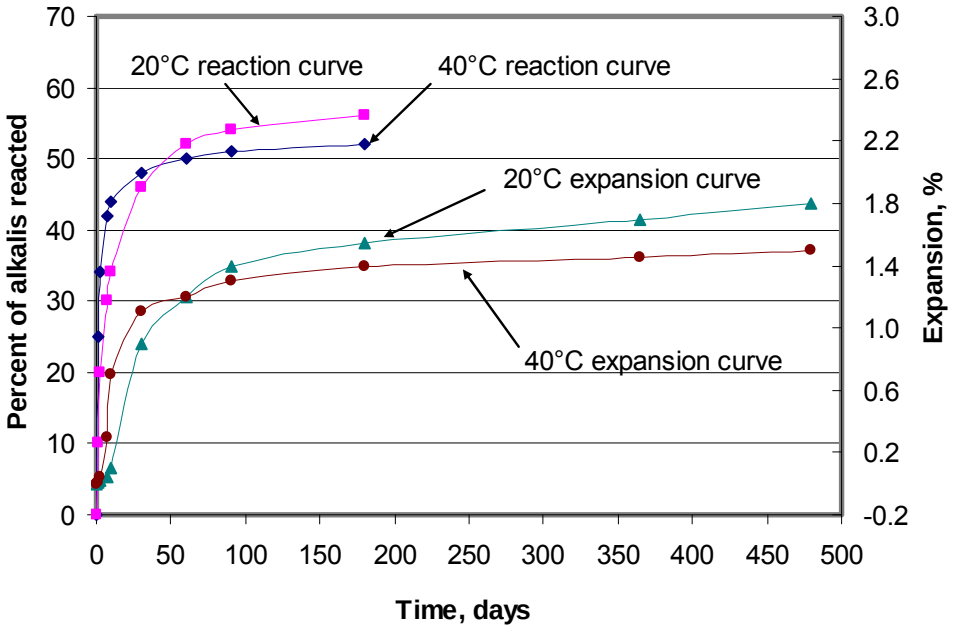

Fig. 3-1. Effect of temperature and alkalinity on ASR expansion (Diamond et al. 1981)

Stanton (1940) and Mindess (2002) found that the expansion due to ASR was dependent on various forms of silica (Table 3-1), amount of reactive silica, and grain size of reactive particles. They reported that the aggregates have different reactivities, depending on the degree of crystallinity, grain size, and the proportion of these reactive phases within the reactive aggregate. This is because of the more disordered the structure the greater the surface area available for reaction. Amorphous, crypto-crystalline, and microcrystalline silica structures are particularly susceptible to ASR.

Hobbs (1988) reported the expansion increases as particle size decreases, which means the particle size of reactive material is also an important age factor (Fig. 3-2). Thus, the greater the fineness the higher the reactivity.

Table 3–1. Forms of Reactive Silica in Rocks that Can Participate in Alkali-Aggregate Reaction (Mindess et al. 2002)

Reactive Component	Physical Form	Rock Type in which it is found	Occurrence
Opal	Amorphous	Opaline limestone (e.g., Spratt limestone), chert, shale, flint	Common as a minor constituent in sedimentary rocks
Silica glass	Amorphous	Volcanic glasses (rhyolite, andesite, dacite) and tuffs; synthetic glasses	Regions of volcanic origin; river gravels originating in volcanic areas; container glass
Chalcedony	Poorly crystallized quartz	Siliceous limestones and sandstones, cherts and flints	Widespread
Cristobalite (tridymite)	Crystalline	Opaline rocks, fired ceramics	uncommon
Quartz	Crystalline	Quartzite, sands, sandstones, many igneous and metamorphic rocks (e.g. granites and schists)	Common, but reactive only if highly strained or microcrystalline

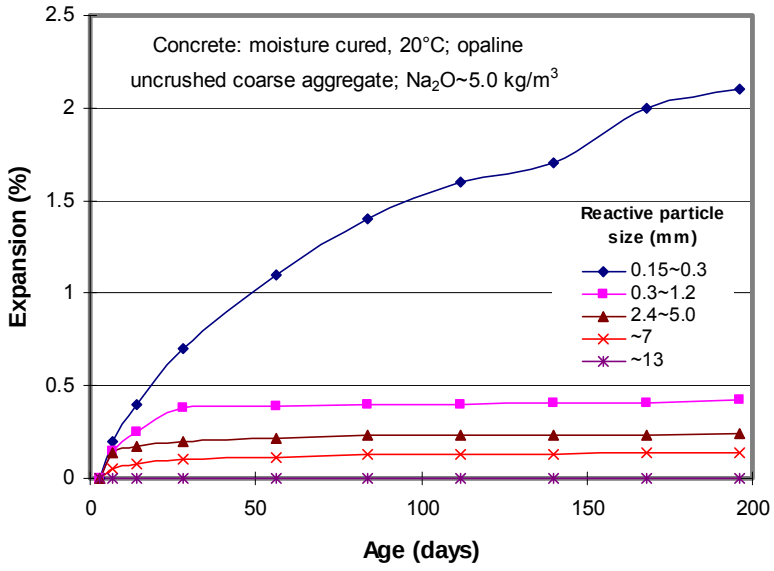

Fig. 3–2. Effect of reactive particle size on the relationship between expansion and age (w/c = 0.41 and aggregate to cement ratio = 0.3)

The dissolution rate and amount of the reactive silica components of aggregate is related to the alkalinity of the pore solution (Fig. 3-3). High pH of concrete pore solution is necessary along with reactive siliceous aggregate for ASR to occur. A reactive aggregate in a low pH solution may not react (or have low potential to react) and can have good field performance. Diamond (1983) and Kelleck et al. (1986) suggests that a threshold concentration required to initiate and sustain ASR is 0.25M (pH=13.4) and 0.2M (pH=13.3), respectively. Therefore, a threshold alkali concentration is a characteristic for each reactive phase below which the reaction does not occur.

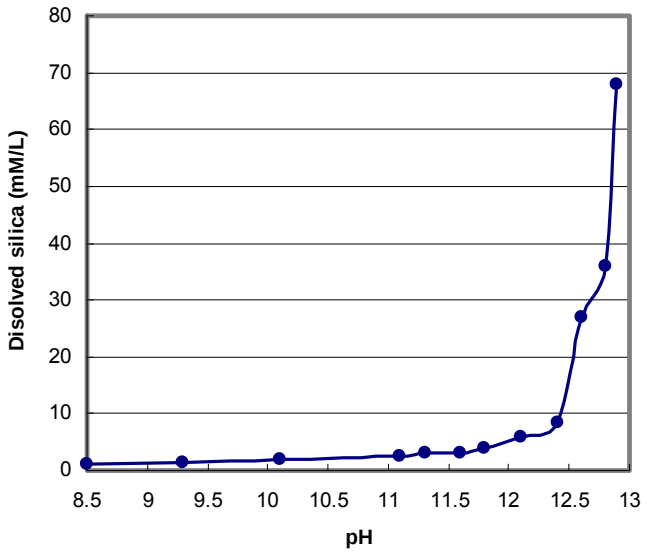

Fig. 3–3. Effect of pH on dissolution of amorphous silica (Folliard et al. 2002)

Hobbs (1988) reported the total alkali content of the concrete on a mass percent volume basis plays an important role in the nature of the reaction products (Fig. 3-4). Concrete containing less than 4 kg/m^3 Na_2O_e was generally resistant to excess expansion. Folliard et al. (2002) from ASTM C 1293 test results stated that the total alkali content below 3.0 kg/m^3 Na_2O_e appears to be the upper criterion of limiting expansion.

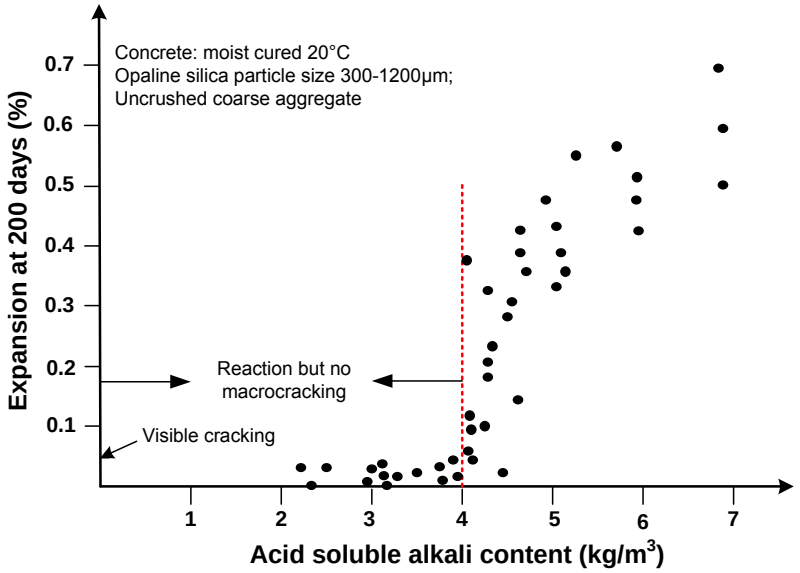

Fig. 3–4. Expansion at 200 days as a function of acid soluble alkali content (Hobbs 1988)

Gaze and Nixon (1983) observed that in the study of the effect of adding mineral admixture, fly ash addition effectively suppressed expansion at cement replacement levels of 20 percent or more on an equal volume basis. However, at a given level of fly ash replacement, the expansion of concrete prisms increased as the calcium or alkali content of the fly ash increased. In general, when a part of the portland cement is replaced by fly ash, reduction in expansion caused by ASR is simply due to the reduction in alkali content, which may result from cement replacement, only when the fly ash itself does not contain water soluble alkali. However, because a number of fly ashes, particularly high calcium fly ashes, may have appreciable amounts of soluble alkalis, there is a danger of increased ASR under some circumstances. A study by Shehata and Thomas (2000) demonstrated that the alkali content of some fly ashes was higher than that of the cement replaced. Consequently, key ASR factors and their characteristics to affect ASR are summarized in Table 3-2.

Table 3–2. Key ASR Factors and Characteristics

Categories	Factors	Properties/Characteristics
Mixture proportions	Amount of water, amount of aggregate, cement and fly ash content, $Na_2O_{equivalent}$, fly ash CaO and alkali contents, mitigating admixtures (e.g., $LiNO_3$)	w/cm, concrete porosity, total concrete $Na_2O_{equivalent}$, fly ash amount and CaO content, dosage rates of mitigating admixtures, ionic diffusion rate, ultimate and rate of expansion
Aggregate reactivity	Type, size, form, degree of crystallinity and amount of eactive silica; internal porosity and crystal strain; dissolution rate	Aggregate reactivity, ultimate expansion
Exposure conditions	Temperature, humidity	Concrete equivalent age

DEVELOPMENT OF PERFORMANCE-BASED MODEL TO ASSESS ASR

As previously mentioned, the basic approach to understanding ASR is to establish how material combinations affect ASR behavior. If expansion of concrete is taken as the primary evidence of ASR damage, it is presumed that this improved understanding will be achieved via establishment of how the expansion of the concrete is a function of concrete material properties and external factors such as the exposure conditions in terms of temperature and humidity. As previously noted, ASR is a chemical reaction that integrates the combined effects of temperature, alkalinity, and time relative to the kinetics of ASR expansion

The protocol developed herein uses the expansion history produced by the dilatometer method. Because, as previously stated, the development of ASR is a thermally activated process that is also sensitive to a given level of alkalinity and the size of the aggregate, the proposed approach is capable of providing direct accountability for a variety of important material related factors that affect ASR behavior of concrete such as temperature, alkalinity, aggregate reactivity, humidity, and age. These parameters are encompassed within a kinetic-type performance model (equation 3-4) that is the proposed primary tool to characterize ASR.

$$\varepsilon = \lambda \cdot \varepsilon_0 \cdot e^{-\left(\frac{\alpha}{t_e}\right)^{\beta}} \quad (3\text{-}4)$$

where, $\varepsilon =$ ASR expansion of concrete; $\lambda =$ SCMs adjustment factor; $\varepsilon_0 =$ ultimate ASR expansion of concrete; α and $\beta =$ concrete parameters representing a combined effects of mixture related parameters such as w/cm and/or porosity, diffusion, permeability matching with testing temperature/alkalinity and ultimately related to the rate of expansion; and $t_e =$ equivalent age.

The determination of the ASR model parameters is accomplished through a series of steps. All aggregate and concrete parameters are tabulated for mitigation of ASR in concrete. They will be used to mixture design which leads to formulate a ASR-resistant mixture using job specific aggregate for new concrete or selecting proper combination of mitigating techniques for old concrete.

- Step 1. Determination of aggregate parameters such as apparent activation energy (E_a) and ultimate expansion of aggregate ($\varepsilon_{aggr.}$) as a function of alkalinity and aggregate size
- Step 2. Calculation of equivalent age using Ea and concrete expansion data over time
- Step 3. Determination of concrete parameters (α, β, and ε_0) as a function of w/cm, temperature, alkalinity, and SCMs' content.

Determination of Aggregate Parameters

In general chemistry, the activation energy (E_a) is related to rate theory as depicted by the Arrhenius function. The Arrhenius function is based on the law of acceleration due to a series of chemical reactions that integrate the coupled effect of temperature and time into a single parameter under different conditions. For instance, Fig. 3-5 shows a general reaction coordinate diagram relating the energy of a system to its geometry along one possible reaction pathway.

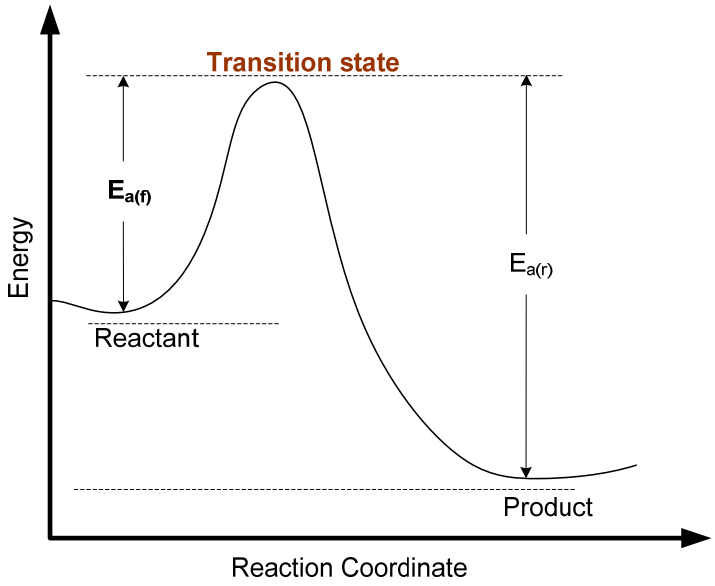

Fig. 3−5. Reaction coordinate diagram

The E_a is the critical minimum energy in a chemical reaction required by reactants to be converted into products. $E_{a(f)}$ or $E_{a(r)}$ are the activation energies for forward and reverse reactions, respectively. The transition state is that point on the energy curve where the activated process passes from reactants to products.

Because the ASR is a thermally activated process that is also phenomenologically sensitive to a given level of alkalinity (Saouma and Perotti 2006), the concept of E_a can serve as a characteristic fundamental reactivity term for performance analysis purposes. E_a relative to ASR can be defined as the energy needed to start ASR as well as serve as a key parameter to characterize the susceptibility of the aggregate to ASR perhaps as a function of alkalinity and size of aggregate. The test for E_a can be conducted on both coarse and fine aggregates and with different levels of test solution alkalinities (e.g., 1N, 0.5N, 0.25N etc.). Testing with different levels of exposed aggregate surface areas (i.e., coarse and fine aggregate) and soak solution alkalinities will allow establishing a relationship between the E_a and the ratio of alkalinity to the size of aggregate. The established relationship will allow adjustment to the E_a based on aggregate size and the level of alkalinity which the concrete is likely to be exposed to under field conditions. Therefore, in the proposed E_a

approach it should be possible to integrate the combined effects of temperature, alkalinity, and time relative to the kinetics of ASR expansion into a single parameter to characterize ASR expansion of concrete.

However, its application to the case of ASR is an approximation because the ASR of the different reactive components of aggregate corresponds to several simultaneous and inter-dependent chemical reactions. Thus, the E_a in ASR is defined as apparent activation energy. This parameter which characterizes aggregate reactivity is the only one which can be found in the expression of equivalent age, and has to be experimentally determined.

The determination of the ASR activation energy of aggregate is accomplished through a series of steps. First, the reaction rate parameter (K_T) and ultimate expansion of aggregate (ε_a) are determined. The expansion over time produced by the reaction products when an aggregate reacts with alkalis is measured by the dilatometer device. The K_T and ε_a are nominally determined from the measured expansion–time relationship at three different temperatures and at a given level of alkalinity using the following empirical equation (Carino and Lew 2001):

$$\varepsilon = \varepsilon_a \frac{K_T(t - t_0)}{1 + K_T(t - t_0)} \tag{3-5}$$

where, ε = expansion; ε_a = ultimate expansion of the aggregate; K_T = reaction rate parameter at temperature T ; t = actual reactive age at temperature T (day); and t_0 = theoretical initial reaction time (day)

Transforming equation (3-5) into a linear format, K_T and ε_a can be evaluated by using $1/\varepsilon$ vs $1/(t - t_0)$.

$$\frac{1}{\varepsilon} = \frac{1}{\varepsilon_a} + \frac{1}{\varepsilon_a K_T (t - t_0)} \tag{3-6}$$

A linear regression analysis is shown in Fig. 3-6. The trend line is used to evaluate K_T and the inverse of the intercept value is the ultimate expansion of aggregate. The E_a is related to the slope of the linear regression between the natural log of the reaction rate parameter and the inverse of temperature $(1/T)$ (Fig. 3-7). The negative slope of the straight line is equal to the activation energy divided by the gas constant (Fig. 3-7).

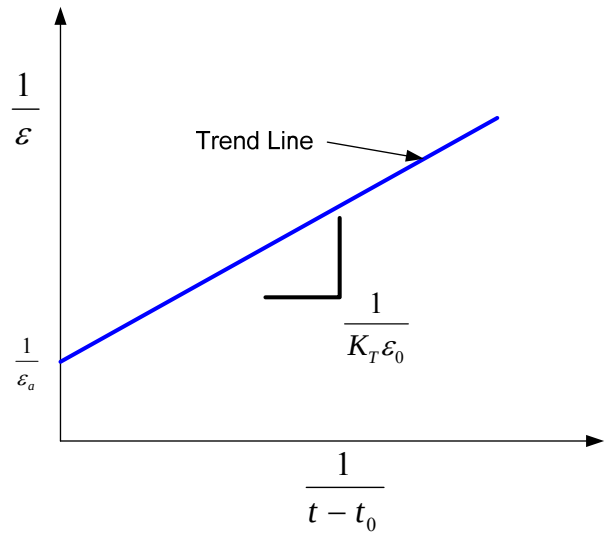

Fig. 3−6. Reciprocal of expansion versus reciprocal of age

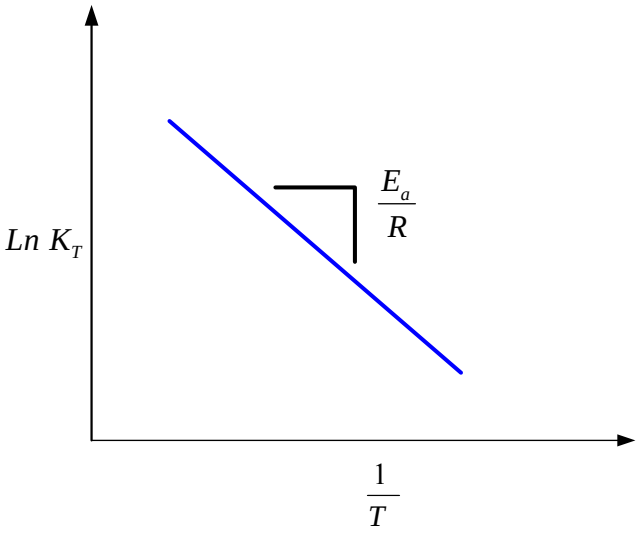

Fig. 3−7. Plot for determining the value of activation energy

Calculation of Equivalent Age

The E_a determined from aggregate parameter study is used to calculate the equivalent age (t_e) in equation (3-7) requiring that the concrete temperature, age, and moisture information be available.

$$t_e = \gamma_H \cdot \sum_0^t e^{-\frac{E_a}{R}\left(\frac{1}{273+T}-\frac{1}{273+T_r}\right)} \cdot \Delta t \qquad (3\text{-}7)$$

where, $\gamma_H =$ relative humidity factor; $E_a =$ apparent ASR activation energy; $R =$ universal gas constant, 8.314 J/mol·K; $T =$ testing temperature (ºC); $T_r =$ reference temperature (°C), and $\Delta t =$ time.

The term t_e is used to account for the combined effect of time and temperature on ASR expansion development at a reference temperature and a given alkalinity of test solution. The t_e is the integral in time of the ratio between the rates of reaction k_1 and k_r of two specimens of the same concrete specimen shown in Fig. 3-8. One is a fictitious specimen and is assumed to be kept t a constant temperature T_r, generally 23 °C. The other specimen is real and has a temperature profile $T_1 = T_1(t)$. At every time t*, the real specimen has an equivalent age $t_{e,1}$ (t*). This means that at the time t*, it has the same degree of reaction that the reference process will have after a total time $t_{e,r}$ (t*), being tested at $T=T_r$. Where time is converted in equivalent age, the temperature of the process assumes the value $T=T_r$. In other words, it is indicates that the rate of ASR at testing temperature T_1 is a certain times that at the reference temperature T_r. For example, if E_a is 37.5 KJ/mol, the reference temperature is 23 °C, and γ_H is assumed to 1, the rate of expansion at temperature 80 °C is 11.70 times that at 23 °C. A given aggregate tested at 80 °C for 1 day has the same degree of reaction (expansion) as that tested at 23 °C for 11.70 day. The equivalent age is of great interest for predictions because it not only allows direct comparisons of concrete specimens that are being ASR at different speed, but also takes into account the so-called cross over effect of concrete with other degree of reaction over temperature.

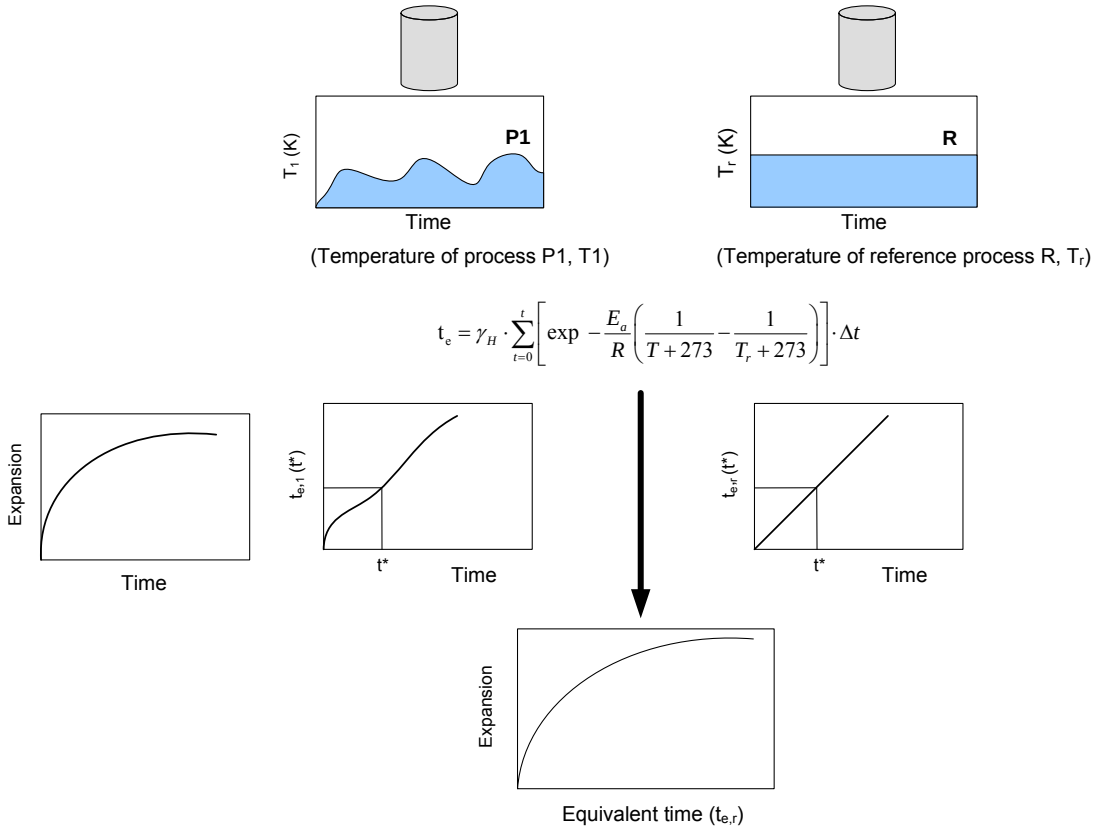

Fig. 3−8. Concept of equivalent age

Determination of Concrete Parameters

The main purpose of the performance-based model (equation (3-4)) is to predict the ASR expansion behavior for new concrete or the residual expansion of ASR affected concrete. "What if" scenarios based on the performance relationship are useful in formulating an ASR-resistant mixture for job specific aggregate and materials combinations or combination of mitigating techniques for old concrete. To this end, further characterization and determination of the α, β, and λ terms are based upon expansion testing of the corresponding concretes using the dilatometer. The parameters α and β in equation (3-4) are anticipated to be mixture specific and ultimately formulated as material models to represent the effect of the w/c, the degree of hydration, or other physical aspects of the mixture on ASR. By taking the double natural logarithm, equation (3-4) can be transformed into the following linearized form:

$$Ln\left[-Ln\left(\frac{\varepsilon}{\varepsilon_0 \cdot \lambda}\right)\right] = \beta Ln\alpha - \beta Lnt_e \qquad (3\text{-}8)$$

α and β can be derived from the slope and intercept/slope of the regressed line in the form of equation (3-8) (as illustrated in Fig. 3-9) provided the ultimate expansion (ε_0) of concrete is known. Therefore, α and β become dependent variables. The ε_0 can be predicted based on minimizing the difference between measured and calculated concrete expansion. In order to adjust or compensate for the errors in prediction, the concept of the sum of the squared errors (SSE) is used. The minimum value of SSE represents the best value of the ε_0:

$$SSE_{\text{min.}} = \sum\left(\varepsilon_m - \varepsilon_c\right)^2 \qquad (3\text{-}9)$$

where, $SSE_{\text{min.}}$ = minimum sum of the squared errors; ε_m = measured concrete expansion; and ε_c = calculated concrete expansion.

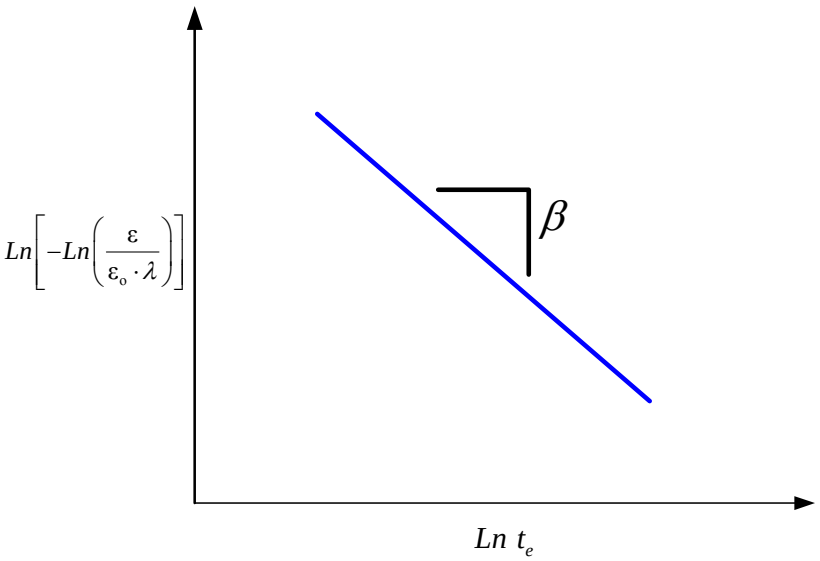

Fig. 3–9. Plot for determining concrete parameters (α and β)

The λ term in equation (3-4) is equal to 1 unless it is used to represent the effect of SCMs on ASR behavior. Equation (3-4) provides a relationship between fundamental material characteristics of a concrete mixture and the ASR expansion characteristics. Consequently, it is feasible that the parameters of equation (3-4) (α, β, and λ) be determined as a function of the mixture design relative to the prediction of performance of concrete using known values of E_a adjusted for the level of alkalinity expected under field conditions.

CHAPTER IV

MATERIALS AND EXPERIMENTAL DETAILS

Designing an experimental program with a science approach is a means to incorporate the performance concepts in a new protocol to assess ASR potential of aggregate and concrete and to improve the understanding of key properties of materials in the ASR mechanism. For the study to be sufficiently broad, several design variables such as aggregate reactivity and particle size are considered for application of the performance-based testing protocol. This chapter presents materials, experimental details, and information on the characteristics and properties of the materials used in this research. Also presented are the details of a testing device and test procedure related to sample preparation and calculation of expansion.

EXPERIMENTAL DESIGNS

This study seeks to develop the performance-based testing protocol to evaluate ASR potential of aggregate and concrete using dilatometer method. The aim of this study is accomplished through three main experimental series:

- Series I: Determination of aggregate parameters (E_a and ε_a)
- Series II: Determination of concrete parameters (α, β, and ε_0)
- Series III: Assessment of the proposed performance-based model (Comparison of concrete and aggregate parameters between dilatometer and C 1260/C 1293 methods)

Each experimental program contributes to the achievement of the different objectives in order to investigate the utility of a performance-based testing protocol. Series I focuses on the use of dilatometer to measure ASR potential of minerals and aggregate as a function of key indicators such as reactivity of constituent minerals with respect to their crystallinities. The ASR reactivity of mineral and aggregates is characterized with the evolution of activation energy of ASR on the basis of the kinetic approach.

Series II is to formulate a frame work for a performance-based testing protocol by combining the laboratory measured material properties and exposure conditions for determining concrete parameters α, β, and ε_0. A series of expansion measurements using the dilatometer were performed on concrete of a specific concrete mixture.

Series III addresses whether the performance-based ASR expansion model can be applied to improve interpretation of the ASR over what could be gained through ASTM C 1260 and C 1293 test method. Consequently, Table 4-1 and Fig. 4-1 list testing factors and test conditions for three main experimental series.

Table 4−1. Experimental Programs of the Dissertation

Experimental Series	Test method	Evaluation items	Testing factor	Materials	Test condition
Series I	Dilatometer	Aggregate reactivity	E_a	4 minerals 3 aggregates	60, 70, 80 °C 1N NaOH
Series II	Dilatometer	Combined material test	Effect of normality of NaOH	Gravel	0.5N & 1N NaOH
				Rhyolite	0.25, 0.5, & 1N NaOH
			Effect of $LiNO_3$	Gravel	0.25, 0.5, & 0.75M $LiNO_3$
			Effect of calcium	Rhyolite	[NaOH+$Ca(OH)_2$] solution
		Concrete parameters	α, β, ε_0	Gravel	0.5N & 1N NaOH 80 °C
				Rhyolite	0.5N & 1N NaOH 80 °C
Series III	ASTM C 1293	Concrete parameters	α, β, ε_0	Gravel	38 °C W/ alkalis
				Rhyolite	38 °C W/ or w/o alkalis
	ASTM C 1260			Gravel	80 °C / 1N NaOH
				Rhyolite	80 °C / 1N NaOH
	ASTM C 1260	Aggregate reactivity	E_a	Rhyolite	60, 70, 80 °C 0.5N & 1N NaOH

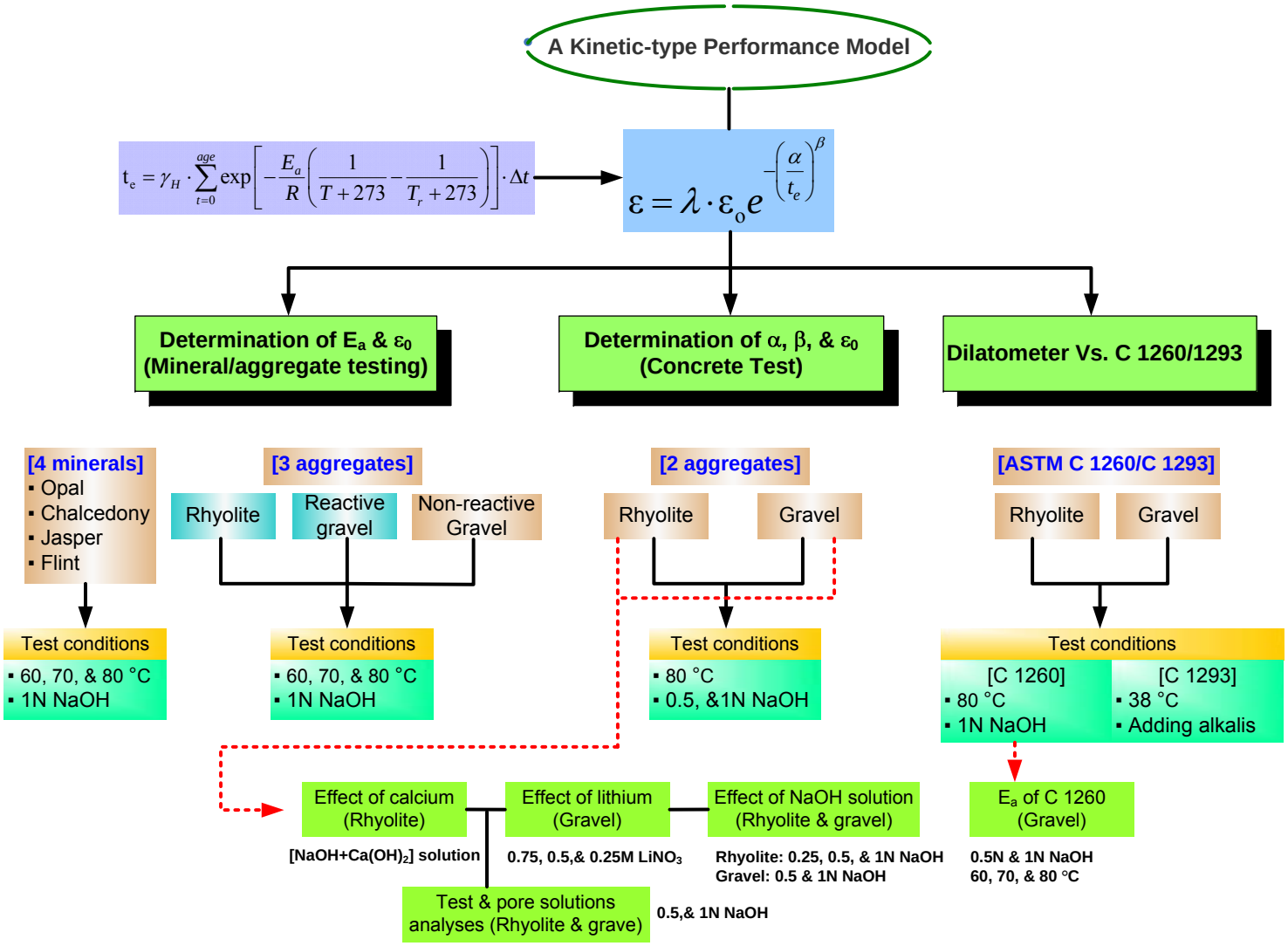

Fig. 4–1. Experimental programs of the dissertation

MATERIALS

The materials selected for this study include four aggregates with different reactivities, ASTM Type I cement, and Class F fly ash. An understanding of material properties and behavior is important in order to assess ASR potential of aggregate and concrete based on the performance approach. The details of characteristics of aggregate and cementitious materials are described below.

Aggregate Properties

For series I to determine aggregate parameters, samples of different forms of reactive silica minerals, namely pure opal, chalcedony, jasper, flint along with non-reactive gravel sand, siliceous reactive coarse gravel, and New Mexico rhyolite (rhyolite) aggregates were used. Mineral samples, which were in an as-received produced, had different particle size distribution (PSD) (Fig. 4-2). Fig. 4-2 shows the PSD of minerals and aggregates used in this study. The NM rhyolite shows relatively finer PSD than that of the tested minerals.

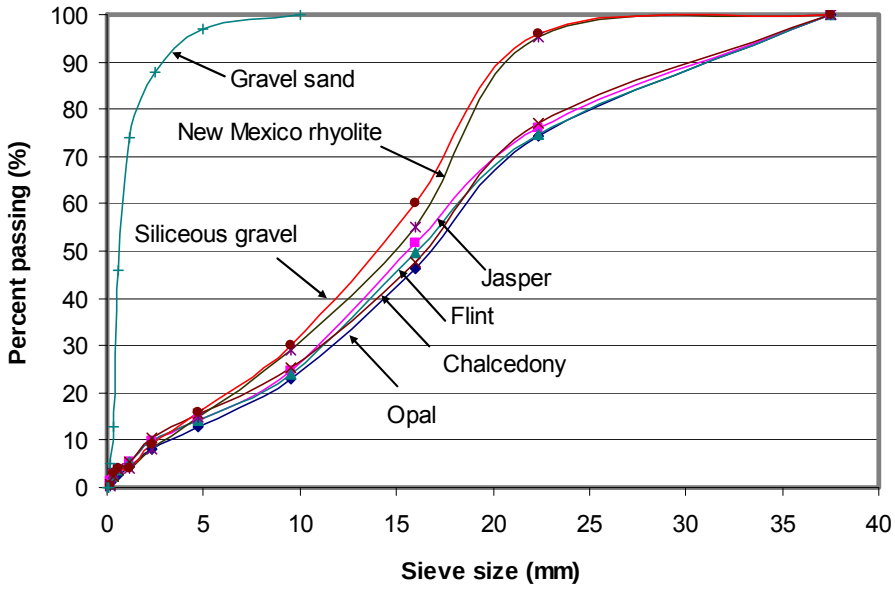

Fig. 4–2. Particle size distribution of minerals and aggregates

In general, the reactivity increases as the size of mineral or aggregate decreases. Increasing aggregate surface area by crushing is a common practice in some existing test

methods (e.g., ASTM C 289, C 441, and C 1260) in order to accelerate the reaction. The reactivity of an aggregate in a crushed condition has a higher specific surface may not represent the reactivity under field conditions. Thus, in order to avoid this problem, aggregates were tested in uncrushed conditions (an as-received condition). However, the amount of passing on each selected sieve was kept constant for all the tested minerals and aggregates to make the PSD a common denominator. The PSD of rhyolite was selected to the target PSD. This allowed for the comparison of the activation energy of different forms of silica minerals and to categorize them based on their reactivity. Additionally, non-reactive gravel sand used to cast concrete specimen was also tested in the dilatomter and its activation energy was calculated.

For Series II, the same aggregates used at Series I experimental program were selected to cast concrete. These aggregates had previously been classified as reactive according to ASTM C 1260 test method using cement with 0.44% Na_2O_e. Reactive gravel aggregate had an expansion of 0.24 percent at 14 days, while the expansion of the non-reactive gravel was 0.08 percent at 14 days. The rhyolite was 1.31 percent at 14 days. The reactive gravel contains a strained quartz which is reactive whereas a glassy (acid volcanic) material is the reactive constituent in NM rhyolite (Fig. 4-3). The non-reactive aggregate was used as a fine aggregate to cast the concrete. Again, Fig. 4-3 shows the particle size distribution (PSD) of the aggregates used in Series II.

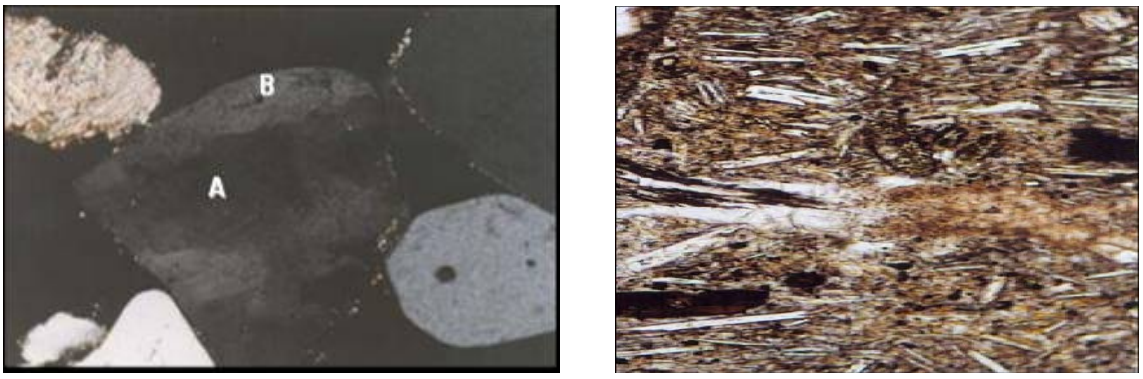

(a) Gravel (reactive strained quartz) (b) New Mexico Rhyolite

Fig. 4−3. Photomicrographs of the tested aggregates

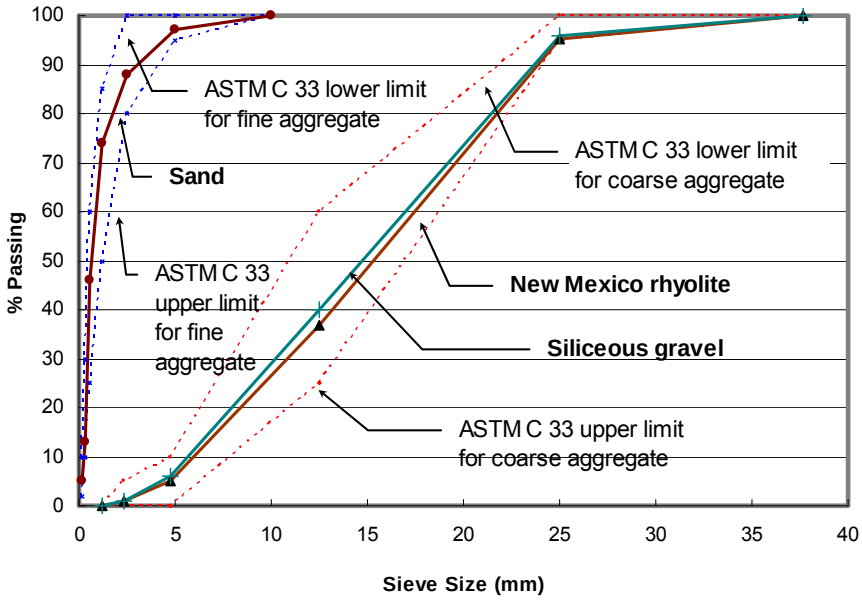

Fig. 4−4. Particle size distribution of the tested aggregates

Series III addresses whether the performance-based ASR expansion model proposed in Chapter III can be applied to improve interpretation of the alkali-silica reaction over what could be gained through ASTM C 1260 and C 1293 test method. The same gravel and rhyolite aggregates used in Series II were also used in this series where their chemical properties are presented in Table 4-2. The mineralogy and petrographic examinations were established from qualitative x-ray diffraction (XRD) analysis and ASTM C 295 method, respectively. Quartz was identified as the principal mineral in the gravel with small amounts of calcite, microcline feldspar and other silicate minerals in both aggregates whereas the rhyolite aggregate includes quartz, feldspar, mica, and amphibole. These coincided with the chemical analyses that indicated the SiO_2 was over 90% in gravel and higher contents of Na_2O and K_2O were found in the rhyolite aggregate.

ASTM C 289 testing was also carried out on the aggregates to determine which elements and what extent were involved in the deleterious reaction. From Fig. 4-4, one aggregate source had been classified as reactive and the other had been classified as non reactive although chemical analyses of aggregates (Table 4-2) show very little difference in

composition. It can be clearly seen that both reactive gravel and rhyolite aggregates were within reactive C 289 criteria, indicating the high sensitivity to alkalis.

Table 4–2. Chemical Analyses of Aggregates

Components	Aggregate Type		
	Non-reactive gravel	Reactive gravel	Rhyolite
SiO_2	93.15	95.67	70.13
Al_2O_3	0.33	0.37	12.05
Fe_2O_3	0.42	0.68	10.12
CaO	2.46	1.98	3.01
MgO	0.08	0.12	0.01
Na_2O	1.40	0.64	1.70
K_2O	0.23	0.22	2.90
TiO_2	0.05	0.04	0.01
MnO_2	0.02	0.04	0.01
SO_3	0.06	0.03	0.03

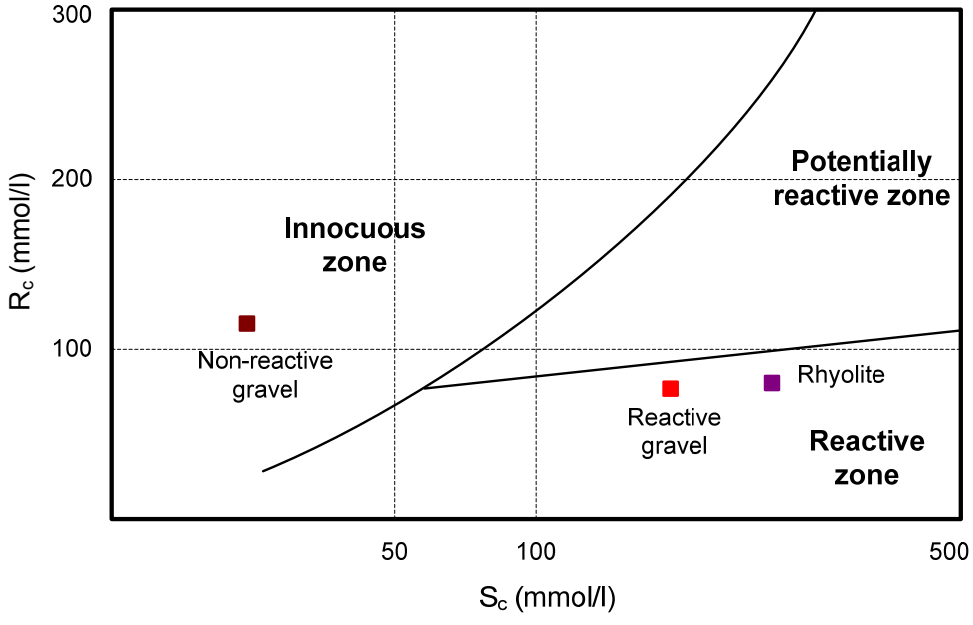

Fig. 4–5. ASTM C 289 chemical test results

Cement Properties

Cementitious materials used in this study were ASTM Type I portland cement.. The physical properties and chemical analysis of the cement are presented in Tables 4-3 and 4-4.

Table 4–3. Physical Properties of Cement

Physical tests	Cement
Fineness, m^2/kg	358
Specific gravity	3.11
Vicat setting time (min.)	
Not less than	103
Not more than	160
Compressive strength (MPa)	
3-day	28.20
28-day	47.80
Autoclave expansion (%)	0.08

Table 4–4. Chemical Analyses of Cement

Chemical analysis	Cement
SiO_2	19.12
Al_2O_3	5.07
Fe_2O_3	1.80
CaO	64.73
MgO	1.43
Na_2O	-
K_2O	-
TiO_2	-
MnO_2	-
SO_3	3.17
[a]Na_2O_e	0.64
Loss on ignition, %	0.90

[a]Available alkali, expressed as $Na_2O_{equivalent}$, as per ASTM C 150.

TEST DEVICE

The apparatus, referred to as the dilatometer is developed to measure actual volume expansion of the ASR gel formed when an aggregate or concrete reacts with alkalis over time and temperature. The cross-sectional diagram of the dilatometer is shown in Fig. 4-5. Briefly, the dilatometer consists of a stainless steel cylindrical container, a lid, a hollow tower standing on the lid, and a float. The container is capable of holding a reasonable amount of as-received aggregate samples and accommodating aggregates with size as large as 75 mm. Furthermore, mortar/concrete cores or cylindrical specimens (101.6 mm diameter x 139.7 mm height) can also be tested in the container. The container is filled with the testing materials and a test solution (typically NaOH solution).

A tower is attached to the lid of the container to install a linear variable differential transducer (LVDT). The inner surface of the lid is configured at a 15 degree angle so that the entrapped air bubbles trapped from between the aggregate particles during vacuum process can move readily along the surface. On the side of the tower, there are three access holes with three screws. When the dilatometer is in use, the aggregate sample and NaOH solution are placed in the container. These screws are used to adjust the initial NaOH solution surface level to the desired height. If highly reactive aggregate is used in the test, the initial solution level should be placed at the lowest position so that it has enough room for large expansion.

The float moves freely along with the NaOH solution surface in the tower. The core of the LVDT is connected to the float to measure the rise of the NaOH solution surface. Electrical signals from the LVDT are generated as the core moves. The signals are acquired and amplified by a signal conditioner and then recorded with a computer data acquisition system. The LVDT used is SCHAEVITZ Model 1000 HCA, which provides a displacement of 50.8 mm (± 25.4 mm). This provides a sufficiently high accuracy (it can measure 0.021mm) in the measurement of a certain volume change in the small area of the NaOH solution surface in the tower. A thermocouple is immersed in the NaOH solution to monitor the test temperature inside the container. The temperature is recorded along with the LVDT signal by the same computer data acquisition system.

In operation, after the container is filled with the material to be tested for ASR related expansion, the lid is closed and the device is immersed in a water bath. The

temperature of the water bath is raised to the desired temperature thus raising the temperature of the aggregate and solution. As ASR commences inside the dilatometer, expansive ASR gel is produced, and then the related expansion due to ASR gel formation is measured. As a result, the float in the tower rises, which is continuously recorded over the testing period. The test period is relatively short, and can be completed within 2 to 3 days, or less..

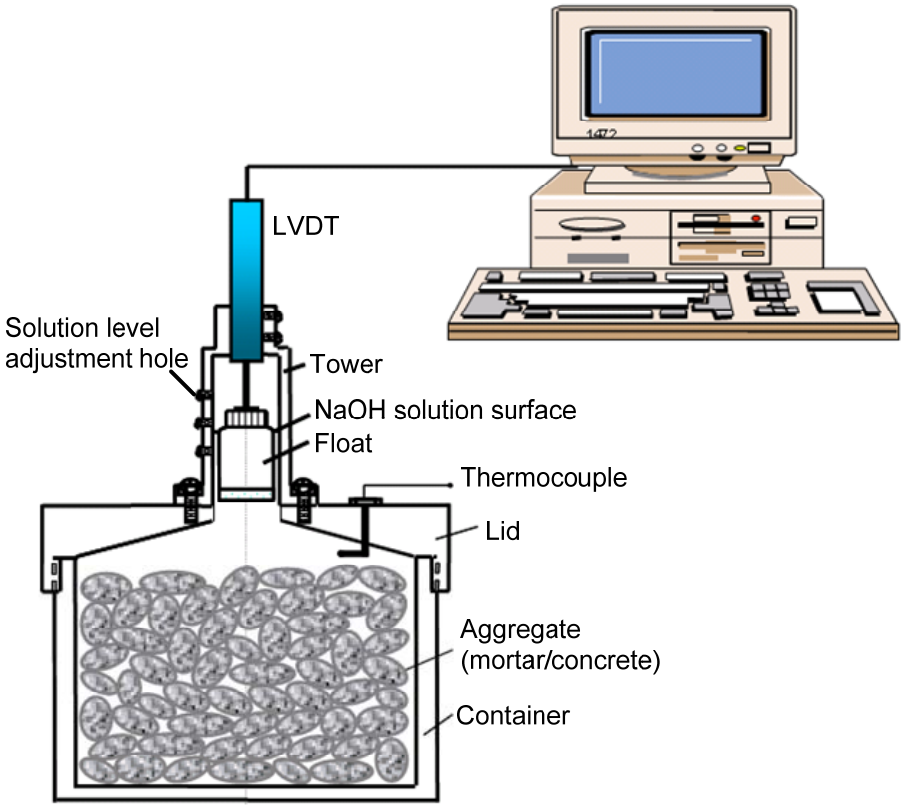

Fig. 4–6. Cross-section of the testing apparatus

TEST PROCEDURE

This section describes the preparation of the test solution and specimens relative to the testing procedure for the dilatometer as a part of developing performance-based testing protocol. Additionally, this section explains test procedure of modified ASTM C 1260 and

C 1293 tests used in evaluating the suitability of the new performance-based model to improve interpretation of ASR as well as comparing the concrete parameters from the new test method to those from these methods.

Preparation of Test Solution

The test solution is prepared from 40 g of sodium hydroxide (NaOH) dissolved in 900 mL of water diluted with additional distilled water to obtain 1.0 L of solution. A 1.0 ± 0.01N NaOH solution is prepared and standardized to ± 0.001N. Similarly, 0.5N and 0.25N NaOH solutions are also prepared.

[$LiNO_3$ + NaOH] solutions with different lithium nitrate ($LiNO_3$) dosages, namely 0.75, 0.5, and 0.25 $NiNO_3$, were also prepared to investigate the effect of $LiNO_3$ for reducing expansion due to ASR. The dosage of $LiNO_3$ was calculated according to molarity (M), which is number of solute per a given volume of total solution.

Finally, in order to investigate the effect of calcium hydroxide [$Ca(OH)_2$] on ASR expansion behavior, 1N NaOH solution containing fully saturated $Ca(OH)_2$ was used.

Preparation of Specimen for Dilatometer Test

Basically, the dilatometer measures the volume expansion from the amount of expansive ASR gel produced. As-received aggregate and concrete samples can be tested, without extraneous size effect associated with the aggregate that are common in the other test methods; some test methods even require the aggregate to be ground into fine particles which introduces wider variability into the test results. For aggregate testing, aggregate samples were tested directly; 80 percent of aggregate (by volume) out of the total volume of the cylindrical container is filled. The details of sample preparation are listed in Appendix B.

However, for concrete testing, a special mold is used to accelerate the test. A 4-inch diameter cylinder with a 1-inch diameter center hole (to increase the exposed surface area) was cast (Fig. 4-6). The mixture proportions are presented in Table 4-4. After 24 hours of curing, the specimen was demolded and placed in a moist-curing room at 23 ± 2ºC. After 7 days of curing, the apparent specific gravity of specimen was measured to

determine initial volume of concrete before testing. The concrete specimen was tested with the same way as aggregate testing and the test was terminated after 7 days.

Table 4−4. Concrete Mixture Proportions for Dilatometer Test

Mixture	w/cm	Unit weight (kg/m^3)				
		Water	Cement	Fly ash	Fine aggregate	Coarse aggregate
Gravel concrete	0.48	133.8	278.9	-	708.3	1150.5
Rhyolite concrete	0.48	133.8	278.9	-	742.2	1147.8

Coarse aggregate factor (CAF) = 0.7

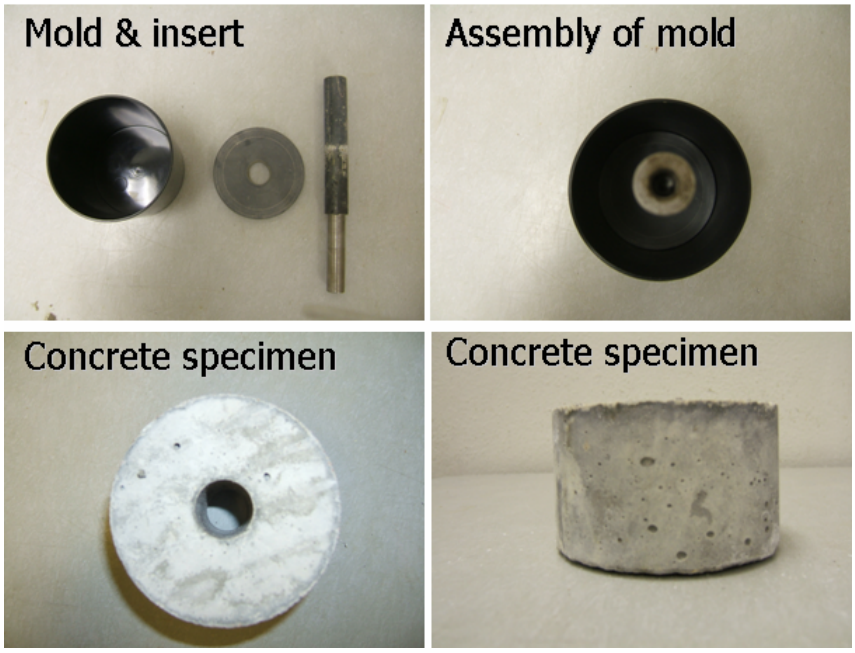

Fig. 4−7. Concrete specimens cast with special mold

Dilatometer Test Procedure

Aggregates are placed in the container in a dry condition, and then NaOH solution is added in the container at room temperature. The aggregates are soaked in NaOH solution for at least 1-day before starting actual test (Fig. 4-7) to make a fully saturated condition to accelerate test. The lid is securely screwed to seal the container. A vacuum is applied for a period of time (approx. 45 min.) to remove entrapped air between aggregate particles. The

container is also shaken periodically to facilitate removal of entrapped air (Fig. 4-8). After vacuuming, the dilatometer is placed in a water bath in which the water temperature is first equilibrated to room temperature. Then the tower access port is opened to drain any excess solution, the LVDT is positioned in the tower with its core connected to the float to measure the rise of the test solution surface. If necessary, more test solution is added in the cavity of the tower until the float is positioned properly.

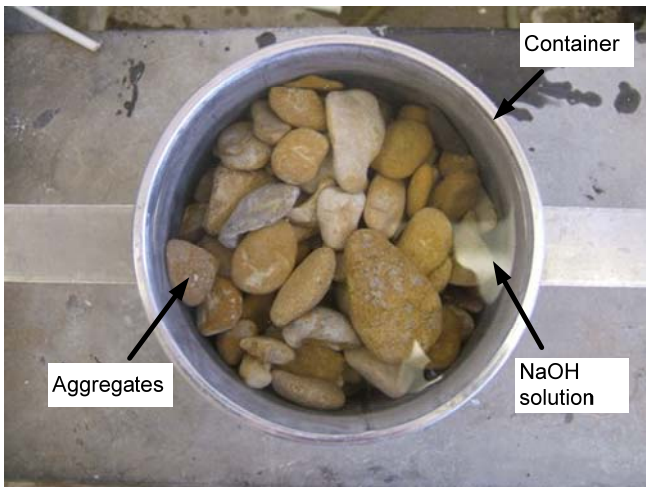

Fig. 4−8. Filled aggregates and NaOH solution in the container at room temperature

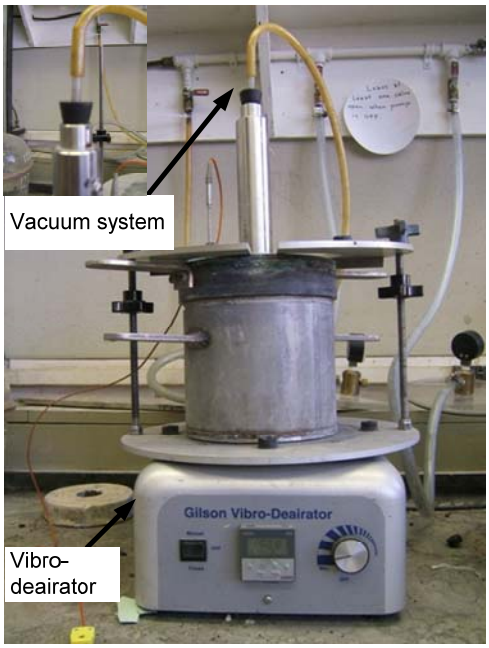

Fig. 4−9. A vacuum to remove entrapped air between aggregate particles

The water bath is heated to the desired temperature (60 °C, 70 °C, or 80 °C), where it is held constant. As ASR expansion of the aggregate inside the specimen container begins, the float rises and electrical signals from the LVDT are generated. The signals are acquired and amplified by a signal conditioner and then recorded by a computerized data acquisition system. A thermocouple is installed inside the dilatometer to monitor temperature inside the container. The data acquisition system records the temperature and LVDT readings simultaneously (Fig. 4-9).

The volume of aggregates used and test solution are kept constant for each test. The test is terminated typically after 2 or 3 days. However, it can be conducted for shorter or longer periods until sufficient data are obtained to define the expansion characteristics. The details of test procedure are listed in Appendix C.

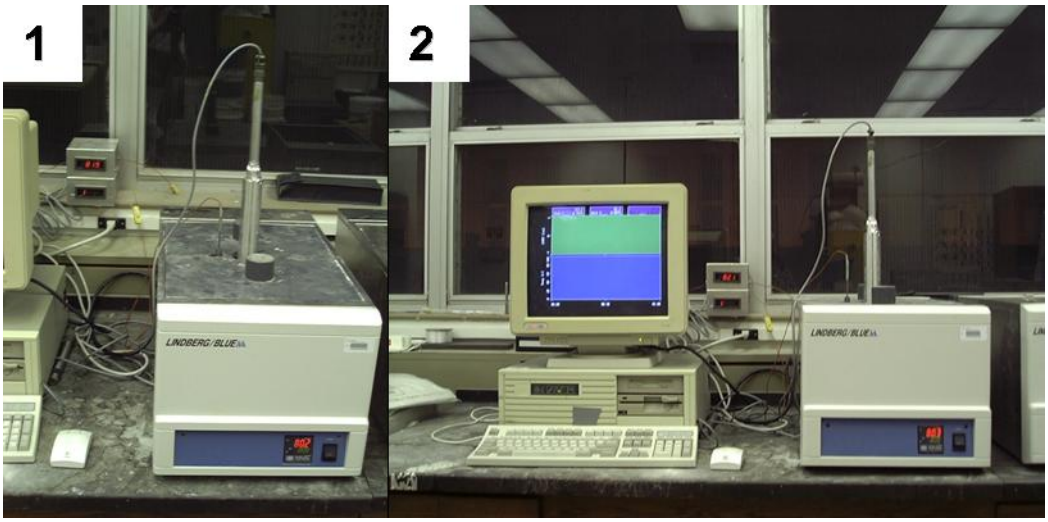

Fig. 4−10. Setup of dilatometer system

Preparation of Specimen for ASTM C 1260 and C 1293 Tests

Because the objective of Series III is to apply a performance-based model to C 1260 and C 1293 expansion data to improve interpretation of the ASR using C 1260 and C 1293 test results as well as evaluate the suitability of model in current test method, mortar and concrete specimens were prepared in accordance with the C 1260 and the C 1293 mix

design guideline, respectively. Two plain cement mortar mixtures were made. Both mixtures were prepared at a ratio of water to cementitious material (w/cm) of 0.48. In case of the concrete mixture, sodium hydroxide (NaOH) was added to increase the alkalinity of the cement from 0.64% Na_2O_e. to 1.25 Na_2O_e. This additional alkali increased the total alkali content of the concrete to 3.49 kg/m^3. The mixture proportions are presented in Table 4-5.

Table 4−5. Mixture Proportions of Mortar and Concrete for C 1260 and C 1293

Mixture	W/CM	kg/m^3					
		Water	Cement	Class F fly ash	*Fine aggr.	*Coarse aggr.	NaOH
Gravel mortar	0.48	133.8	278.9	-	1867.5	-	-
Rhyolite mortar	0.48	133.8	278.9	-	1920.5	-	-
Gravel concrete	0.48	133.8	278.9	-	708.3	1150.5	2.20
Rhyolite concrete	0.48	133.8	278.9	-	742.2	1147.8	2.20

*Fine and coarse aggregates.

Test Procedure of Modified ASTM C 1260 and C 1293 Tests

Nine mortar bars, each 25 x 25 x 275mm in size, were cast. After casting, the test specimens were kept immediately in a moist room and retained in the molds for 24 hours. On the next day, they were demolded, identified properly and an initial reading is taken with a vertical length comparator instrument, as per ASTM C 490. To maintain consistency of readings, the same end of the specimens was kept up each time. After tabulating the readings, the specimens were immersed in water in a sealed container, which was placed in an oven kept at constant temperatures of 60 °C, 70 °C, and 80 °C. Selection of the three temperatures was arbitrary. It is pointed out that the prisms were kept in water at room temperature for 2 to 3 hours and then the container was introduced in the oven at three different temperatures. This is to avoid initial thermal shock to the prisms. After 24 hours in the oven, the prisms were taken to a room, which have ambient temperature (23 °C ± 2 °C), and before significant cooling took place, their lengths were measured. This is the zero reading. After the zero reading, the prisms were immersed in 0.25N, 0.5N, and 1N NaOH solutions kept at 60 °C, 70 °C, and 80 °C. These solutions were stored in a

tightly covered plastic container, which was large enough to totally immerse all the prisms. The prisms were periodically measured over a 1 year period (Fig. 4-9).

Three concrete specimens of 275 x 75 x 75 mm dimension for each aggregate were cast with a water to cement ratio of 0.48 (Table 4-5). After 24 hours of curing, specimens were demolded the initial measurement of the specimens was taken. After the length was measured, a set of 3 specimens was placed in a plastic container with sealed lids and three PVC pipe spacers at the bottom, and water was added to approximately a 25 mm depth. The prisms were kept in a vertical position without touching the water (Fig. 4-10). The container was kept in an environment room maintained at 38 ± 2 ºC. The expansion was measured periodically for 1 year.

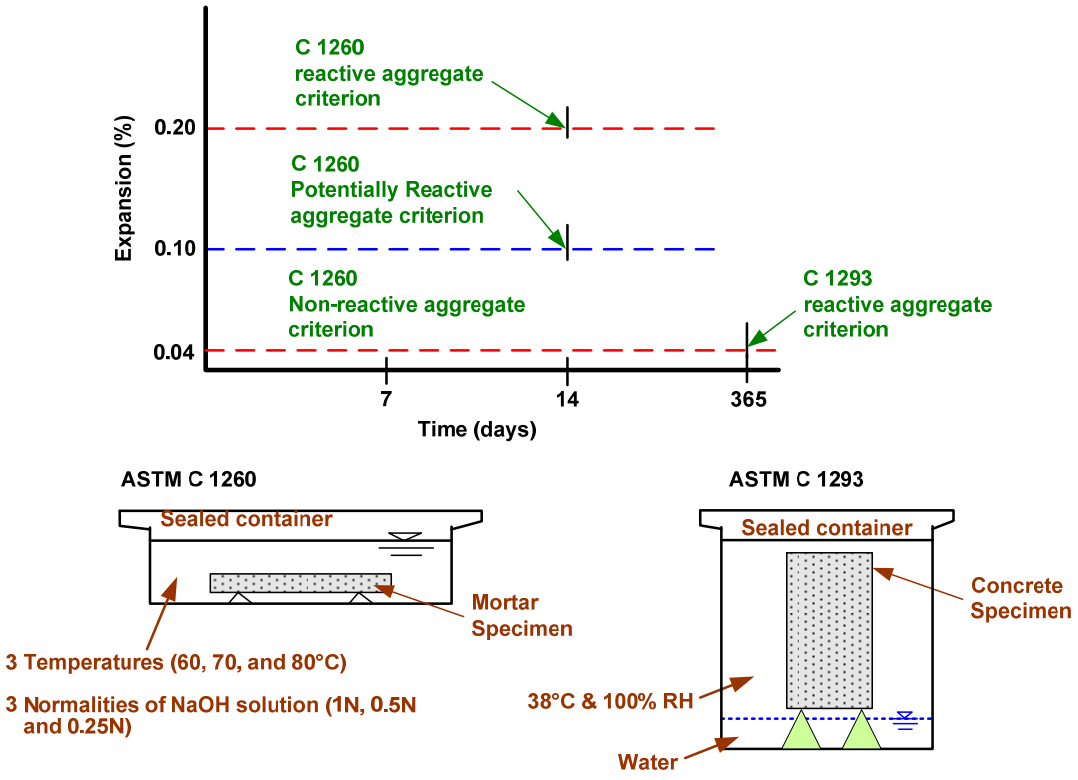

Fig. 4−11. Modified ASTM C 1260 and C 1293 test methods

CALCULATION OF EXPANSION

The volume change of aggregate, mortar, and concrete specimen is generally considered the most sensitive index of internal micro-cracking due to ASR. For dilatometer tests, Fig. 4-12 shows measuring volume change. The volume change due to ASR was calculated as follows:

$$\varepsilon_n(\%) = \frac{\Delta V_{ASR}}{V_{aggregate}} \times 100 \qquad (4\text{–}1)$$

Where, $\varepsilon_n(\%) =$ percent expansion at n hours; $V_{aggregate} =$ initial aggregate volume; $\Delta V_{ASR} =$ the volume changes due to ASR at n hours at a given normality and target temperature.

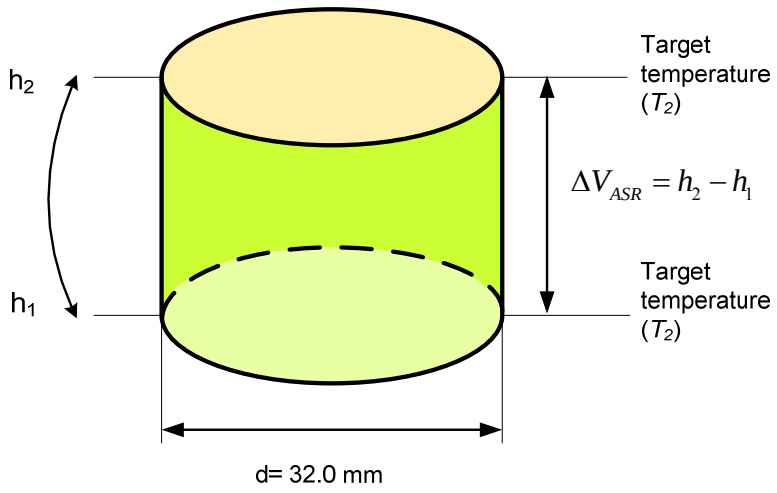

Fig. 4−12. Diagram of specimen volume change due to ASR of concrete

For ASTM C 1260 test method, subsequent length measurements are made periodically. The specimens are measured immediately after being removed from the NaOH solution (i.e. at 1N NaOH and 80°C). Percent expansion is calculated as follows:

$$\varepsilon\ (\%) = \frac{L_m - L_0}{L_0} \times 100 \qquad (4\text{–}2)$$

where, $\varepsilon\ (\%)$ = percent expansion at n days; L_m = measured length at n days; and L_0 = gauge length at zero days.

Corrections are made to compensate for changes in the length of the invar bar (reference bar). The average expansion of the three specimens was reported as the expansion of the sample at that particular age. For ASTM C 1293 test method, length changes are measured and calculated the same way as for the mortar bars in the C 1260 test, with the exception that the concrete prism samples are measured after being taken out of the curing chamber and maintained at room temperature (23 ± 2 °C) for 16-20 hours.

CHAPTER V

ACTIVATION ENERGY OF ALKALI-SILICA REACTION FOR MINERALS AND AGGREGATES

In Chapter III, a performance-based testing protocol was proposed as a means to incorporate the effect of aggregate reactivity, w/c, porosity, SCM, and lithium compounds on ASR in order to formulate job specific ASR resistant mixtures. In the protocol, aggregate reactivity in ASR is characterized relative to the activation energy (E_a) which is defined as energy needed to initiate ASR as well as a key parameter to characterize aggregate ASR susceptibility. Because the development of ASR is a thermally activated process that is also sensitive to a given level of alkalinity and mineralogy of the aggregate, the proposed E_a approach is capable of providing direct accountability for a variety of important material related factors that affect ASR expansion of aggregate such as mineralogy and crystallinity of aggregate. These parameters are encompassed within a kinetic-type approach that is the primary tool to characterize aggregate ASR.

In general, natural aggregates consist of different minerals in different proportions and some of them are reactive. The kinetics of alkali aggregate reaction depends on (i) whether the whole aggregate particle is reactive or some constituent(s) of aggregate is reactive, (ii) textural disposition of minerals and porosity, and (iii) reactivity of the reactive constituents. For instance, opal (SiO_2, nH_2O) is a highly reactive form of amorphous silica (CANMET 1991) and amounts as small as 1% (by mass) can cause damaging expansion in the aggregates due to ASR. Opal may be present as constituent of cherts, flints, volcanic rocks, some limestones and sandstones. Chalcedony and jasper belongs to the cryptocrystalline silica group composed of mainly radiating fibers of quartz with sometimes minute quartz crystals (CANMET 1991) and is considered to be a reactive (medium) with cement alkalis. Chalcedonies present as the main constituent of flints, cherts, jaspers, and as a cementing agent in quartzites. Flint is a rock mainly composed of chalcedony/submicroscopic quartz. By testing chalcedony, jasper and flint, some light can be shed on the prediction of aggregate activation energy based on mineral activation

energy. The gravel aggregate contains strained (deformed) quartz which is highly reactive in alkaline solution. The highly reactive acid (siliceous) volcanic glassy material is the reactive components of the New Mexico rhyolite (NM rhyolite).

The combined effect of the above factors may ultimately alter the diffusion/penetration process in different alkalinities and therefore, may manifest ASR activation energy as a function of alkalinity. However, it is anticipated that a normalized E_a (i.e., E_a/normality of test solution) should be a constant parameter for a given aggregate source. This approach provides a means for activation energy to be used to characterize the ASR susceptibility of aggregate.

The present study as described in Chapter IV was mainly focused on measuring ASR expansion of selective siliceous minerals and aggregates by dilatometer and introducing activation energy (calculated based on the time-expansion relationship as a function of temperature) as an indicator of ASR reactivity with respect to their crystallinity of aggregate and mineralogy. Although the test apparatus measures the expansion directly, it does not provide absolute values of expansion, but characteristics of it. In other words, the expansion data are used to define material-related parameters related to the formation of ASR product.

The ultimate goal, in this regard, is to introduce a performance-based (i.e., model to predict the rate and ultimate expansion of concrete) testing protocol by combining the laboratory measured material properties and exposure conditions through a kinetics-based mathematical formulation for predicting concrete ASR performance under field conditions for a given set of moisture and temperature conditions. The present work represents an initial effort towards this ultimate goal.

TESTING PROTOCOL APPROACH

The test was conducted using three different temperatures, namely 60 °C, 70 °C, and 80 °C and 1N NaOH solution to establish the concept of activation energy as an indicator of ASR reactivity with respect to their crystallinity of aggregate and mineralogy according to the test procedure described in Chapter IV.

EXPANSION CHARACTERISTICS

Figs. 5-1 through 5-4 shows the bulk volume expansion test results from the opal, jasper, flint, and chalcedony at 1N NaOH solution and three different temperatures, namely 60 °C, 70 °C, and 80 °C. Low initial expansion (up to 5 to 10 hours) followed by a rapid increase of expansion was characteristic of the 4 tested minerals. Interestingly, the mineral opal shows lower expansion than that of the other three minerals up to 10 hours, but showed significant expansion after 15 hours irrespective of the testing temperature. Furthermore, results show that by lowering the testing temperature from 70 °C to 60 °C, the amount of overall expansion decreased. The most rapid and highest ultimate expansion was observed in the opal at all three testing temperatures.

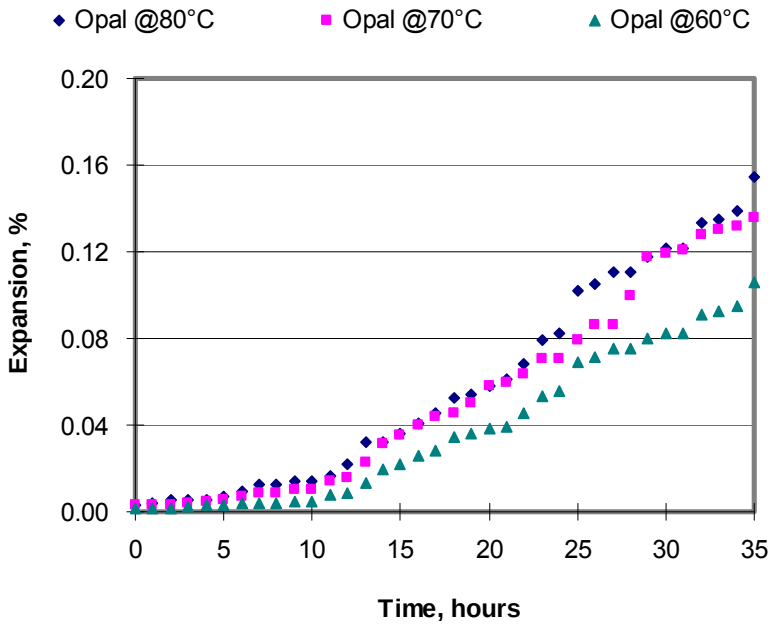

Fig. 5–1. Expansion development of opal mineral

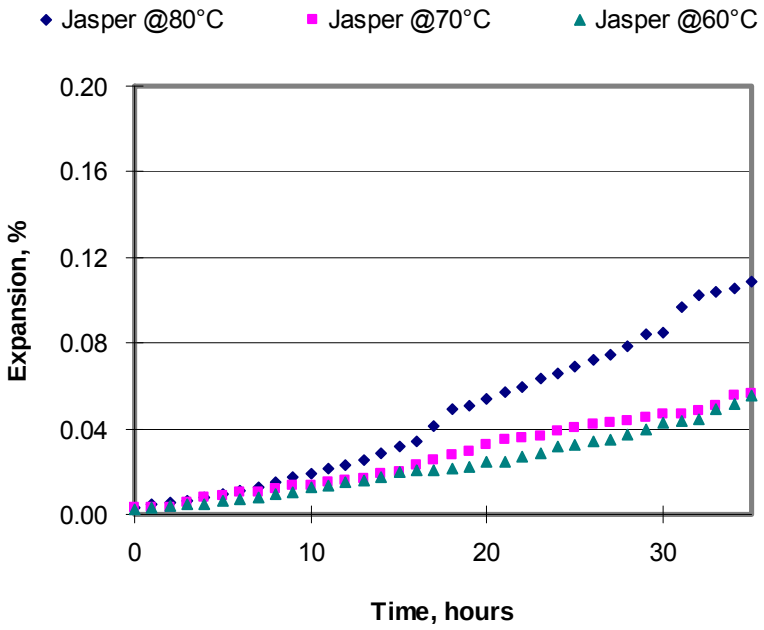

Fig. 5–2. Expansion development of jasper mineral

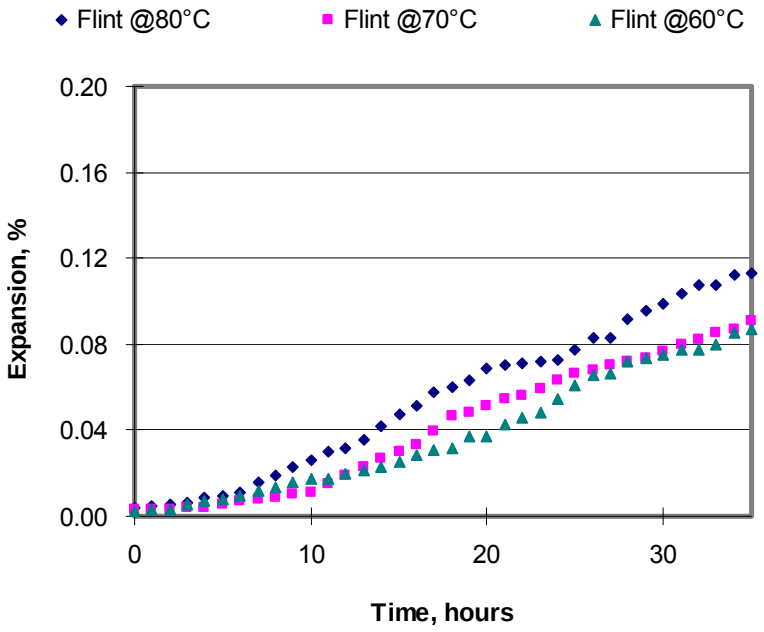

Fig. 5–3. Expansion development of flint mineral

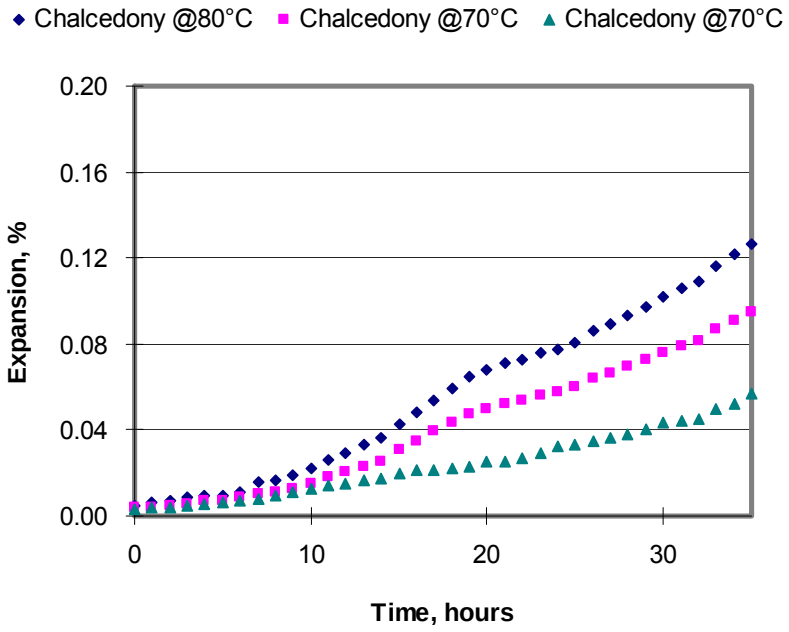

Fig. 5–4. Expansion development of chalcedony mineral

Figs. 5-5 and 5-6 show aggregate volume expansion results for siliceous reactive gravel and rhyolite aggregates. As expected, all expansion curves display the same characteristic patterns, i.e., initial low expansion up to 10 hours, followed by a steep rise from 10 hours to 30 hours. These aggregates, however produced lower expansion than that of the tested minerals (Figs. 5-1 though 5-4) at a given temperature. It must be recognized that in this test method, expansion produced due to ASR products, not amount of soluble silica produced, is measured after each operating temperature is reached at the desired temperature (e.g. 60 °C, 70 °C, and 80 °C). From these results, it is apparent that this new test method can categorize minerals and aggregates based on their reactivity within a very short period of time. It is interesting to note that expansion for all the tested minerals and aggregates occurred without any calcium in the system as all the testes were conducted with only NaOH solution.

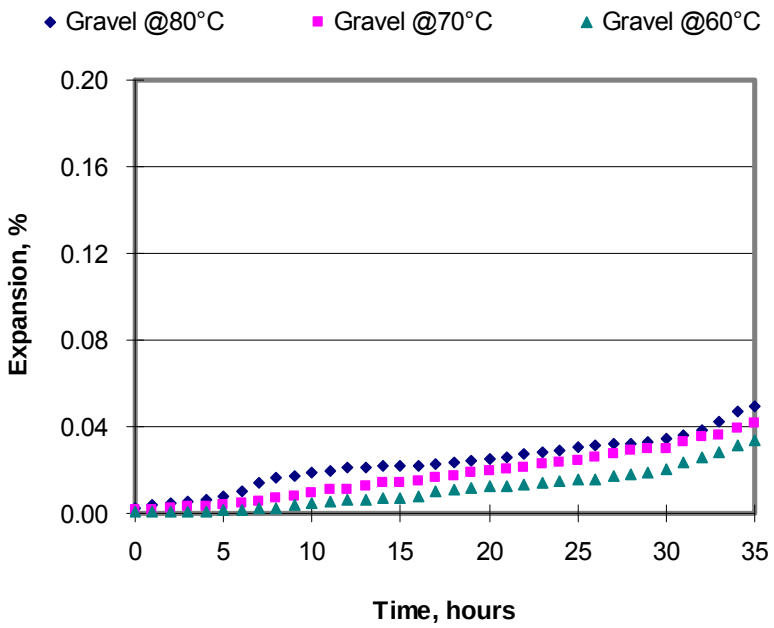

Fig. 5–5. Expansion development of gravel

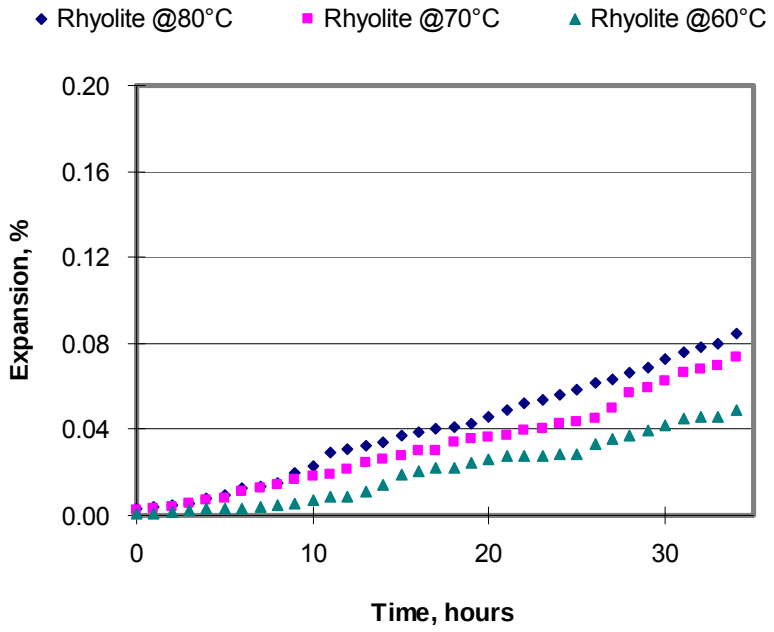

Fig. 5–6. Expansion development of New Mexico rhyolite

Fig. 5-7 shows the expansion characteristics of non-reactive aggregate. Although the PSD of non-reactive aggregate is finer than that of the reactive aggregate (Fig. 4-2), the reactive gravel aggregate produced higher expansion than that of non-reactive gravel, irrespective of temperature. From chemical composition analysis (Table 4-2), both oxide compositions of the reactive aggregate and non-reactive aggregate are siliceous. It can be surmised that some of non-reactive siliceous aggregate was also solubilized in the presence of 1N NaOH solution and produced little expansion. It must be recognized that in this test method expansion produced due to ASR gel, not the amount of soluble silica produced is measured. From these results, it emerges that this new test method can not only distinguish between non-reactive aggregate and reactive aggregate within a very short period of time, but also categorize aggregates based on their reactivity.

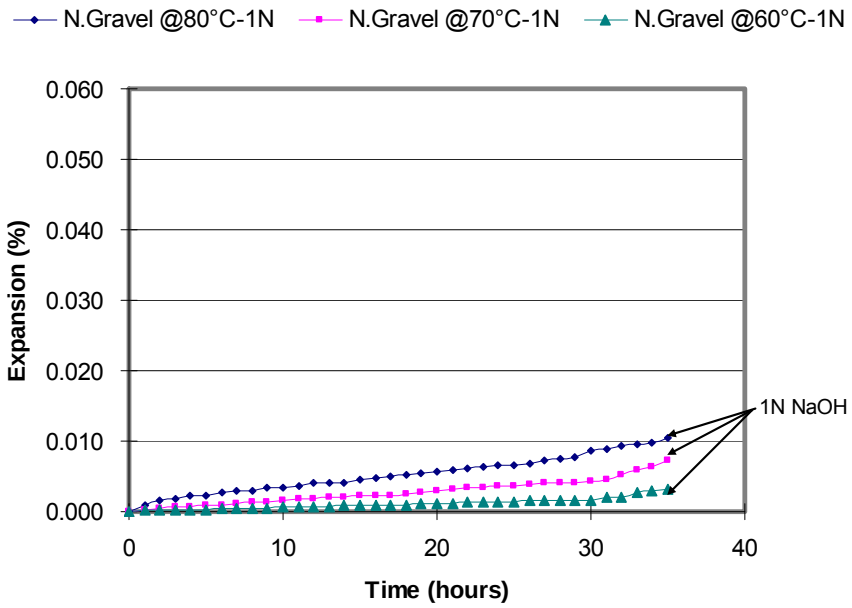

Fig. 5−7. Expansion development of non-reactive gravel aggregate

(N.Gravel=non-reactive gravel aggregate; N=normality)

EFFECT OF TEMPERATURE

The expansion values of different minerals as a function of the time and temperature of the NaOH test solution are presented in Fig. 5-8. Three elevated temperatures (i.e., 60, 70, and 80 °C) were used to accelerate the reaction. For all minerals, expansion increases with increasing test temperature of the test solution from 60 °C to 80 °C. At 80 °C the expansion is higher than that at 70 °C and 60 °C at a given age, irrespective of mineral type. This suggests that the increase in temperature causes more ASR due to high reaction kinetics at a high temperature. Larger overall expansion at higher temperature is possibly due to a higher amount of reaction product formation. An image of the reacted particles and reaction products revealed some relevant observations pertaining to this conclusion.

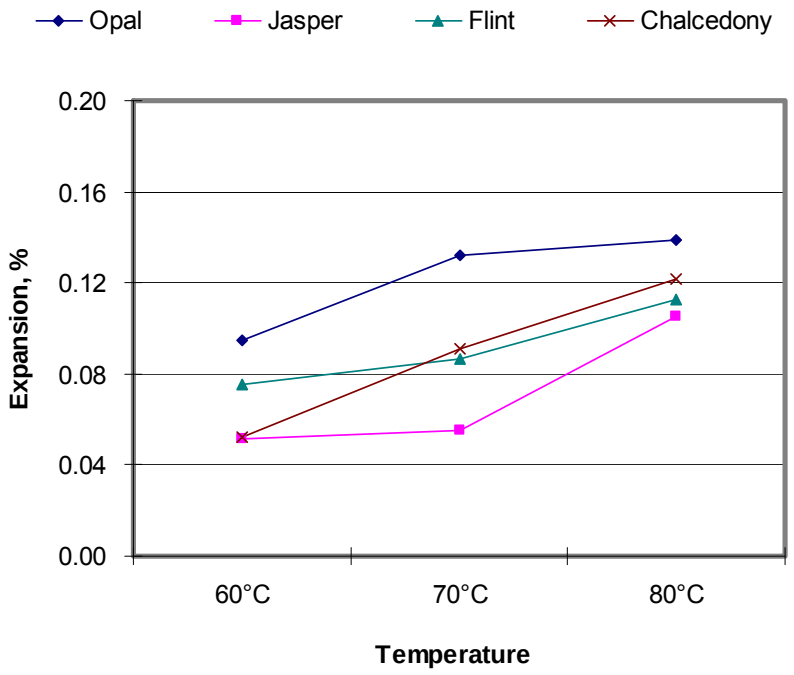

Fig. 5–8. Expansion as a function of temperature (at 35 hours)

IMAGE OF THE REACTION PRODUCTS

Environmental scanning electron microscope (ESEM) was used to investigate the nature of ASR products in the tested mineral samples and is presented in Figs. 5-9, 5-10, and 5-11. Fig. 5-9a shows that the reaction started on the opal surface and gradually progressed in

the opal particle. The noncrystalline, extremely fine-grained nature of opal is clearly visible from the enlarged view of the un-reacted inside portion of the particle (Fig. 5-9b).

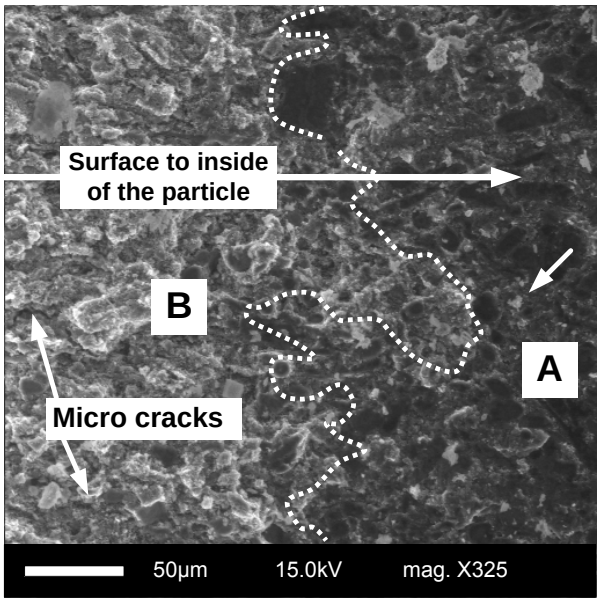

(a)

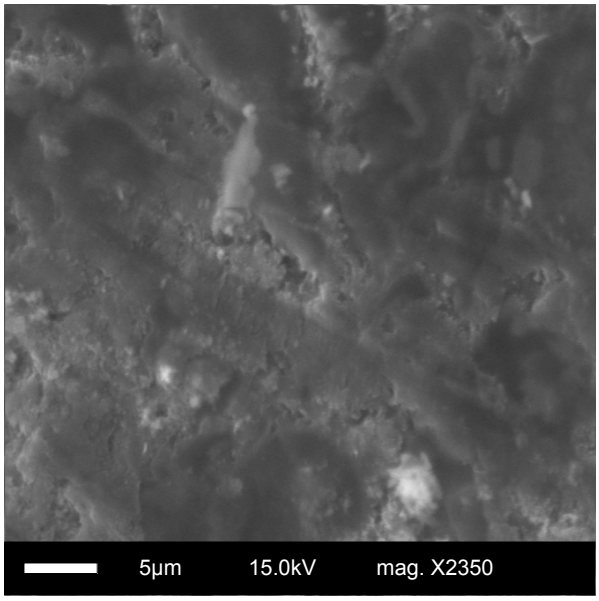

(b)

Fig. 5–9. ESEM images of opal particles. (a) Fractured surface image showing reaction front in an opal particle at 80°C (A–un-reacted inner portion, B–reacted outer portion), (b) Enlarged view of un-reacted portion

The reaction between alkaline solution (NaOH) and opal particles caused dissolution and in-situ precipitation of reaction products (Fig. 5-10a) followed by accumulation of ASR products (Fig. 5-10b). A representative energy dispersive spectroscopic (EDS) elemental analysis of the ASR products is presented in Fig. 5-10b, and it shows the presence of elements Na and Si (the peaks for Au and Pd came from Au-Pd coating that used during sample preparation). This is an indication that ASR product without calcium is expansive.

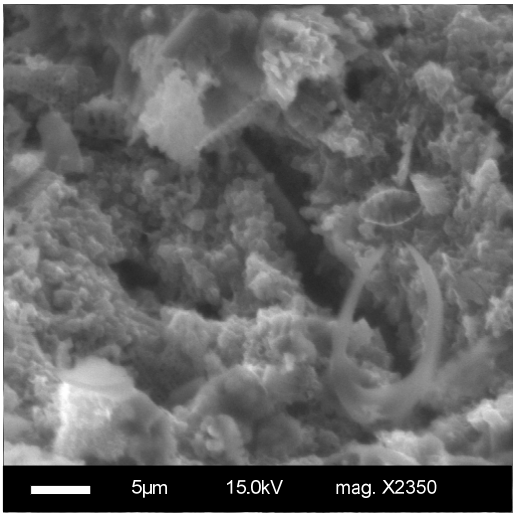

(a)

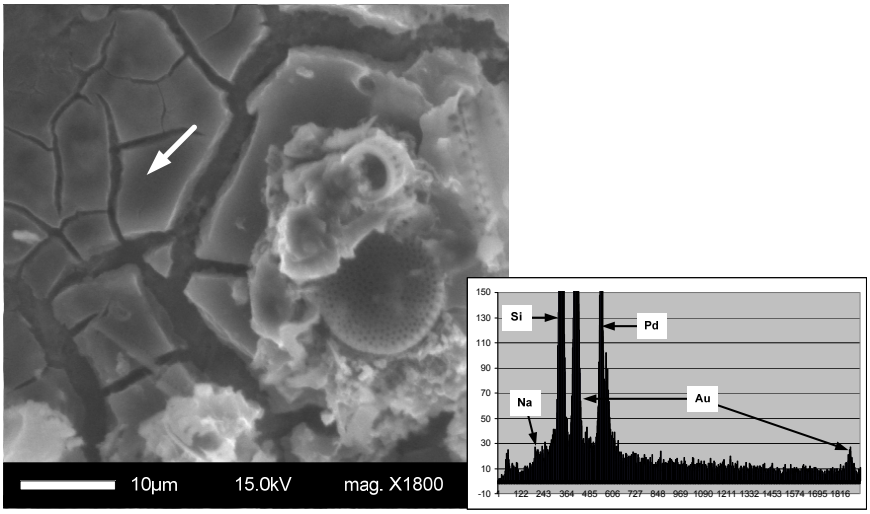

(b)

Fig. 5-10. Enlarged view of reacted portion in Fig. 5-8b. (a) In-situ gel formation through dissolution and precipitation, (b) Accumulation of gel

ESEM observations on the reaction products of some reacted jasper particles are presented in Fig. 5-11. Fig. 5-11a shows that jasper consists of fine crystals (cryptocrystalline). Fig. 5-11b and 5-11c show that the reaction started on the surface and formation of in-situ product was evident. However, the overall intensity of reaction is somewhat lower in jasper than that of opal. This is in accordance with the observed expansion behavior, i.e., jasper produce lower expansion than opal.

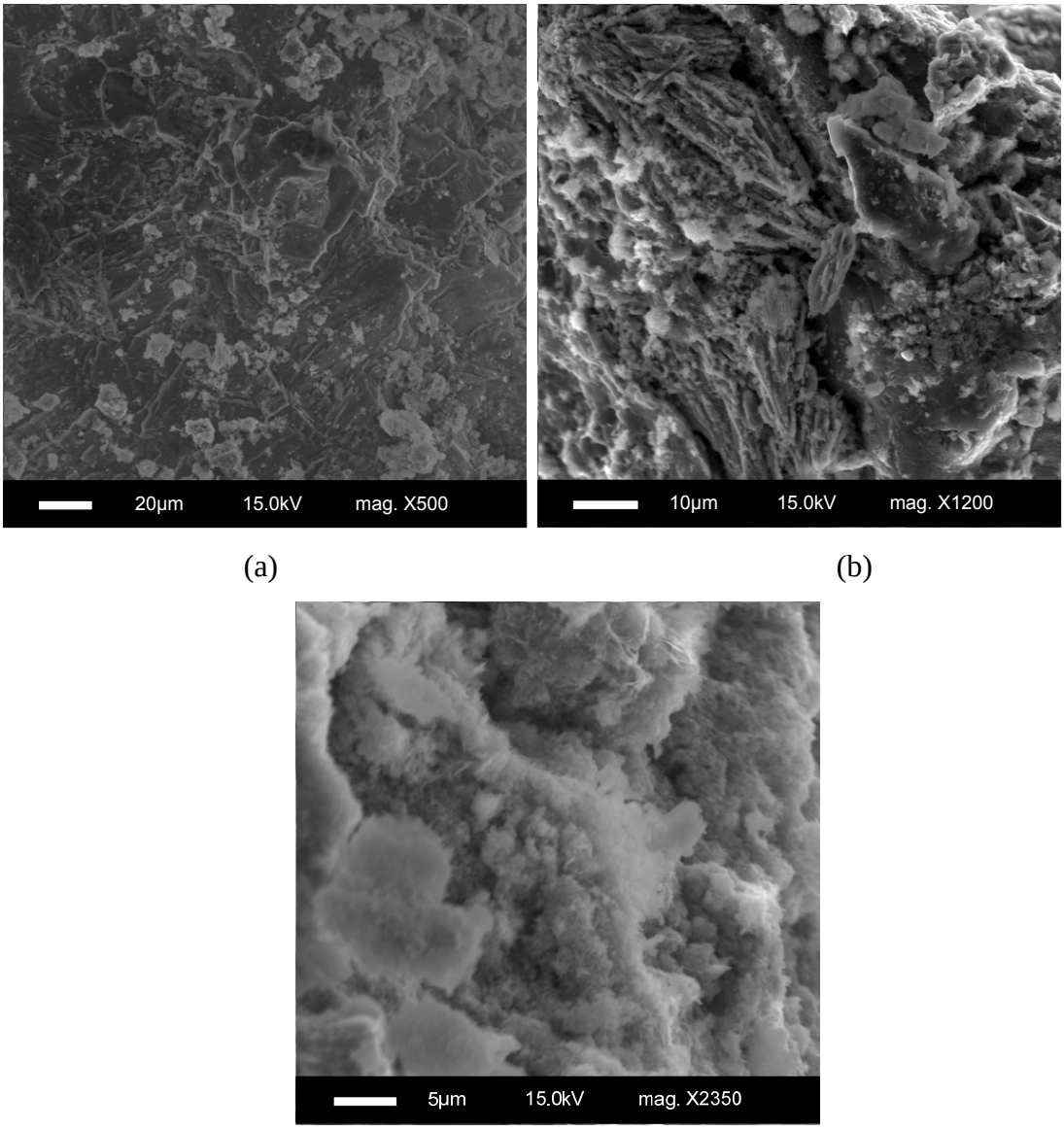

(a) (b)

(c)

Fig. 5-11. Fractured surface image of ASR in jasper at 80 °C. (a) Un-reacted portion of a jasper particle, (b) Dissolution and in-situ precipitation of gel, and (c) In-situ ASR gel

DETERMINATION OF ASR ACTIVATION ENERGY (E_a) OF MINERALS AND AGGREGATES

It is known that there are some initial conditions related to alkalinity, aggregate reactivity, humidity, and temperature conditions that must be met to initiate ASR. Therefore, ASR is a chemical reaction that integrates the combined effects of temperature, alkalinity, and time relative to the kinetics of ASR expansion into a single parameter (activation energy, E_a). At early ages, a rise in temperature leads to an acceleration of chemical reactions between alkali and silica and hence, causes the expansion development to occur at a faster rate. This notion fits well within the concept of activation energy, which characterizes energy needed to start the reaction. The use of the activation energy provides a unique parameter to evaluate ASR susceptibility of aggregate.

The following steps are an example to calculate activation energy of the corresponding minerals or aggregates. As an example, the expansion versus age data for the NM rhyolite aggregate (Fig. 5-6) were used to define the alkalinity and temperature dependence of the reaction rate parameter. The expansion-age data for each operating temperature were plotted as $1/\varepsilon$ versus 1/(assuming $t - t_0 = t$) to find the ultimate expansion (Fig. 5-12).

From linear regression analysis, the intercepts at 60°C, 70°C, and 80°C are 11.3, 16.1, and 11.9 respectively, which equal to the reciprocal of the ultimate expansion. Therefore, the ultimate expansions as a function of temperature are ε_0 = 1/11.3 = 0.084 (60°C), 1/16.1 = 0.062 (70°C), and 1/11.9 = 0.089 (80°C), respectively.

Next, in order to determine the activation energy, the reaction rate parameters (K_T) at the three temperatures are plotted as in Fig. 5-13. The negative of the slope of the straight line is equal to the activation energy divided by the gas constant. Therefore, the E_a at 1N NaOH alkalinity of the NM rhyolite aggregate is 61.65 KJ/mol.

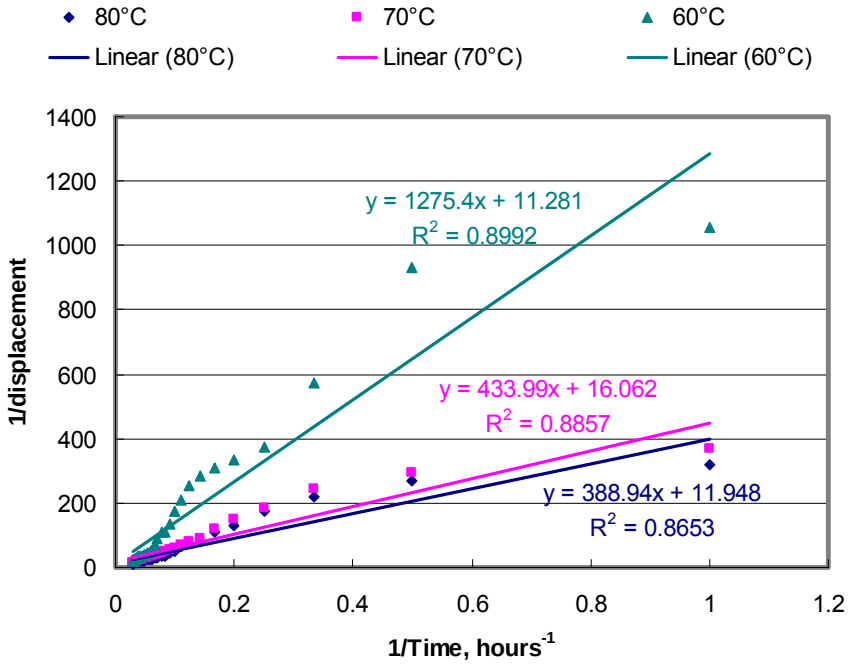

Fig. 5-12. Plot of reciprocal expansion vs. reciprocal age to evaluate ultimate expansion

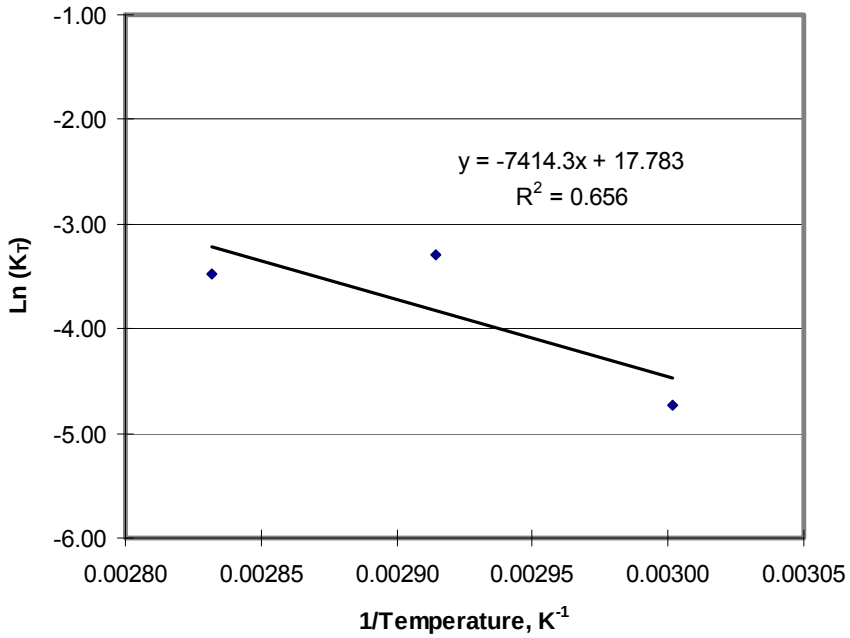

Fig. 5-13. Natural logarithm of reaction rate parameter vs. the inverse of the absolute temperature

RECALCULATION OF ASR E_a OF MINERALS AND AGGREGATES

As shown in earlier section, from the plot of $1/\varepsilon$ versus $1/(t-t_0)$, or $1/\varepsilon$ versus $1/($ t if t_0 is smaller than t), one can determine the ultimate expansion as the reciprocal of the intercept at infinite time, and the reaction rate parameter as the intercept divided by the slope. Determination of the slope and intercept of the best fitting straight line through the data appears to be very sensitive to t_0 value. From Fig. 5-12, an overall linear regression results in an insufficient slope and intercept, thereby it is likely to have misleading values of K_T and ε_0.

Figs. 5-14 and 5-15 show the calculated K_T value changes rhyolite and gravel aggregates tested at 1N and 0.5N NaOH solution according to time. K_T value has a big variation at initial time, and then is stabilized regardless of aggregate type and normality of test solution. If only short-term data are selected to calculate K_T, it may have misleading results. Therefore, it is likely that the early-stage data need to be ignored. The value of K_T and ε_0 must be determined by extrapolating sufficient available data instead of by regression on the whole range of data. This means that the choice of a parameter, t_0, has significant impact on the calculation of K_T because the t_0 defines how much of the valuable expansion data is included into the K_T calculation.

The initially low reaction rate parameter value was found in Fig. 5-14. As well known, ASR products form and are accumulated on the surface of reactive aggregate. Amount of ASR gel formation depends on the availability of reactive silica grains and alkalis. The initially low reaction rate parameter value is attributed to the formation of a thin ASR gel layer on the surface of reactive grains in aggregate. ASR gel coating on the reactive grains temporarily retards further ASR. The thin ASR gel layer, however, does not completely prevent ASR of aggregate. ASR gel is gradually converted to a semi-permeable rigid film which allows the penetration of the alkali solution through the rigid film into the aggregate for further reaction. With time, as a result of diffusion process, ASR gel is accumulated on the surface of aggregate and causes expansion forces. Further ASR gel formation and its accumulation on the surface of aggregate increase the thickness of ASR gel. Therefore, the diffusion of alkalis from solution across the growing gel layer

toward the reaction front at the surface of an unreacted remnant of the particle is reduced. This explains the relative decrease in reaction rate parameter with time.

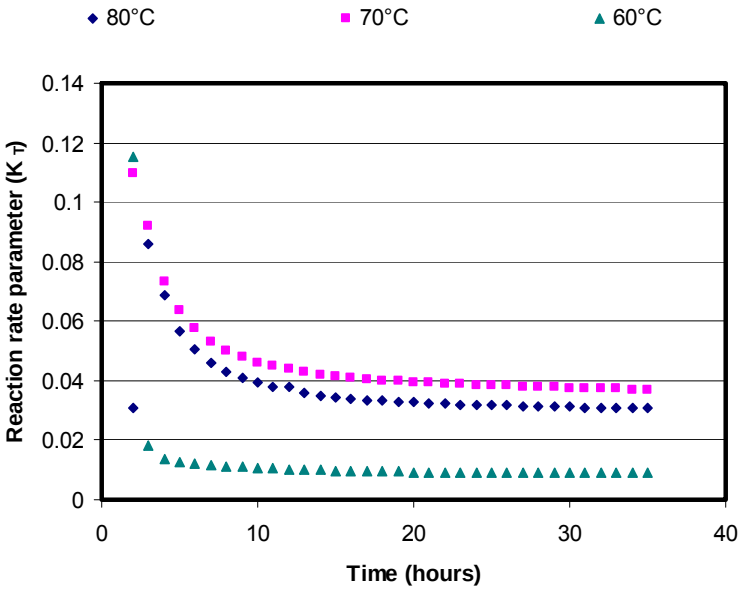

(a) New Mexico rhyolite aggregate

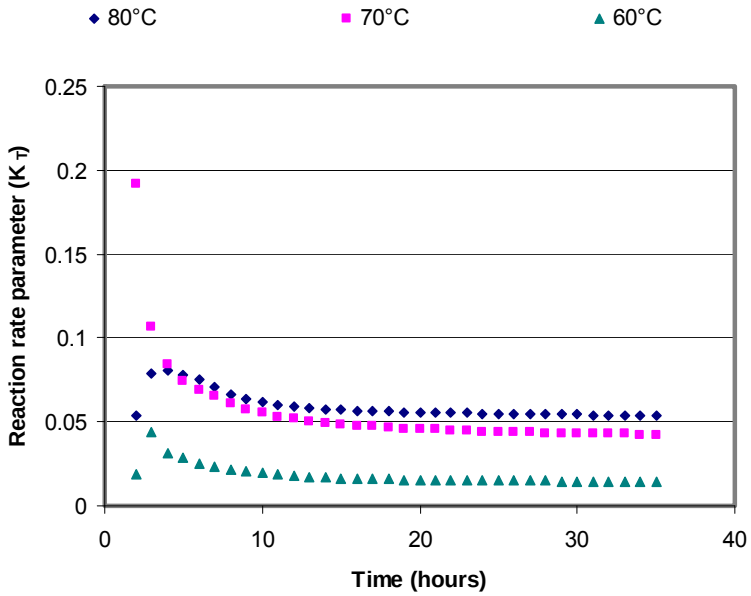

(b) Gravel aggregate

Fig. 5-14. Reaction rate parameter (K_T) changes according to time (at 1N NaOH)

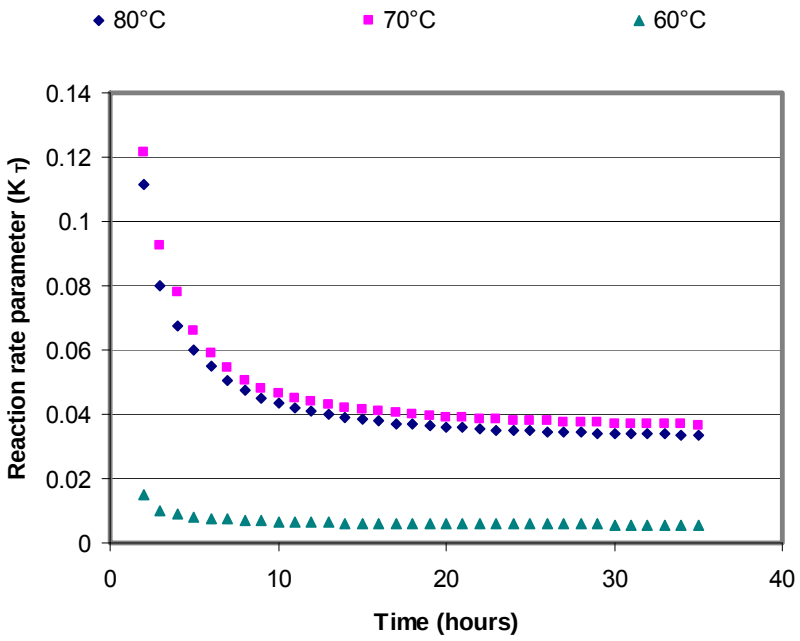

(a) New Mexico rhyolite aggregate

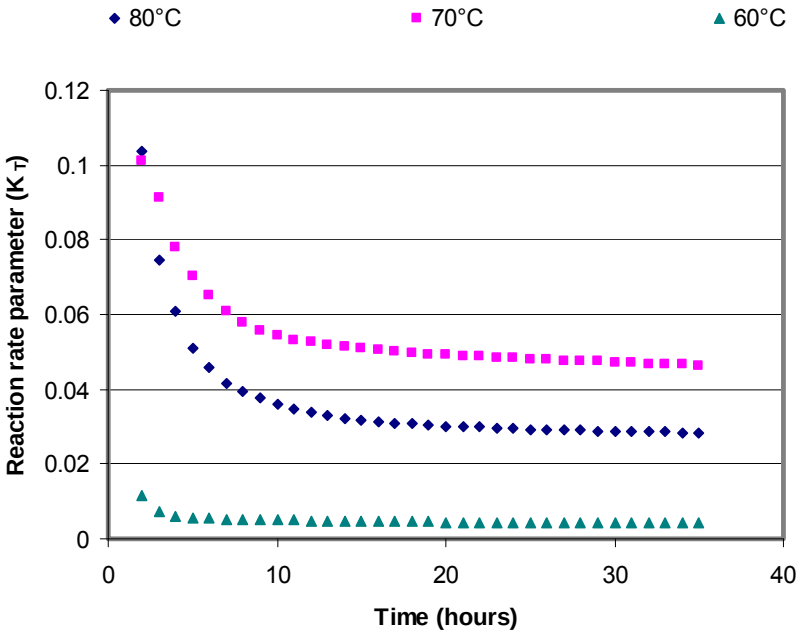

(b) Gravel aggregate

Fig. 5-15. Reaction rate parameter (K_T) changes according to time (at 0.5N NaOH)

From Fig. 5-14, it was selected that the t_0 value is 14 days and the reaction rate parameter of rhyolite aggregate was determined for each different temperature at 1N NaOH solution (Fig. 5-16). The E_a of rhyolite aggregate was determined from the plot of Ln (K_T) versus 1/Temperature, Temperature being in Kelvin (Fig. 5-17). All reaction rate parameter versus inverse temperature plots for each mineral and aggregate are listed in Appendix D.

Fig. 5-18 and Table 5-1 show the activation energy of opal, jasper, flint, and chalcedony minerals and siliceous reactive sand and New Mexico rhyolite within the studied temperature range and age. As previously noted, activation energy (E_a) indicates the energy needed to start the ASR. The activation energy of opal (11.1 KJ/mol) is lower than that of other minerals.

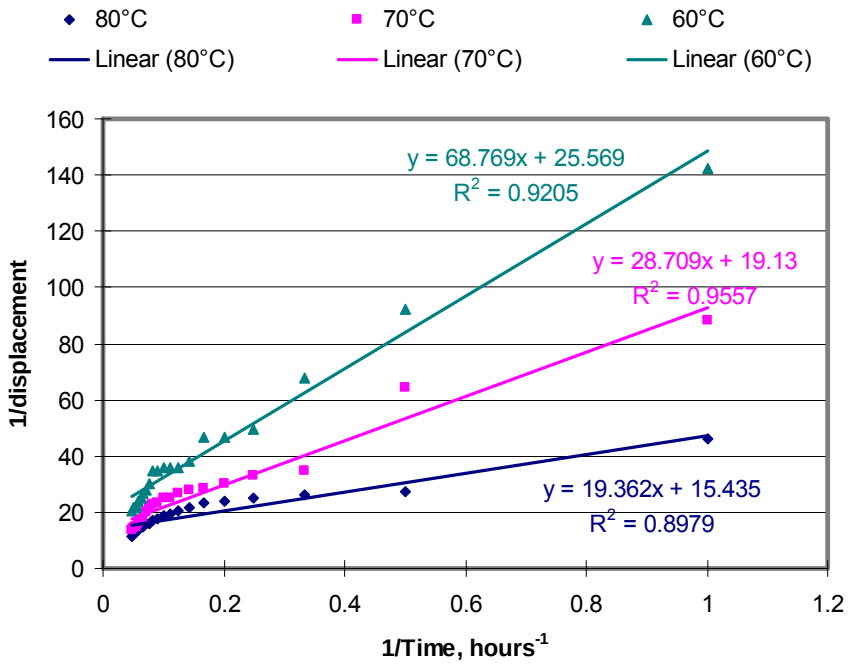

Fig. 5-16. Plot of reciprocal expansion vs. reciprocal age to evaluate ultimate expansion

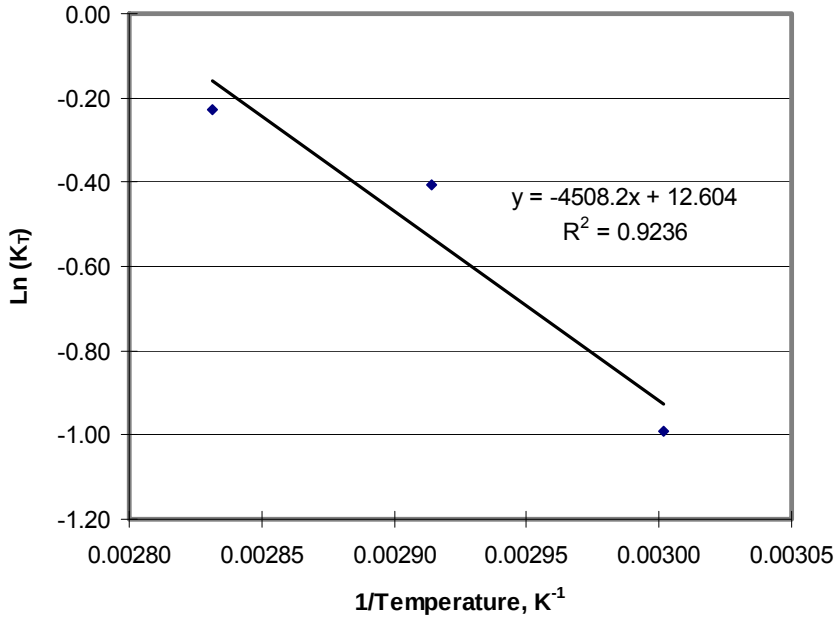

Fig. 5-17. Natural logarithm of reaction rate parameter vs. the inverse of the temperature

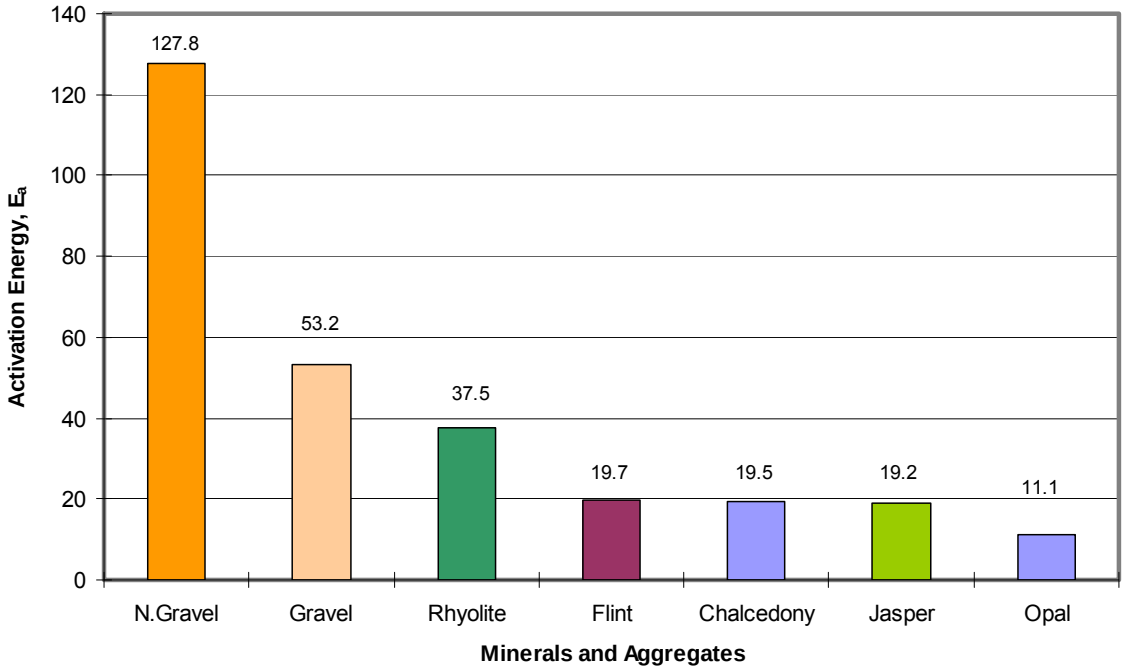

Fig. 5-18. Activation energy (KJ/mol) of silica minerals and aggregates (at 1N NaOH)

Table 5−1. Characteristics of Expansion Development of Mineral and Aggregate

Type of Aggregate	Normality of NaOH (N)	Temperature (°C)	Aggregate properties			Mineralogy/Morphology
			Reaction rate parameter (K_T)	Ultimate expansion (ε_a)	[a] E_a (KJ/mol)	
Opal	1N	60	0.269	0.075	11.1	Amorphous silica
		70	0.331	0.099		
		80	0.337	0.106		
Jasper	1N	60	0.322	0.041	13.1	Cryptocrystalline
		70	0.347	0.049		
		80	0.421	0.082		
Chalcedony	1N	60	0.305	0.044	19.5	Cryptocrystalline
		70	0.397	0.075		
		80	0.453	0.098		
Flint	1N	60	0.429	0.065	19.7	Rock mainly composed of chalcedony
		70	0.508	0.073		
		80	0.643	0.092		
Rhyolite	1N	60	0.372	0.039	37.5	Acid volcanic glass
		70	0.666	0.052		
		80	0.797	0.065		
Reactive gravel	1N	60	0.465	0.018	53.2	Strained quartz
		70	0.744	0.027		
		80	1.384	0.032		
Non-reactive gravel	1N	60	0.249	0.012	127.8	Quartz
		70	1.066	0.067		
		80	3.388	0.069		

[a]Activation energy was calculated with expansion data at 1N NaOH.

From the expansion behavior (Figs. 5-1 through 5-4), it is observed that opal is more reactive than jasper, flint, and chalcedony. This is an indication that the energy needed to start the ASR reaction is comparatively low in the case of minerals with high reactivity (e.g., opal). On the other hand, the mineral with high ASR reactivity needs less energy to initiate the reaction. It is important to note that opal is an amorphous form of silica whereas chalcedony, jasper and flint are cryptocrystalline forms of silica. Therefore, it is obvious that the amorphous form of silica should be more reactive than the micro-crystalline or crypto-crystalline forms and it supports the results of activation energy.

The reactive siliceous gravel consists of deformed (highly strained) crystalline quartz. It is known that strained quartz is reactive because of crystal defects imposed through deformation. It is to be noted that crystalline quartz without any deformation (strain) is non-reactive. The New Mexico rhyolite is reactive because of the presence of devitrified volcanic glass. Chalcedony and jasper are both crypto-crystalline form of silica and shows similar activation energy. It is interesting to note that flint also shows the E_a similar to jasper and chalcedony. Flint is a rock and mainly contains chalcedony. This indicates that E_a of a monomineralic rock (e.g., flint) is very similar to the activation energy of the constituent mineral (e.g., chalcedony). It is anticipated that the aggregate E_a is a function of the E_a of the constituent minerals and can be formulated in a form of a model (on the basis of bulk volume expansion). However, further work such as (i) determination of activation energy of different aggregates with varying mineralogy and reactivity, (ii) the effect of degree of crystallinity, mode of occurrence and size of the reactive constituents and others needs to be performed in order to explore the viability of modeling such effects for performance prediction purposes.

SUMMARY

Using the dilatometer to measure expansion of mineral and aggregate due to ASR represents a new approach to the characterization of ASR. In this chapter, the new test method was used to determine ASR reactivity of mineral and aggregate as a function of temperature, time, and alkalinity of the test solution. The results indicate that the concept of activation energy can be used to represent the reactivity of mineral and aggregate

subjected to ASR as well as to categorize minerals and aggregates based on their ASR potential. Based on the results, the following conclusions can be drawn:

1. Increasing temperature of the test solution accelerates the rate of expansion due to ASR regardless of mineral and aggregate reactivity.
2. The activation energy appears to be useful approach to categorize different form of silica minerals based on their reactivity. Degree of crystallinity of different forms of silica minerals matches with the activation energy results.

The work described in this study, however, was based on 1N NaOH test solution and limited particle mineral and aggregate sizes. It may be a more realistic approach to test every mineral and aggregate using three different levels of alkalinity in order to (i) determine a threshold alkali level for a particular aggregate and (ii) to establish the relationship between E_a and alkalinity. Furthermore, size and shape effects of mineral and aggregate also need to be considered in order to interpret the testing results. It is observed from the present study that ASR products without calcium are expansive. Therefore, it would be worthwhile to investigate the role of calcium (experiments with different dosages of $Ca(OH)_2$) on the ASR expansion behavior.

CHAPTER VI

PERFORMANCE-BASED APPROACH TO EVALUATE ASR POTENTIAL OF AGGREGATE AND CONCRETE USING DILATOMETER METHOD

For more than sixty years since the discovery of ASR (Stanton, 1940a and b), extensive research has been carried out on ASR throughout the world. Main areas of research have addressed fundamental understanding of the mechanism of ASR and developing quick reliable test methods to assess the ASR potential of aggregate and concrete. A number of accelerated test methods for determining potential reactivity of aggregate have been developed over the past 15 years. Despite a wealth of data that exists on alkali reactivity of aggregates from different sources by using these methods, doubts remain as to whether the current tests used to predict ASR are sufficiently performance-based to address how different combination of concrete materials may interact to affect ASR behavior; most of current methods are more suited as a screening tool rather than a fundamental assessment of ASR potential.

The advantage of a performance-based approach is the consideration of the expansion history which encompasses unique characteristics of each combination of material components used in the mixture; identifying these characteristics in terms of the material performance of field concrete will form the foundation of a unified procedure and guideline to evaluate ASR potential of aggregate and concrete. Furthermore, they can address how different combinations of concrete materials may affect ASR behavior.

This chapter describes a new rapid performance-based ASR testing protocol to predict ASR potential of aggregate and concrete using dilatometery. The performance-based approach is founded on the relationship between expansion and temperature over time as an aggregate reacts with alkalis. The dilatometer can be used to carry out tests for characterizing ASR of both aggregates and concrete. This procedure can be done within a fairly short period of time (e.g., within 3 days), and is based on the direct measurement of expansive ASR products under conditions that are definable at realistic levels of alkali and temperatures representative of field concrete. Expansion is measured on both aggregate

and concrete. The test is accelerated significantly by testing at elevated temperatures of 60, 70, and 80 °C.

Although the test apparatus measures the expansion directly, it does not provide absolute values of expansion, but characteristics of it. In other words, the expansion data can be used to define parameters related to the formation of ASR gel. It is intended to help engineers in designing ASR resistant concrete mixes for new construction. A series of expansion measurements using the dilatometer are first performed on aggregates, followed by expansion tests on concrete of a specific concrete mixture for a given application. In continuation with the evaluation of performance-based approach, ASTM C 1260/C1293 data for the tested aggregates through the proposed model is analyzed to draw a comparative assessment between dilatometer and C 1260/C1293 based material properties and ultimate expansion.

EXPANSION CHARACTERISTICS OF AGGREGATE

Figs. 6-1 and 6-2 show the expansion results for the New Mexico rhyolite (rhyolite) and siliceous reactive gravel at different normalities and NaOH and temperatures during the first 35 hours. The results indicate that aggregates are very susceptible to normality of test solution. In 1N NaOH solution, the expansion of rhyolite at 80 °C and 70 °C reached 0.02 at 25 hours while that at 60 °C was 0.02 at 35 hours. However, in 0.5N NaOH solution it was only at 35 hours that the expansion reached 0.02 percent, irrespective of the testing temperature. In 0.25N NaOH solution, the expansion was still below 0.2 percent at 25 hours. The rhyolite produced higher expansion than that of siliceous gravel, irrespective of temperature and normality of test solution, although the PSD of both aggregates is same. This is an indication that the reactivity of the rhyolite is greater than that of gravel.

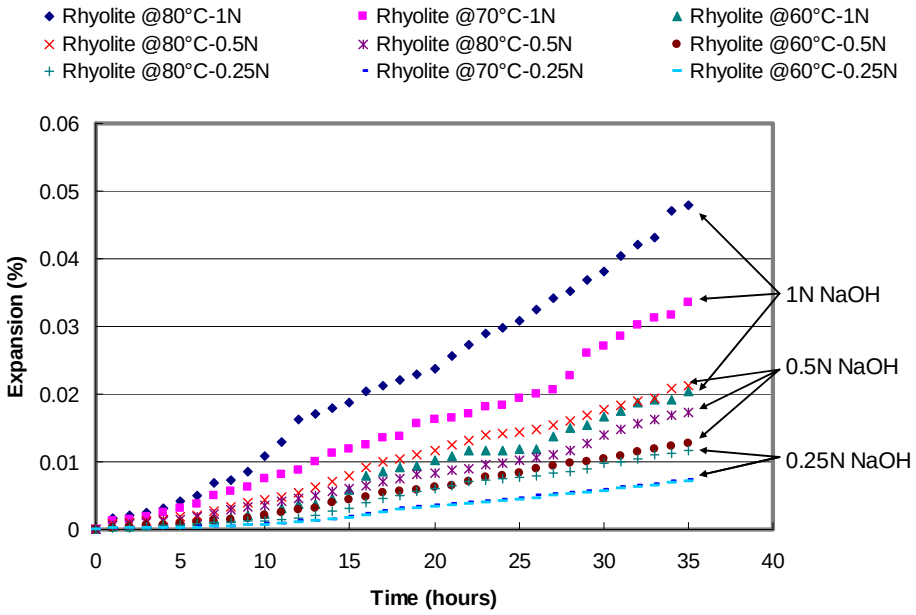

Fig. 6−1. Expansion of New Mexico rhyolite aggregate (N = normality)

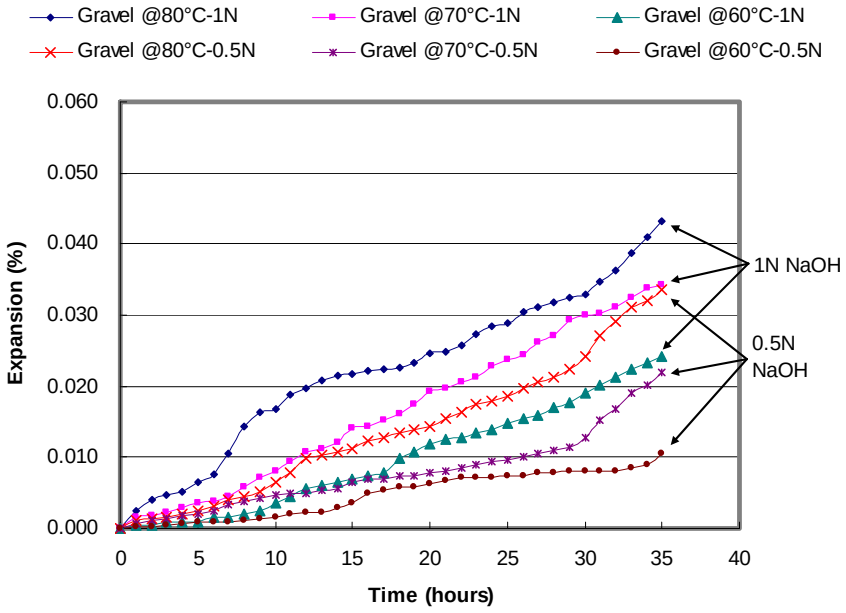

Fig. 6−2. Expansion of gravel aggregate (N = normality)

EFFECT OF TEMPERATURE AND NORMALITY OF TEST SOLUTION ON EXPANSION BEHAVIOR

The expansion values of rhyolite aggregate as a function of temperature of NaOH solution are given in Fig. 6-3. As expected, the rate of expansion increases with increasing temperature of the test solution for both test methods. Although the slope of the expansion curve from 60 °C to 80 °C is fairly uniform regardless of age, the expansion of both aggregate and mortar at 80 °C is higher than that at 60 °C. This indicates that the temperature of the test solution is an important factor in the expansion characteristics due to ASR.

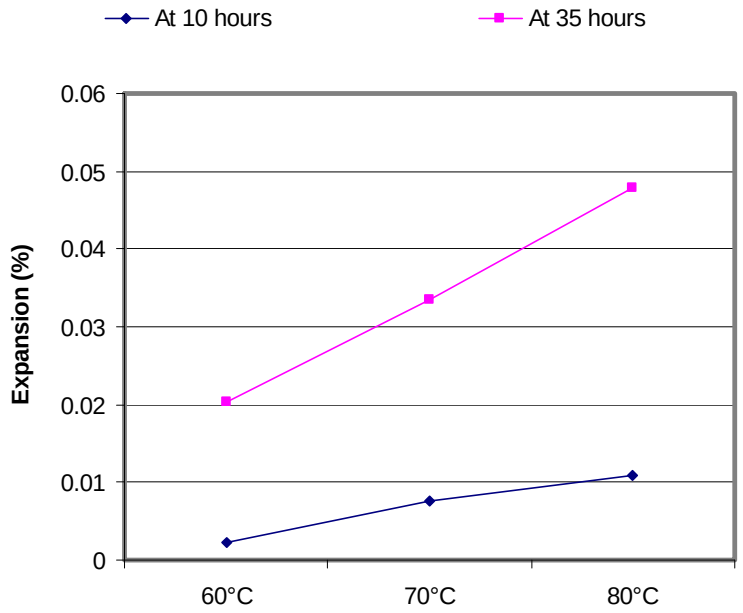

Fig. 6−3. Effect of temperature of NaOH solution (at 1N NaOH)

Fig. 6-4 presents the expansion values of rhyolite aggregate as function of NaOH test solution normality. All expansion curves display the same characteristic pattern: the expansion increases with increasing the normality of NaOH solution form 0.25N to 1N. When the normality of NaOH solution increases from 0.25N to 0.5N, the slope of expansion is gradual. The rate of expansion, however, increases significantly when the normality increases from 0.5N to 1N NaOH. At 1N NaOH the expansion is higher than those at 0.25N and 0.5N NaOH, irrespective of test method. The initial reaction due to a

higher normality of test solution seems to induce the formation of higher amount of ASR gel, and this leads to larger overall expansion. This suggests that the increase of the test solution not only accelerates expansion, but also increase the ASR gel formation (higher the temperature higher, the rate of reaction due to higher reaction kinetics).

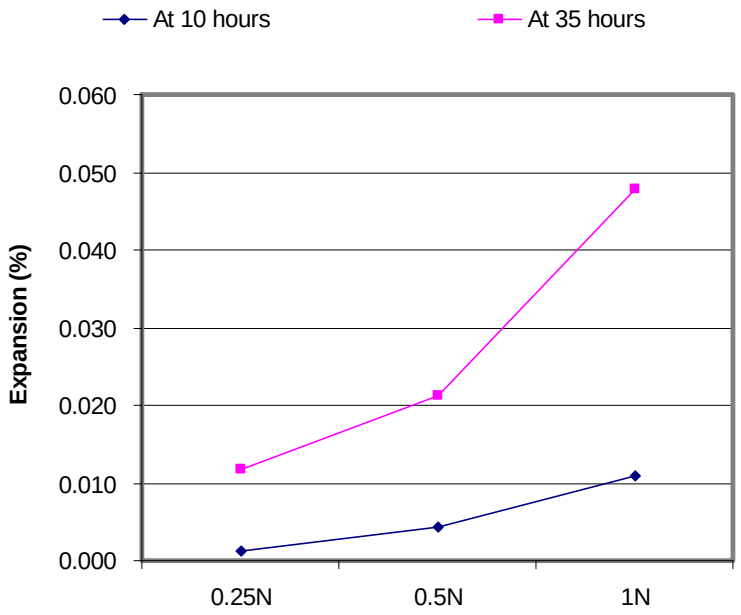

Fig. 6−4. Effect of normality of NaOH solution (at 80°C)

EFFECT OF CALCIUM HYDROXIDE ON EXPANSION CHARACTERISTICS

Classic theories describing ASR in concrete generally do not consider calcium in the primary role of reaction and expansion. The mechanism of expansion proposed by McGowan and Vivian (1952) does not consider calcium to influence the chemistry of ASR or the mechanisms of expansion. In her study on the structure of ASR gels, Dent Glasser (1979) proposed that the alkali-silica gel acts as a semi-permeable membrane, but does not consider calcium as a contributory factor.

However, a number of workers have suggested that the presence of $Ca(OH)_2$ is required for ASR induced damage. Powers and Steinour (1955) considered the expansive nature of the reaction product to depend upon its calcium to silica ratio which in turns relies upon the availability of $Ca(OH)_2$. However, in contrast to this view, other researchers feel

that the role of calcium hydroxide is more involved than previously thought (Powers and Steinour 1995). It was suggested that the presence of $Ca(OH)_2$ and its availability for reaction is required for the formation of potentially destructive expansive gel (Chatterji, 1979, 1989a, 1989b; Chatterji and Thaulow 2000; Thomas 2000).

The effect of $Ca(OH)_2$ on ASR expansion is presented in Fig. 6-5. Expansion due to ASR is increased in the presence of $Ca(OH)_2$ regardless of temperature.

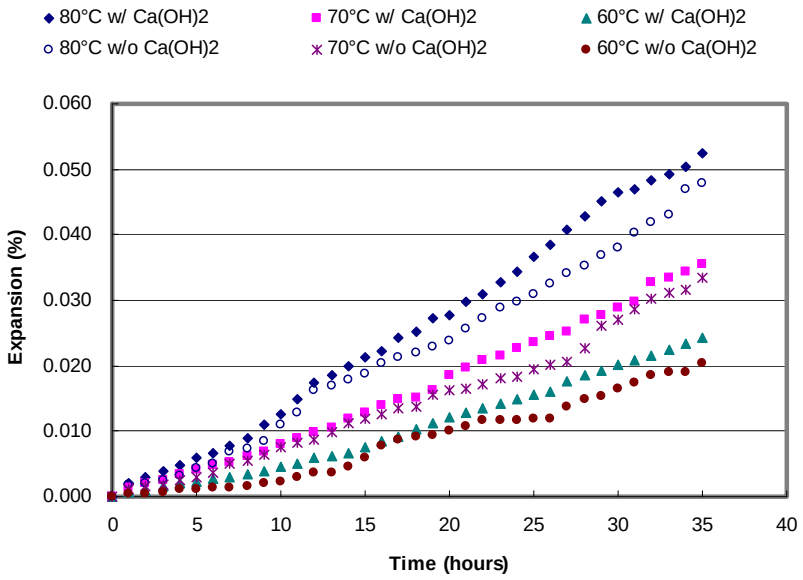

Fig. 6−5. Effect of calcium hydroxide on ASR expansion of NM rhyolite aggregate

From these results, it is apparent that (i) ASR can be expansive without calcium and (ii) that in the presence of calcium on the expansion is enhanced but not an absolute element to make ASR a destructive product, and (iii) this new test method can differentiate between calcium bearing expansive gel and non-calcium bearing expansive gel produced by ASR.

EFFECT OF LITHIUM NITRATE ON EXPANSION CHARACTERISTICS

The Strategic Highway Research Program (SHRP) looked on the role of lithium in preventing ASR in new concrete and mitigating ASR in afflicted concrete (Stark et al. 1993). Eventually, the Federal Highway Administration (FHWA) and the American

Association of State Highway and Transportation Offices (AASHTO) Lead States program promoted a round robin evaluation of mitigation schemes, and produced a guide specification for the prevention of deleterious ASR in concrete. As for the lithium interaction, Stark (1992) proposed that a less-expansive or non-expansive product can form in the presence of lithium. Diamond (1999) demonstrated that as the amount of lithium present in the gel increased, as compared to the amount of sodium and potassium present, mortar bar expansion decreased, confirming Stark's view.

Currently, one test method is recommended for assessing lithium compounds as ASR-preventive agents. ASTM C 1260 is modified by adding the lithium to the alkaline test solution to achieve the same lithium-alkali ratio as that used in the mortar mixture. In addition, ASTM C 1293 is yet to formulate proper guidance on using this test for assessing lithium compounds. However, only limited data are available for these tests.

The dilatometer was used to evaluate the dosage of lithium nitrate ($LiNO_3$) required to suppress ASR (Fig. 6-6). Comparative evaluation of aggregate expansion results for three different dosages shows that a Li:Na molar ratio of 0.75 reduced the expansion to a very low value, while 0.5M $LiNO_3$ dosage was slightly less effective in reducing expansion. When a Li:Na molar ratio of 0.25 was used, it leads to the lowest reduction in expansion than the other two. Although the reason for such a significant reduction of expansion in the presence of $LiNO_3$ cannot be fully explained at this stage, it is possible that increase of tetrahedral coordination hydrated ions of Li in higher normality occupies more space than the octahedral coordination hydrated ions of Na in gel formed by ASR. From these test results, it is deduced that the inhibiting effect of $LiNO_3$ on the expansion due to ASR depends on the dosage of $LiNO_3$. Although modified ASTM C 1260 test method is used to assess the effectiveness of $LiNO_3$ in reducing ASR expansion, the dilatometer method can also be used to evaluate the dosage of $LiNO_3$ at realistic levels required for a particular aggregate.

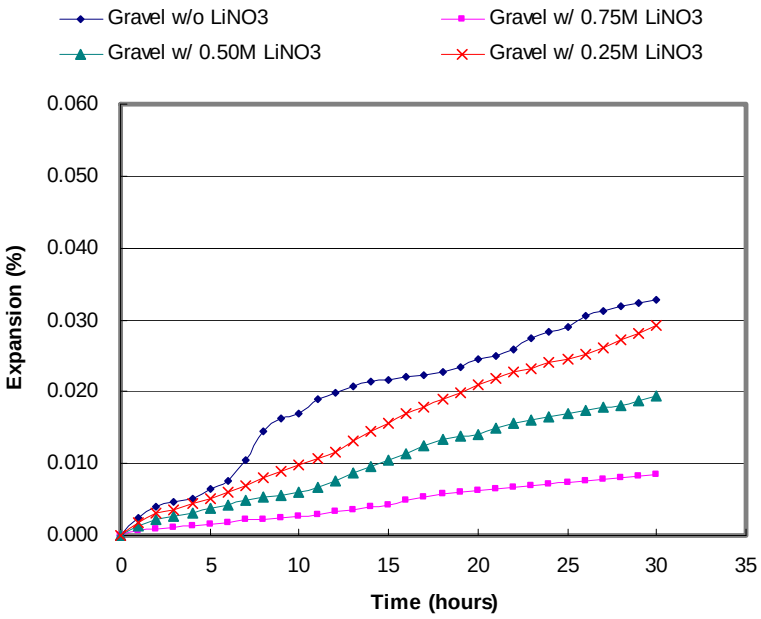

Fig. 6−6. Effect of lithium nitrite on ASR expansion of gravel aggregate (at 80 °C)

CHEMISTRY OF TEST AND PORE SOLUTION

As previously mentioned in Chapter II, ASR in concrete is the deleterious chemical reaction between aggregate containing reactive forms of silica and alkali and hydroxyl ions in the pore solution from hydrating cement. The amount of alkalis and hydroxyl ions in the pore solution plays a critical role in ASR. Contrary to ASTM C 1260 test method, aggregate in the dilatometer method is directly in contact with sodium hydroxide (NaOH) solution and forms ASR gel. If the ASR gel is soluble in the NaOH solution, it may cause shrinkage instead of expansion. Thus, it is important to investigate how alkali ions in the solution change before and after testing. The change in the chemistry of solutions will be discussed in this section.

In conjunction with the aggregate expansion analyses, the chemistry of test solutions before and after dilatometer test was analyzed. Additionally, the pore solution of concrete specimen composed of New Mexico rhyolite was extracted under high pressure (1000 MPa) according to the procedures developed by Barneyhack and Diamond (1981) before and after dilatometer test. The test and pore solutions were chemically analyzed using inductively coupled plasma (ICP) for sodium (Na^{+}), potassium (K^{+}), and calcium (Ca^{2+}) ions concentration and pH of both solutions was measured using pH meter.

Chemistry of Test Solution

Comparative evaluation of all ion concentrations and pH is given in Table 6-1. As expected, the concentration of Na^+ ions decreased substantially after dilatometer test regardless of normality of test solution and aggregate type. A drop in Na^+ ions concentration is contributed to the fact that Na^+ ions react with siliceous reactive component of aggregate and its concentration is reduced by Na^+ ions trapping by ASR reaction: As shown in Fig. 6-7, the ASR is initiated by the hydroxyl ion (OH^-) attack to dissolute reactive silica present in the aggregate, which results in the formation of acidic silanol bonds (Si–OH). As additional OH^- ions penetrate into the structure, the second acid-base dissolution (Si–O^-) occurs between OH^- ions in the pore solution and the existing silanol groups or silanol groups produced by hydroxyl ion attack. To maintain charge equilibrium, the formation of negatively charged Si–O^- ions from the aggregate attract positively charged ions (Na^+) from the test solution.

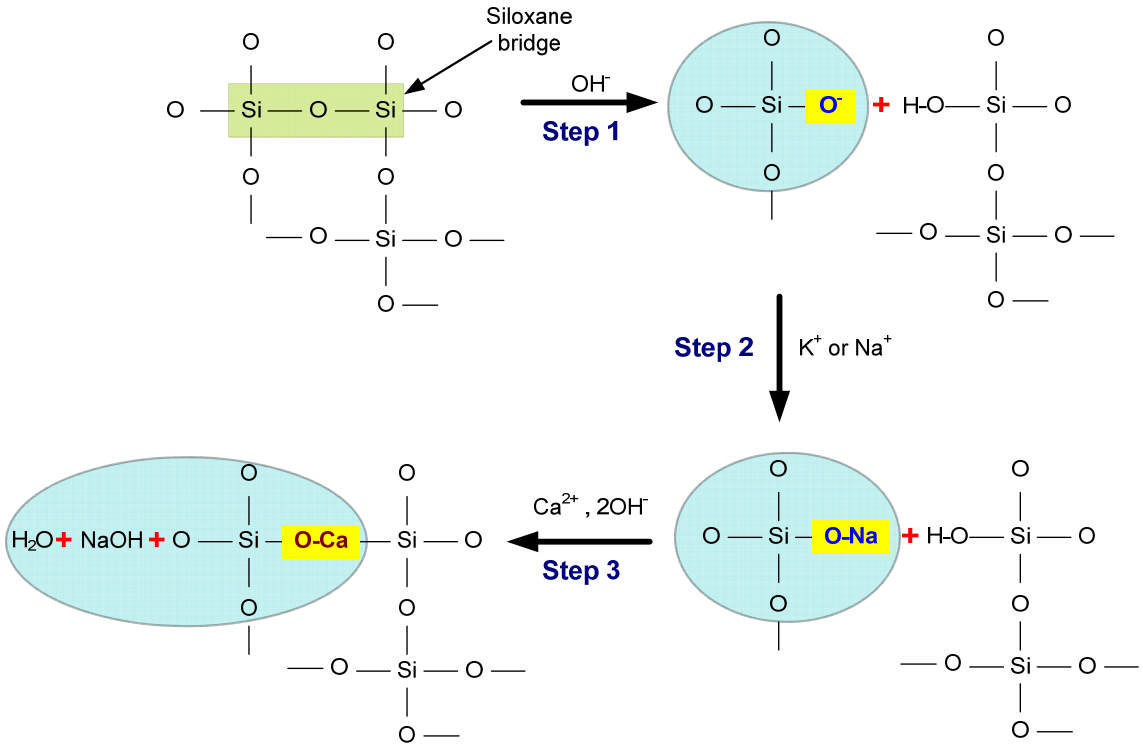

Fig. 6–7. Schematic illustration of alkali-silica reaction

Table 6−1. Chemistry of Test and Pore Solution

Aggregate	Temperature (°C)	Normality of test solution (N)	Chemistry of solution before testing (mol/L)				Chemistry of solution after testing (mol/L)			
			Na	K	Ca	pH	Na	K	Ca	pH
Gravel	80	1	1.73990	0.00000	0.00000	13.78	0.32633	0.00127	0.00007	13.28
	80	0.5	0.86995	0.00000	0.00000	13.77	0.29940	0.00095	0.00005	13.22
	80	0.25	0.43498	0.00000	0.00000	13.75	0.19898	0.00059	0.00005	13.06
New Mexico Rhyolite	80	1	1.73990	0.00000	0.00000	13.78	0.19071	0.00330	0.00011	13.11
	80	0.5	0.86995	0.00000	0.00000	13.77	0.13870	0.00180	0.00009	13.08
	80	0.25	0.43498	0.00000	0.00000	13.75	0.13387	0.00107	0.00006	13.04
Concrete*	80	1	0.34924	0.26855	0.00072	13.43	0.62202	0.21638	0.00030	13.75

*Alkali ion concentrations in pore solution of concrete were measured instead alkali ion concentration of test solution.

The driving force of alkali ions that diffuse to the aggregate grain is dependent on the concentration of alkali hydroxides such as KOH, NaOH, and $Ca(OH)_2$. Provided that sufficient amounts of alkali hydroxides are available, more siloxane bridges (Si-O-Si) are broken in the presence of more OH^- ions. With further breaking of the siloxane bridges, the Na^+ ions which attached to the oxygen to form alkali-silica gel (ASR gel), which consume Na^+ ions due to binding of alkalis by ASR products.

Figure 6-8 shows the reduction in Na^+ ions concentration calculated with following equation:

$$R_{Na} = \left(C_{initial} - C_{final}\right) / C_{initial} \times 100$$

where, R_{Na} is the reduction in Na^+ ion concentration; $C_{initial}$ is the concentration of Na^+ ion before dilatometer test; C_{final} is the concentration of Na^+ ion after dilatometer test.

Reduction in Na^+ ion concentration of gravel at 1N NaOH solution was approximately 81 percent whereas those at 0.5N and 0.25N NaOH solution were 66 percent and 54 percent respectively. New Mexico rhyolite aggregate shows the trend similar to that of gravel, but it yield higher reduction in Na^+ ion concentration.

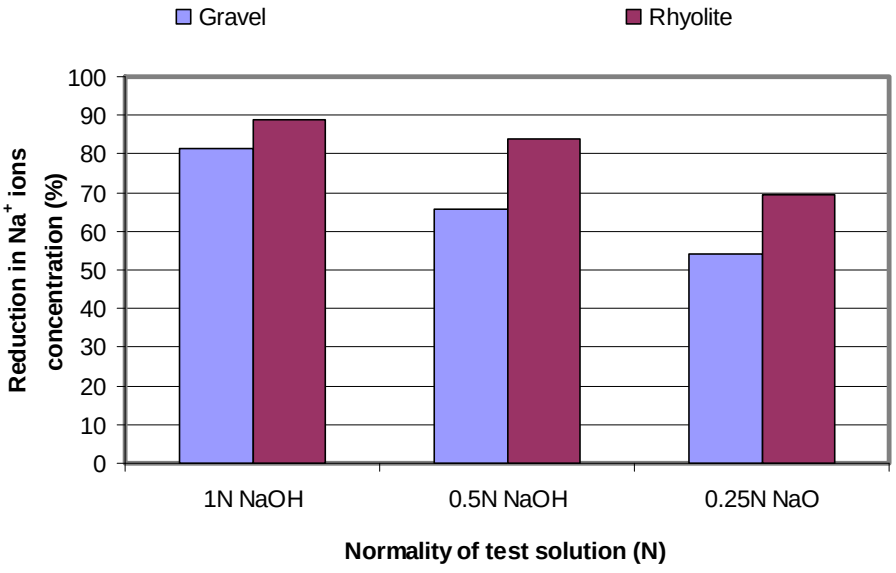

Fig. 6–8. Reduction in Na^+ ion concentration

For K^+ and Ca^{2+} ion concentrations, Table 6-1 shows the substantial augmentation in both ions with increasing the normality of NaOH solution irrespective of aggregate type. This is obviously due to a release of K^+ and Ca^{2+} ions from aggregate and supports the findings by Poulsen et al. (2000), Bérubé et al. (2002), and Constantiner and Diamond (2003): When alkali-bearing aggregates present, some alkalis from aggregates are released into external solutions of alkali hydroxide and calcium hydroxide. Some of these released alkali ions are taken up into ASR products.

Interestingly, released K^+ and Ca^{2+} ion concentrations from rhyolite aggregate are higher than those of gravel aggregate. This can be explained by the chemical analyses results in Table 4-2 shown in Chapter IV. In general, the rhyolite aggregates are formed by the process of molten silica-rich magma flowing toward the earth surface. They typically have 70 to 75 weight percent of silicon dioxide (SiO_2) and more potassium oxide (K_2O) than sodium oxide (Na_2O) as shown in Table 4-2. Finally, a slight decrease in the pH of solution is observed after dilatometer test irrespective of aggregate type and normality of test solution, but the difference in not significant.

Chemistry of Pore Solution in Concrete

For concrete pore solution analyses, Table 6-1 shows Na^+ ion concentration increases with increasing normality of NaOH solution whereas K^+ and Ca^{2+} ion concentrations decrease after dilatometer test. The increase in Na^+ ion concentration is attributed to the readily availability of Na^+ ion from NaOH solution. The normality of test solution strongly contaminates the pore solution alkalinity of the concrete specimen.

A drop in K^+ and Ca^{2+} ion concentrations is attributed to alkali leaching. It should be noted that the concrete specimen was immersed in 1N NaOH solution during the testing, which can allow for leaching of both ions initially present in the specimen and lead to dilution by external solution. As previously explained, the consumption of alkali ions by the formation of ASR gel also can explain the reduction in K^+ and Ca^{2+} ion concentrations.

Solubility of ASR Gel

From an assessment of pore and test solution chemistry, ASR gel seems to be less soluble in the NaOH solution. If ASR gel is very soluble in the NaOH solution, the concentration

of Na^+ ion after dilatometer test should be similar to that before testing. Therefore, the solubility of ASR gel looks low not to cause noticeable shrinkage in volume in dilatometer test. This can be explained by the recent study performed by Ichikawa and Miura (2007):

The consumption of Na^+ or K^+ and OH^- ions by the formation of ASR gel decreases the concentration of OH^- ions surrounding the aggregate, which lead to the dissolution of Ca^{2+} ions into the solution because the solubility of Ca^{2+} ions is proportional to $1/[OH^-]^2$, where $[OH^-]$ is the concentration of OH^- ions. The Ca^{2+} ions then react with ASR gel to generate calcium silicate (Step 3 in Fig. 6-7). The fluid and homogeneous alkali silicate shells are therefore formed on the surfaces of the ASR-affected aggregate. By successive reactions with OH^- and Ca^{2+} ions, it is gradually converted to a semi-permeable rigid film, which is dense enough for preventing the leakage of fluid alkali silicate gel generated after formation of the a semi-permeable film and allowing the penetration of the alkaline solution through the rigid film into the aggregate (Fig. 6-9). Because the rigid film prevents the deformation of the aggregates, the expansion pressure generated by the penetration of the solution is accumulated in the aggregates. When the accumulated pressure exceeds the tolerance of the shells, the pressure explosively cracks the aggregates, which causes the volume expansion in dilatometer test.

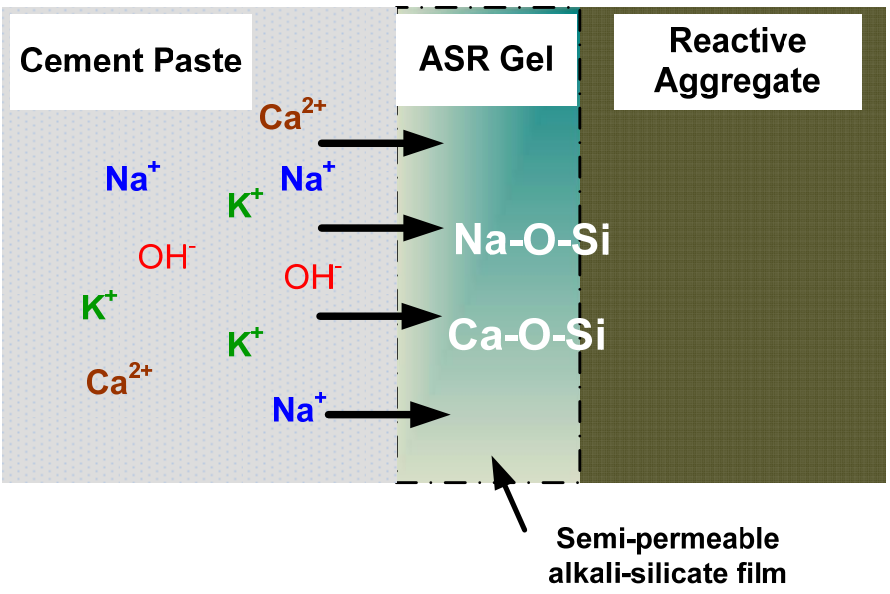

Fig. 6–9. Formation of a semi-permeable alkali-silicate film

DETERMINATION OF AGGREGATE PARAMETERS (ε_a and E_a)

As previously mentioned in the Chapters III and V, the E_a concept integrates the coupled effects of temperature, alkalinity, and time relative to the kinetics of ASR expansion into a single parameter. It was reported that the E_a of different forms of silica mineral matches with degree of its crystallinity (reactivity). In this regard, the E_a can serve as an overall indicator of ASR potential of aggregate. The activation energies corresponding to rhyolite and gravel at both 1N and 0.5N NaOH were calculated and presented in Table 6-2.

Table 6-2 shows the activation energy of siliceous reactive gravel and New Mexico rhyolite within the studied temperature range and age. As previously noted, activation energy (E_a) indicates the energy needed to initiate ASR. The activation energy of rhyolite (37.5 KJ/mol) is lower than that of gravel (53.2 KJ/mol). The reactive siliceous gravel consists of deformed (highly strained) crystalline quartz. It is known that strained quartz is reactive because of crystal defects imposed through deformation. It is to be noted that crystalline quartz without any deformation (strain) is non-reactive. The rhyolite is reactive because of the presence of devitrified volcanic glass.

It is also interesting to note that the E_a shows lower values when normality of test solution is decreased, irrespective of aggregate types. It is indicated that the E_a is a function of alkalinity in aggregate system.

Table 6−2. Characteristics of Expansion Development of Aggregate

Type of Aggregate	Normality of NaOH (N)	Temperature (°C)	Aggregate properties		Type and normality of concrete testing	Concrete/mortar properties			
			Ultimate expansion (ε_a)	E_a (KJ/mol)		Ultimate expansion (ε_0)		$\log\alpha$	β
						volume	[c]linear		
New Mexico Rhyolite	1N	60	0.037	37.5	Dilatometer (at 1N NaOH)	1.90	0.63	14.08	0.18
		70	0.028						
		80	0.046						
	0.5N	60	0.041	50.0	[a]Dilatometer (at 1N NaOH)	1.70	0.57	14.51	0.18
		70	0.014						
		80	0.019						
	0.5N	60	0.041	50.0	[b]Dilatometer (at 0.5N NaOH)	1.20	0.40	16.32	0.16
		70	0.014						
		80	0.019						
Gravel	1N	60	0.026	53.2	Dilatometer (at 1N NaOH)	1.45	0.48	13.97	0.23
		70	0.029						
		80	0.044						
	0.5N	60	0.044	68.9	[a]Dilatometer (at 1N NaOH)	1.23	0.31	14.49	0.23
		70	0.015						
		80	0.030						

[a]Concrete parameters were calculated with activation energy at 0.5N NaOH and concrete expansion data at 1N NaOH.

[b]Concrete parameters were calculated with activation energy at 0.5N NaOH and concrete expansion data at 0.5N NaOH.

[c]Volume expansion was divided by 3 to get the linear expansion (linear expansion = volume expansion / 3).

DETERMINATION OF CONCRETE PARAMETERS (α, β, and ε_0)

Once the activation energy has been determined from testing the aggregate source, the equivalent (t_e) can be estimated by using equation (3-5) with known values of concrete temperatures (T and T_r), age (t), and humidity (γ_H). If the reference temperature (T_r) in equation is 23 ºC, the t_e equals 11.7 hours. The relative expansion ($\varepsilon/\varepsilon_0$) is obtained by dividing the directly measured concrete expansion profiles (Fig. 6-10) by their corresponding ultimate expansion.

Using a linear relationship between double natural logarithm of the relative expansion and natural logarithm of the equivalent age, the coefficients α and β were back-calculated (Fig. 6-11). Because SCMs are not used in concrete mixture, λ is assumed to 1. The $\log\alpha$ and β are found to be 14.08 and 0.18, respectively when the ultimate expansion of concrete (ε_0) of rhyolite is 1.90 percent (volume). The predicted expansion (using equation 3-4) is compared with the dilatometer measured expansion in Fig. 6-12. A perusal of Fig. 6-12 shows that the calculated expansion compares well with the measured one with only a slight deviation.

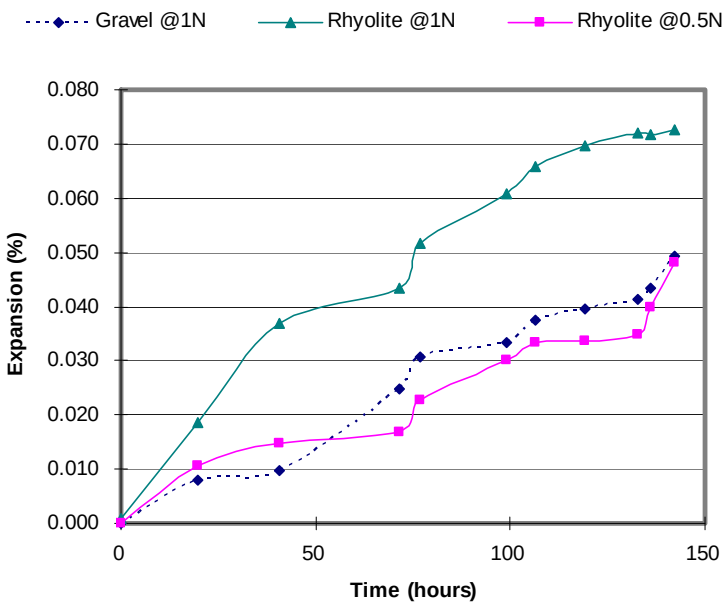

Fig. 6−10. Expansion development of concrete (N = normality)

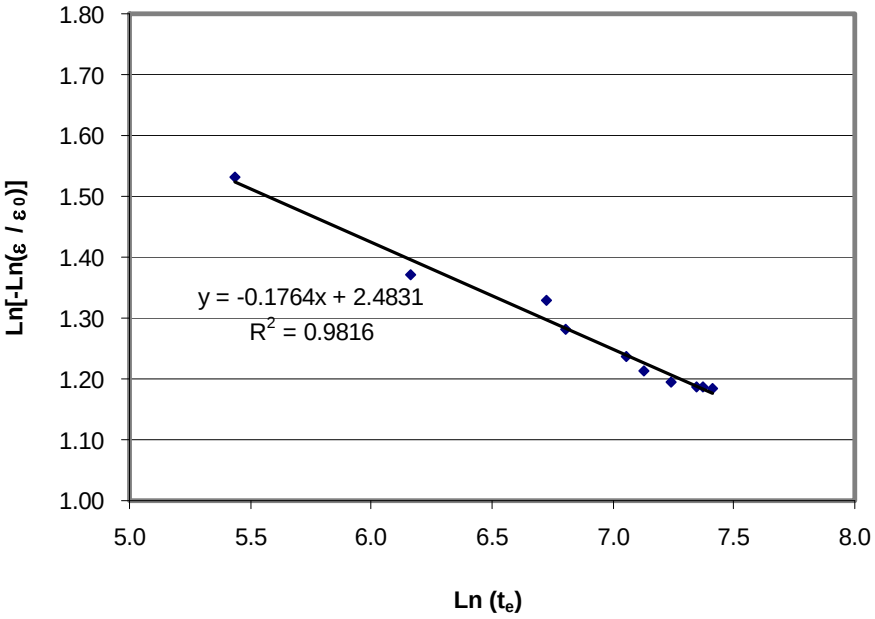

Fig. 6−11. Plot for determining concrete parameters (α and β)

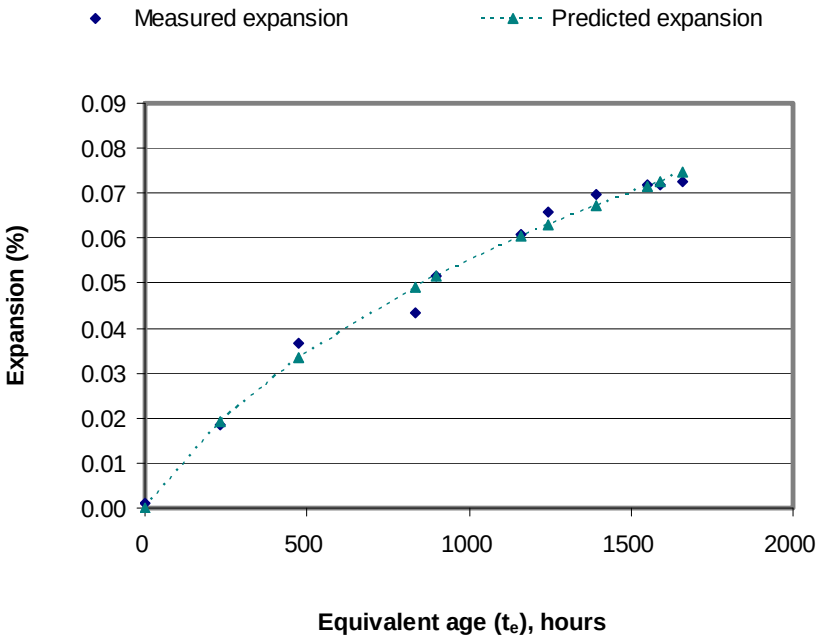

Fig. 6−12. Predicted expansion curves of New Mexico rhyolite concrete

The same calculation procedure was applied to the gravel concrete and the predicted expansion curves of concrete and its ε_0, α, and β values are presented in Fig. 6-13 and Table 6-2, respectively. Similarly, although there is some deviation of the expansion data from actual testing vs. the estimated expansion as calculated from equation (3-4), Figure shows the calculated expansion is in good agreement with the tested expansion.

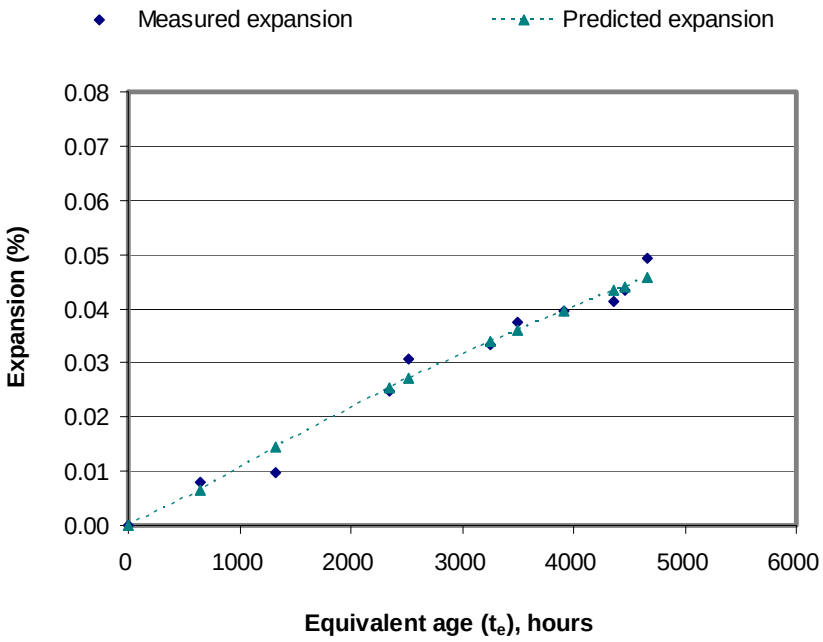

Fig. 6−13. Predicted expansion curves of gravel concrete

Table 6-2 shows the comparison of model parameters determined on the basis of equation (3-4) for each test condition. The ultimate expansion (ε_0) of concrete containing rhyolite is slightly higher than that of concrete containing gravel at the same normality of NaOH solution irrespective of normality of test solution. This is not unexpected as it is observed that rhyolite aggregate is more reactive than reactive gravel aggregate from the expansion behavior (Figs. 6-1 and 6-2).

Concretes in 1N NaOH solution shows higher ultimate expansion than in 0.5N NaOH solution at a given temperature though the same activation energy (50.0 KJ/mol) is used (rhyolite aggregate at 0.5N NaOH). This suggests that normality of the test solution plays a predominant role in the expansion characteristics. From this test result, it can be

interpreted that in the field situation, concrete exposed to a stronger alkali environment condition causes higher ultimate expansion.

Interestingly, as the E_a of aggregate itself increases, the ε_0 of concrete decreases regardless of using the same concrete expansion data and alkali exposure condition. As previously mentioned in the Chapter III, the activation energy associated with ASR indicates the energy to initiate ASR as well as to characterize an aggregate susceptibility to it. It is true that concrete made with more ASR susceptible aggregate produces more rapid and higher expansion in the field if concrete is exposed to the same environment condition. Therefore, the E_a may truly represent aggregate reactivity in concrete as well as aggregate.

In Chapter III, α and β were defined as concrete parameters representing a combined effect of mixture related parameters such as porosity, w/c, diffusion/permeability matching with test condition including temperature and alkalinity. Table 6-2 shows concretes exposed to different test solutions and made with different aggregates have different values of α and β, and consequently achieve different ultimate expansion.

A COMPARATIVE ASSESSMENT BETWEEN DILATOMETER, ASTM C 1260, AND C 1293

Furthering the capability to identify the potential for concrete ASR deterioration and performance is accomplished in part by addressing the suitability of the new performance-based model for assessing ASR potential of concrete; determining if the prediction of ultimate expansion (ε_0) of concrete based on a 2-day aggregate test and a 7-day concrete test is reasonable; and determining if concrete having different mixture proportions and curing temperatures will yield different concrete parameters (α, and β). Furthermore, it may be of interest to bridge the gap between the performance-based method and the ability of current methods to evaluate concrete relative to the field performance.

ASTM C 1293, commonly referred to as the concrete prism test, is currently considered the most accurate and effective test in predicting the field performance of aggregate, but the test is typically run for one year. When testing SCMs or lithium compounds, the test is typically carried out for two years. ASTM C 1260 is also one of the most commonly used methods because test results can be obtained within as little as 14

days, but it represents the worst case scenario (high surface area and high alkalinity) for reactivity for most aggregate tested. If the new approach has correlation with those existing methods, it would be helpful to understand whether or not it can be applied to actual field performance. This section evaluates the correlation between the C 1260 and C 1293 test methods and the performance method.

Value of Activation Energy

As previously mentioned in Chapter III, the E_a associated with ASR indicates the energy to initiate ASR as well as characterize an aggregate's susceptibility to it, which is calculated based on the reaction rate theory that integrates the combination effect of temperature, alkalinity, and time into a single parameter.

In fact, the activation energy of any chemical reactions involving pure phases is a function of aggregate surface area and freshness of the exposed surface, not a function of concentration of the reactants. The E_a of different forms of silica minerals and its correlation with the degree of its crystallinity was confirmed in Chapter V. The value of E_a of aggregate only or mineral would be referred to as a 'pure' value at a given alkalinity. Any other modifications of E_a beyond this must be further delineated.

The E_a capability as a tool to qualify ASR of aggregate relative to a combination of material and alkali conditions in mortar or concrete depends on transport characteristics of mortar or concrete. It relates to either moisture or ionic transport which is broken down into physical and chemical aspects of the concrete's resistance to the potential for ionic ingress, migration, and concentration. Physical resistance of concrete to ionic transport is increased by increasing the tortuosity of the concrete matrix and reducing its permeability or by sealing it against intrusion of surface moisture and keeping the humidity in the concrete at low levels. Chemical resistance to ionic movement is increased by limiting the availability of calcium or the ASR related to ions to reaction sites associated with the aggregate particles. In mortar or concrete systems, each of these mechanisms should be carefully referred to key material properties in order to be useful for the E_a as an indicator of aggregate reactivity. Therefore, the E_a in mortar or concrete may be overestimated or underestimated due to accessibility of calcium or the ASR related ions to reaction sites associated with the aggregate particles. The E_a in mortar or concrete would be an

'effective' value, not the base value to evaluate ASR susceptibility of aggregate because the tortuosity of the combination of its component affect transport performance mechanism.

Fig. 6-14 summarizes the activation energies of aggregates and mortar mixtures within studied temperatures, normalities of NaOH solution, and ages. The E_a of rhyolite aggregate is lower than that of gravel aggregate regardless of normality of test solution regardless of test method (dilatometer and C 1260). From expansion behavior (Figs. 6-1 and 6-2), it is observed that rhyolite aggregate is more reactive than that of gravel aggregate. This is an indication that the energy needed to initiate ASR is relatively low in the case of aggregate with high reactivity. Therefore, aggregate reactivity may be truly represented by activation energy.

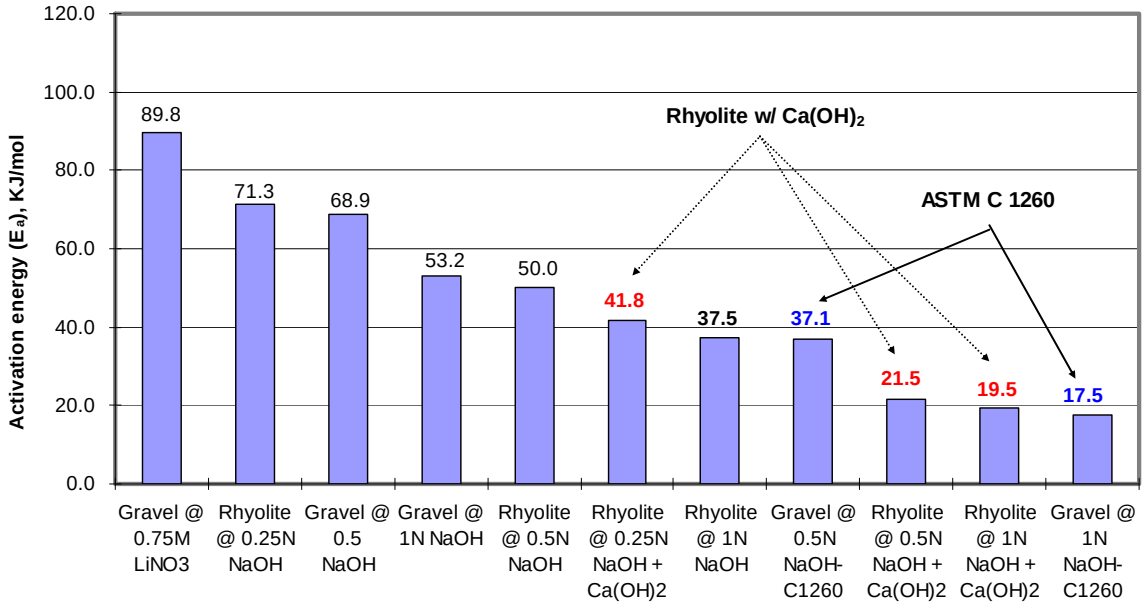

Fig. 6−14. Activation energy of aggregates

On the other hand, the E_a decreases drastically when normality of the test solution is increased from 0.25N to 1N NaOH and when $Ca(OH)_2$ is present, irrespective of the aggregate type and mortar. It can be explained in terms of ionic transport characteristics (Chatterji 1993). As the increasing ionic strength of the solution increases surface charge on the silica grains and the rate of cleaving of the Si-O-Si bonds, the rate of dissolution of silica grains increases. This reaction opens the reactive grains for further attack and forms

acceleration of formation of ASR gel when alkali cations (Na^+ or K^+) enter a reacting grain. Consequently, this causes more rapid and higher expansion and comparatively low E_a.

Interestingly, the values of E_a of mortar mixture containing gravel aggregate at 0.5N and 1N NaOH (the C 1260 test) have been determined to be 37.1 and 17.5 KJ/mol, respectively while the E_a of only aggregate at the same normalities of test solution (dilatometer test) recorded 68.9 and 53.2 KJ/mol. It is important to note that the mortar mixture needs less energy to initiate the ASR. It may contribute to large specific surface area of aggregate as well as the pre-existing internal alkali ions within the cement paste used in the C 1260 test.

Ultimate Expansion of Aggregate (ε_a)

As shown in Table 6-3, the ultimate expansion of aggregate (ε_a) varied with the combination of temperature and normality of NaOH solution while the ε_a of mortar increases with decreasing temperature regardless of testing period. Although it is not clear precisely why this trend is not matched, it can be explained in terms of freshness of the exposed surface area of aggregate exposed to pore solution relative to reaction.

In the dilatometer test, alkali ions directly contact reaction sites associated with the aggregate particles. The reaction is totally dominated by the degree of cystallinity and mode of occurrence and size of the reactive constituents of aggregate exposed to alkali ions. In spite of low normality of NaOH solution, if more reactive sites of each aggregate particle contacts alkali ions, it causes larger ultimate expansion due to high reaction kinetics of aggregate.

In case of mortar specimen, the initial reaction depends on reaction temperature and availability of alkali ions within the cement paste. At later age, the reaction is controlled by the permeability of matrix (the supply alkali ions from the external NaOH solution) along with hydration process. Thus, whereas reaction rate and expansion rate are high but decline with time at elevated temperatures, at low temperature the rate are slower but total expansion may eventually reach or exceed that at higher temperature, regardless of normality of solution (Hobbs 1988; Diamond et al. 1981).

Table 6−3. Characteristics of Expansion Development of Aggregate and Concrete

Type of Aggregate	Normality of NaOH (N)	Temperature (°C)	Aggregate properties		Type and normality of concrete testing	Concrete/mortar properties			
			Ultimate expansion (ε_a)	E_a (KJ/mol)		Ultimate expansion (ε_0)		$\log\alpha$	β
						volume	linear		
New Mexico Rhyolite	1N	60	0.039	37.5	Dilatometer (at 1N NaOH)	1.90	0.63	14.08	0.18
		70	0.052						
		80	0.065						
	1N	60	0.039	37.5	C 1293	2.60	0.87	15.80	0.12
		70	0.052						
		80	0.065						
	1N	60	0.039	37.5	[a]C 1293	1.25	0.42	10.39	0.73
		70	0.052						
		80	0.065						
	1N	60	0.039	37.5	C 1260	12.30	4.10	10.14	0.55
		70	0.052						
		80	0.065						
New Mexico Rhyolite	0.5N	60	0.032	50.0	Dilatometer (at 1N NaOH)	1.70	0.57	14.51	0.18
		70	0.032						
		80	0.041						
	0.5N	60	0.032	50.0	Dilatometer (at 0.5N NaOH)	1.20	0.40	16.32	0.16
		70	0.032						
		80	0.041						
	0.5N	60	0.032	50.0	C 1293	2.40	0.80	18.08	0.12
		70	0.032						
		80	0.041						
	0.5N	60	0.032	50.0	C 1260	12.30	4.10	9.38	0.55
		70	0.032						
		80	0.041						

[a] Concrete without any additional alkali.

Table 6−3. (Cont'd)

Type of Aggregate	Normality of NaOH (N)	Temperature (°C)	Aggregate properties		Type and normality of concrete testing	Concrete/mortar properties			
			Ultimate expansion (ε_a)	E_a (KJ/mol)		Ultimate expansion (ε_0)		$\log \alpha$	β
						volume	linear		
Reactive gravel	1N	60	0.018	53.2	Dilatometer (at 1N NaOH)	1.45	0.48	13.97	0.23
		70	0.027						
		80	0.032						
	1N	60	0.021	89.8	Dilatometer (at 0.75M $LiNO_3$)	1.08	0.36	15.54	0.25
		70	0.026						
		80	0.032						
	1N	60	0.018	53.2	C 1293	1.60	0.53	12.62	0.46
		70	0.027						
		80	0.032						
	1N	60	0.018	53.2	C 1260	15.35	5.12	12.32	0.37
		70	0.027						
		80	0.032						
Reactive gravel	0.5N	60	0.010	68.9	Dilatometer (at 1N NaOH)	1.23	0.41	14.49	0.23
		70	0.013						
		80	0.022						
	0.5N	60	0.010	68.9	C 1293	1.50	0.50	13.39	0.48
		70	0.013						
		80	0.022						
	0.5N	60	0.010	68.9	C 1260	11.30	3.77	12.80	0.41
		70	0.013						
		80	0.022						

[a] Concrete without any additional alkali.

Expansion Characteristics of Mortar and Concrete

Figs. 6-15 through and 6-17 show ASR expansion characteristics of mortar/concretes made with rhyolite and gravel aggregates obtained from different test methods. The expansion differs significantly according to the aggregate type, and the expansion of rhyolite concrete is greater than that of gravel concrete both in dilatometer and ASTM C 1293 testing. This tendency is the same as the test results of aggregate using dilatometer test (Figs. 6-1 through 6-3). As shown in the aggregate test, either increasing normality of test solution or increasing internal alkali content results in a higher expansion.

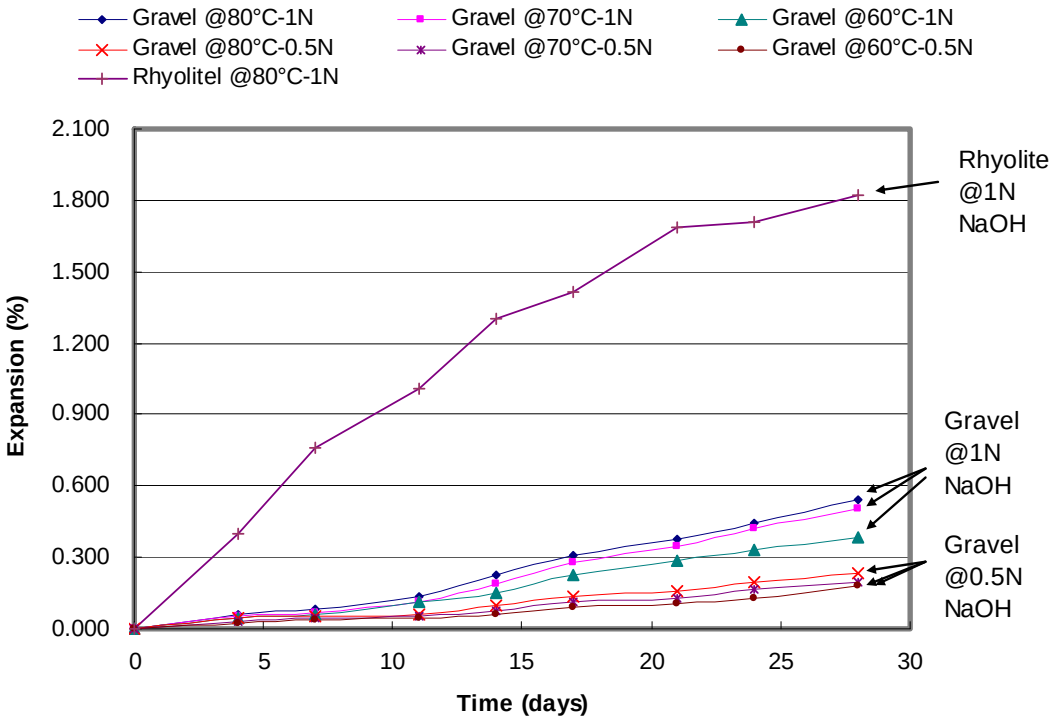

Fig. 6−15. Expansion development of mortar (ASTM C 1260)

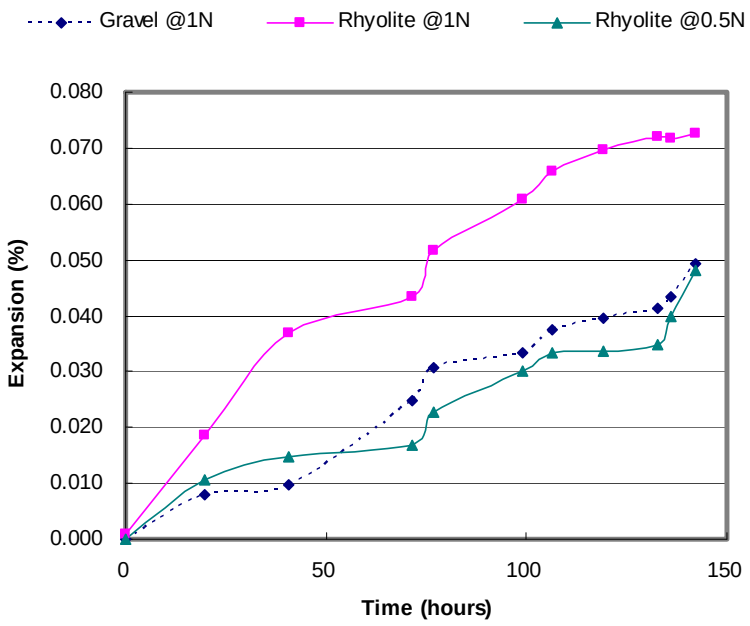

Fig. 6−16. Expansion development of concrete (Dilatometer)

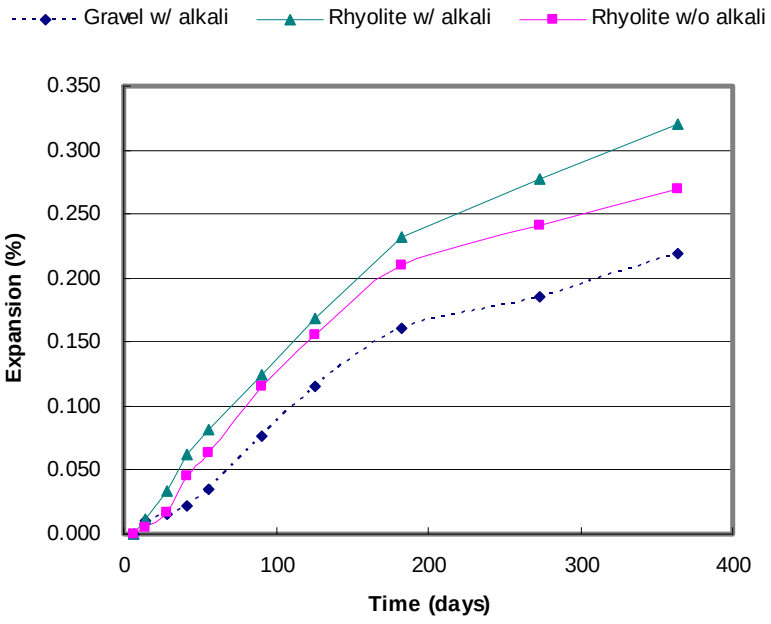

Fig. 6−17. Expansion development of concrete (ASTM C 1293)

Concrete Parameters (ε_0, α, and β)

As described in Chapter III, concrete parameters, ε_0, α, and β, can be determined from interactive calculations between aggregate parameter (E_a), equivalent age, and concrete expansion data at given temperatures and alkalinities. Concrete parameters representing a combined effect of concrete mixture related parameters are a function of the conditions which expansion data was collected and porosity of the concrete. If concrete has similar mixture designs and properties, though test conditions are different, it is expected that concrete will have the similar ultimate expansion.

Activation energies of rhyolite and gravel aggregates obtained from dilatometer test at 1N and 0.5N NaOH were used to evaluate how concrete parameters are affected by different concrete test conditions and methods. The C 1293 linear expansion data was multiplied by 3 to obtain the bulk volume expansion data as measured in the dilatometer (volume expansion = 3 x linear expansion). The factor of 3 was rigorously analyzed and reported by Mukhopadhyay et al. (2004). Like the dilatometer test, the coefficients α and β for C 1260 and C 1293 were derived from the slope and intercept of regressed line in the linearized from of equation (3-8). The comparison of concrete parameters determined on the basis of equation (3-4) with concrete or mortar expansion data using C 1260, C 1293, and dilatometer methods is summarized in Tables 6-3 and 6-4.

Tables 6-4 present the calculated ultimate expansion (ε_0) of mortar/concrete based on the expansion-time relationship of dilatometer, C 1260, and C 1293 for both rhyolite and gravel aggregates. The ε_0 calculated with dilatometer expansion data is slightly lower than that using the C 1293 expansion data, but is in the similar ranges although dilatometer shows higher expansion than that of the C 1293 at early ages. It is noted that higher testing temperature (80 °C) as well as normality of testing solution at dilatometer method are possibly responsible for the higher dilatometer expansion at early age. However, early age expansion and ultimate expansion from both dilatometer and the C 1293 test methods are higher than that of concrete without any additional alkali. The alkalinity level in the both the test was higher than the normal concrete alkalinity (alkali supplied by used cement) because dilatometer test was conducted at 1N NaOH solution whereas in the C 1293 NaOH additional alkali was added in the mix to increase the alkalinity up to 1.25 Na_2O_e.

Table 6–4. Comparison of Expansion Characteristics of Concrete

Days	New Mexico Rhyolite								Gravel					
	C 1260		C 1293		[a] C 1293		Dilatometer		C 1260		C 1293		Dilatometer	
	Linear	Volume (Calc.)	Linear	Volume (Calc.)	Linear	Volume (Calc.)	Linear (Calc.)	Volume	Linear	Volume (Calc.)	Linear	Volume (Calc.)	Linear (Calc.)	Volume
3	0.40	1.19	0.00	0.00	0.00	0.00	0.02	0.07	0.06	0.19	0.00	0.00	0.01	0.04
7	0.76	2.28	0.01	0.03	0.00	0.00	0.02	0.07	0.08	0.24	0.00	0.00	0.02	0.05
14	1.30	3.90	0.01	0.04	0.01	0.02	-	-	0.22	0.67	0.01	0.03	-	-
28	1.82	5.46	0.03	0.10	0.02	0.05	-	-	0.54	1.62	0.02	0.05	-	-
90	-	-	0.13	0.38	0.12	0.35	-	-	-	-	0.08	0.23	-	-
365	-	-	0.32	0.96	0.27	0.81	-	-	-	-	0.22	0.66	-	-
ε_0 (calc.)	4.10	12.30	0.87	2.60	0.42	1.25	0.63	1.90	5.12	15.35	0.53	1.60	0.48	1.45

[a] Concrete without containing additional alkali.

The ε_0 in C 1260 is exceptionally high compared to the C 1293. As previously mentioned, in the C 1260 the aggregates are ground to a specific size for testing. This effect may tend to cause excessively high rate of expansion that are non-existent under field conditions. This higher specific surface characteristic of the C 1260 test method may not be a true representation of ASR reactivity in field concrete. Consequently, the prediction of the ε_0 of concrete based on the only C 1260 expansion history may not be a realistic approach.

Interestingly, when the E_a of 0.75M $LiNO_3$ is used, the ε_0 of gravel concrete is determined to be 0.36 percent linear expansion from dilatometer test (Table 6-3). The effect of lithium compound on reducing ASR expansion of concrete is clearly reflected by the proposed model. Thus, it is concluded that the performance-based model can evaluate the expansion development according to the use of lithium compound.

Figs 6-18 through 6-21 also show that the comparison between the measured and predicted expansion of C 1260 and C 1293 for both rhyolite and gravel aggregates. The predicted expansion matches well with the measured one with a slight deviation regardless of aggregate type.

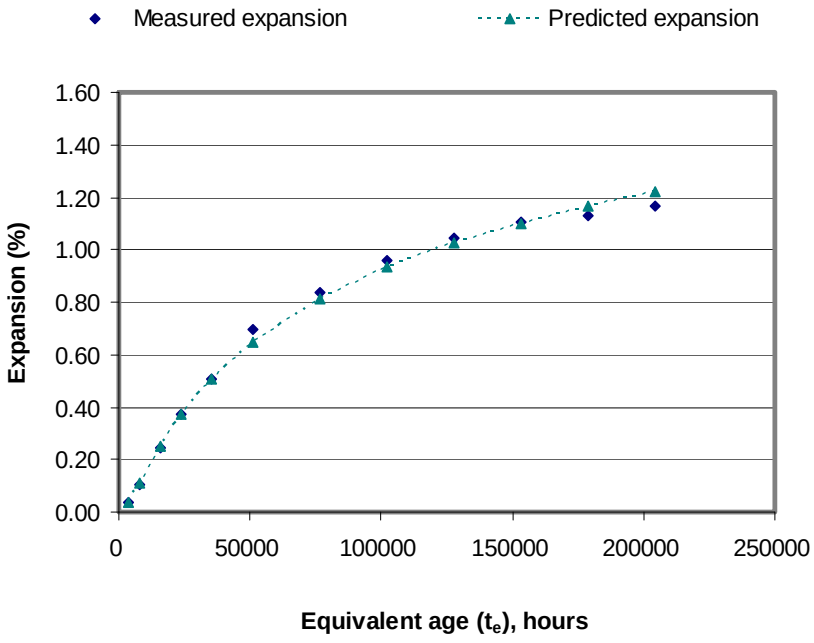

Fig. 6−18. Predicted expansion curve of rhyolite concrete (ASTM C 1293)

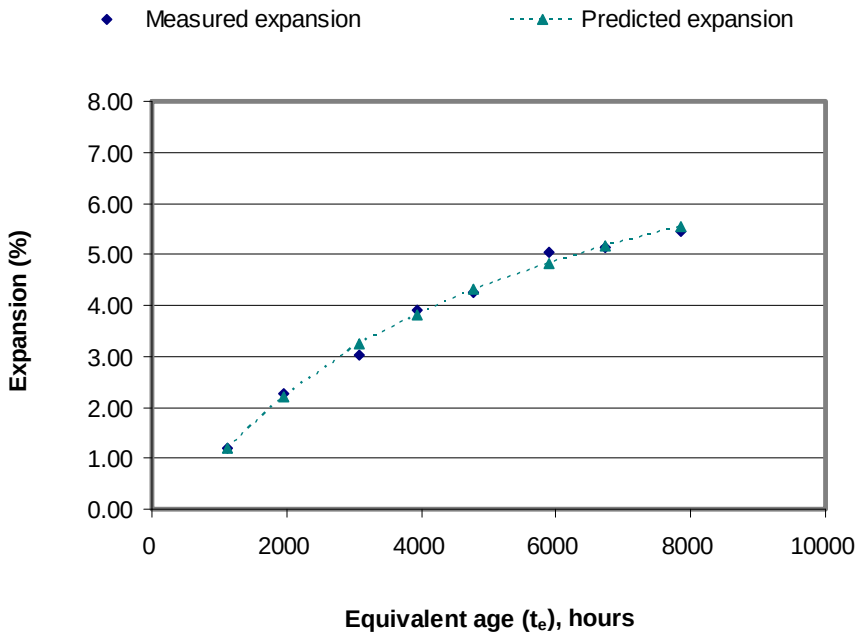

Fig. 6−19. Predicted expansion curve of rhyolite concrete (ASTM C 1260)

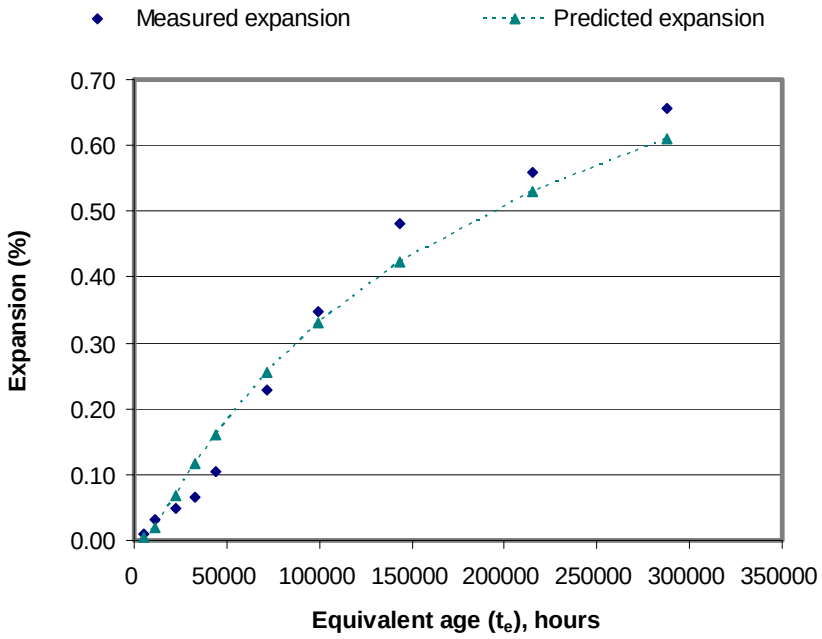

Fig. 6−20. Predicted expansion curve of gravel concrete (ASTM C 1293)

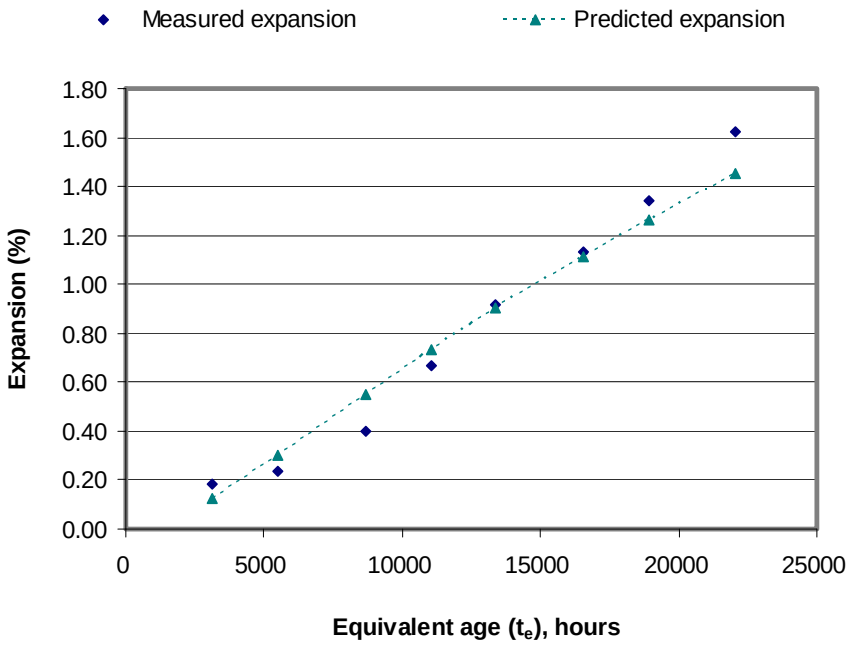

Fig. 6−21. Predicted expansion curve of gravel concrete (ASTM C 1260)

Evaluation of Performance-Based Model

The relative C 1293 expansion estimated on the basis of the performance-based model using equation (3-4) compared with the measured expansion are shown in Figs. 6-22 and 6-23. Concrete parameters α and β obtained from model analyses for C 1260 and dilatometer tests were used to predict the C 1293 expansion behavior. The expansion profiles predicted by the proposed model with α and β parameters in the dilatometer were lower than the measured C 1293 expansion regardless of rhyolite and gravel aggregates. It is noted that the alkalinity level in the C 1293 is possibly responsible for the higher C 1293 expansion (The additional alkali was added to the mixture in order to increase the alkalinity up to 1.25 Na_2O_e in the C 1293). If the total alkali content of the specimen in the dilatometer test by the penetration of available alkalis from NaOH solution matches well to that of C 1293, it is anticipated that the calculated expansion curve corresponds well to the measured one.

When parameters α and β of mortar bar was used, the predicted C 1293 expansion curve is exceptionally high compared to the measured one although the total alkali content in the C 1293 specimen is higher than that of the C 1260. As previously mentioned, the

prediction of the concrete expansion using parameters α and β obtained from C 1260 test may not be a realistic approach because the increased specific surface area of aggregate in the C 1260 using artificially crushed aggregate.

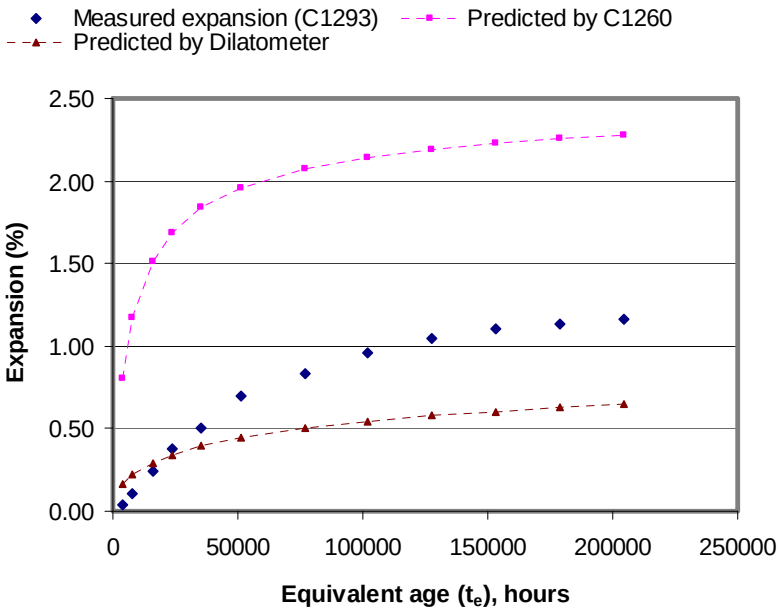

Fig. 6−22. Predicted 1293 expansion of rhyolite concrete

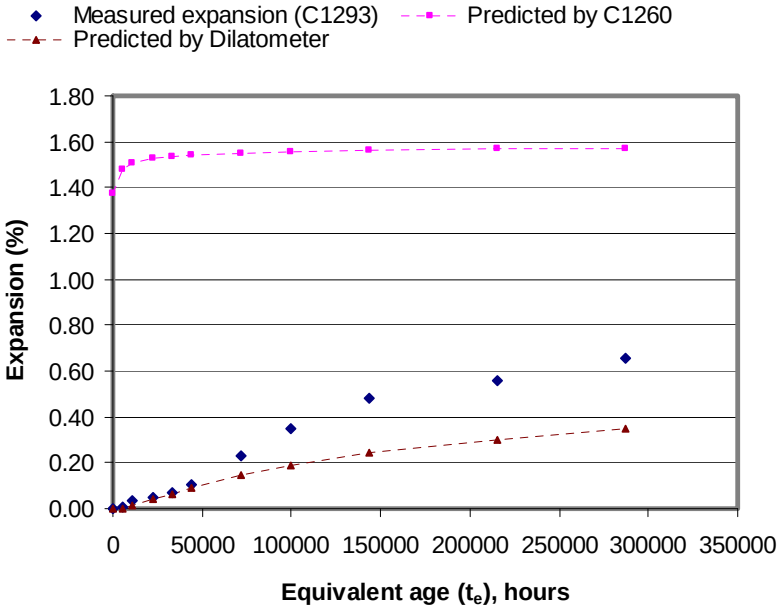

Fig. 6−23. Predicted 1293 expansion of gravel concrete

As previously noted, α and β represent combined effects of mixture related parameters such as w/c and/or porosity at a given temperature and age. If concrete has different mixture designs and properties, though test conditions are same, it has different values of α and β, resulting in the different ultimate expansion due to ASR. Effect of concrete material parameters (α and β) on the expansion-time relationship are given in Fig. 6-24. Curve B has the same value of β as curve A, but has a higher value of α. Curve C has the same value of α as curve A, but has a higher value of β. Changing the value of α preserves the shape of the curve while shifting it to the left to right. Changing the value of β alters the shape of the curve. Therefore, α and β can be used as shape and scale parameters which govern how quickly the ultimate expansion will be achieved in terms of concrete properties such as w/cm and porosity as well as test condition.

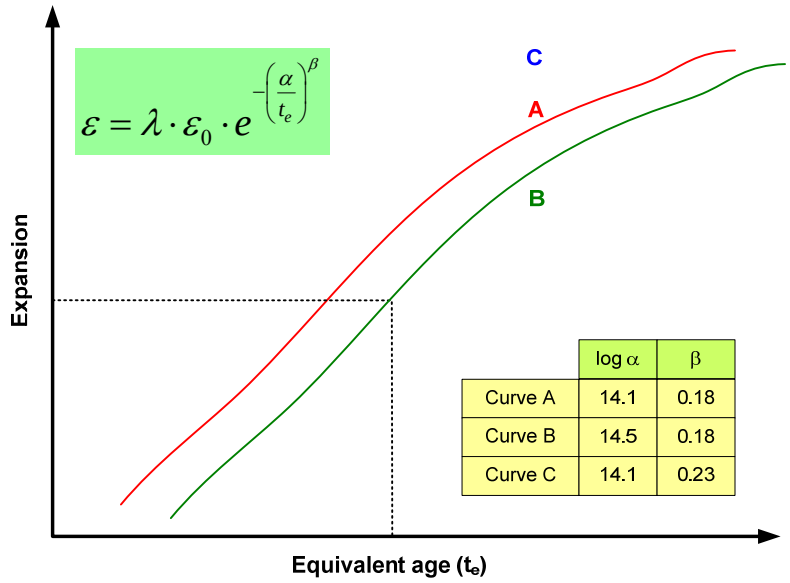

Fig. 6–24. Effect of concrete material parameter (α and β) on the expansion-time relationship

For instance, Table 6-5 shows the comparison of concrete parameters between gravel concrete and rhyolite concrete using dilatometer at different normalities, namely 1N and 0.5N NaOH. Rhyolite concrete at 1N NaOH has the same value of β as at 0.5N NaOH, but has a higher value of α, which indicates that the expansion curve of rhyoite is

shifted to the left to right. As a result, the ultimate expansion of rhyolite concrete at 0.5N NaOH is lower than that at 1N NaOH. The gravel concrete shows the same trend.

Table 6–5. Comparison of Concrete Parameter of Rhyolite Concrete to Gravel Concrete from Dilatometer Test

Type of aggregate	Normality of NaOH (N)	Activation energy (KJ/mol)	Concrete parameters			
			Ultimate expansion (%)		Log α	β
			Volume	Linear		
New Mexico rhyolite	1N	37.5	1.90	0.63	14.08	0.18
	0.5N	50.0	1.70	0.57	14.51	0.18
Reactive gravel	1N	53.2	1.45	0.48	13.97	0.23
	0.5N	68.9	1.23	0.41	14.49	0.23

Concrete parameter values (α and β) obtained with concrete or mortar expansion data using C 1260, C 1293, and dilatometer methods differ in spite of using the same activation energy. It should be noted that the differences in (i) testing temperature (80 °C in dilatometer vs. 38 °C in the C 1293), (ii) alkalinity of concrete (alkalis intruded from test solution in dilatometer vs. internal added alkali in the C 1293), (iii) age (7 days data of dilatometer vs. 1 year of the C 1293) between test methods are clearly manifested by difference in α and β values although the ultimate expansions of concrete are in the similar range. It is also interesting to note that α and β values of concrete with different reactivity of aggregate differ even though the same test method is used.

SUMMARY

To assess ASR potential of aggregate and concrete using the dilatometer test method, a performance-based model has been developed. The idea stems from relating mathematically laboratory and field exposure conditions to field performance based on in part on knowledge of ASR behavior as well as the combination of expansion history over a short period of time. Experimental results indicate that the proposed model can provide the predictability capability of the ASR expansion development in concrete.

Conclusions from this study are based on the limited experimental results presented herein. Further studies are required prior to field implementation of the proposed model.

Because there are some initial conditions related to alkalinity, aggregate reactivity, humidity, and temperature conditions that must be met to initiate ASR, the basis for a more comprehensive laboratory experiments related to key ASR properties is evident.

CHAPTER VII

CONCLUSIONS

Current test methods to assess ASR of aggregate and concrete focus heavily, if not exclusively, on screening aggregate with ASR potential as an empirical approach. Such an approach does not always render satisfactory explanations of all observed phenomena. By introducing a holistic approach, a performance-based model has been developed which couples physical and chemical factors of the aggregate with those of the concrete and mortar. Consistent with observed behavior, a new testing protocol lays the framework for the prediction of concrete expansion due to ASR for a given set of conditions (exposure alkalinity, temperature, etc.), given properties and proportions of individual materials. This research has largely been based on the experimental study of fundamental aspects of ASR with aggregates using a new test device referred to as a dilatometer. This study reports the initial effort to test for and model of selected aggregate and concrete properties with respect to alkali-silica reactivity. Relevant laboratory tests were performed using the dilatometer that directly measures volume changes of aggregate due to reaction products perceived to be ASR.

The basis of the concept of performance-based approach is embedded in a kinetic approach using rate theory (an Arrhenius relationship between temperature and the alkali solution concentration). Because ASR is largely a chemical as well as a thermally activated process, the use of rate theory on dilatometer time-expansion relationship, provides a fundamental aggregate-ASR material property known as “activation energy”. Activation energy is defined as an indicator of aggregate reactivity which is a function of alkalinity, particle size, crystallinity, calcium concentration etc. Test results showed that the E_a varies considerably with aggregate reactivity and alkalinity of test solution.

The noted concrete ASR parameters from performance-based model, E_a, ε_0, α, β, and λ, represent a combined effects of mixture related properties (e.g., w/cm, porosity, presence of SCMs, etc.) and maturity. Therefore, the present performance-based approach provides a direct accountability for a variety of factors that affect ASR, such as aggregate

reactivity, temperature, moisture, calcium concentration, solution alkalinity, water-cementitious material ratio, etc.

Based on the experimental results, the following conclusion can be drawn concerning the performance-based approach to evaluate ASR potential of aggregate and concrete using dilatometer method; (i) the concept of activation energy can be used to represent the reactivity of aggregate subjected to ASR, (ii) the activation energy depends on the reactivity of aggregate and phenomenological alkalinity of test solution, and (iii) The proposed performance-based model provides a means to predict ASR expansion development in concrete.

RECOMMENDATIONS FOR FUTURE STUDY

The work described in this study was based on the limited samples using four minerals and two aggregates. Further studies considering other parameters such as mortar or concrete specimens with different w/cm, SCMs, and aggregates with different reactivities are needed to define the α, β, and λ parameters on a broader scale. Futhermore, size and shape effects of aggregate also must be considered in order to interpret the test results. To this end, it is anticipated the parameters of the proposed model, α, β, and λ, can be selected as a function of the mixture designs enabling the performance prediction of concrete using the tested aggregates at levels of alkalinity predicted for the field condition coupled with the expected temperature and time conditions relative to the kinetics of the ASR expansion mechanism. The determination of E_a, ε_0, α, β, and λ is accomplished from data generated from dilatometer test and that the approach here is much less simulative in nature and much more focused on determining material parameters to ascertain the ASR potential of a given combination of materials.

REFERENCES

ASTM. (1995). “ASTM C 1293-95: Concrete aggregates by determination of length change of concrete due to alkali-silica reaction.” *Annual Book of ASTM Standards*, American Society for Testing Materials, West Conshohocken, PA, 656-661.

ASTM. (1999). “ASTM C 1260-94: Standard test method for potential alkali reactivity of aggregate (mortar-bar method).” *Annual Book of ASTM Standards*, American Society for Testing Materials, West Conshohocken, PA, 646-649.

ASTM. (1999). “ASTM C 227-90: Standard test method for potential alkali reactivity of cement-aggregate combinations (mortar-bar method).” *Annual Book of ASTM Standards*, American Society for Testing Materials, West Conshohocken, PA, 125-129.

ASTM. (1999). “ASTM C 289-94: Standard test method for potential alkali reactivity of aggregate (chemical method).” *Annual Book of ASTM Standards*, American Society for Testing Materials, West Conshohocken, PA, 156-162.

ASTM. (1999). “ASTM C 295: Standard guide for petrographic examination of aggregate for concrete.” *Annual Book of ASTM Standards*, American Society for Testing Materials, West Conshohocken, PA, 175-182.

ASTM. (1999). “ASTM C 441-89, Standard test method for effectiveness of mineral admixture or ground blast-furnace slag in preventing excessive expansion of concrete due to the alkali-silica reaction.” *Annual Book of ASTM Standards*, American Society for Testing Materials, West Conshohocken, PA, 225-227.

Bera, M., Mangialardi, T., and Paolini, A.E. (1994). “Application of the NaOH bath test method for assessing the effectiveness of mineral admixtures against reaction of alkali with artificial siliceous aggregate.” *Cem. Concr. Comp.*, 16, 207-218.

Berube, M.A. and Fournier, B. (1990). “Testing field concrete for future expansion by alkali-aggregate reactions: Canadian developments in testing concrete aggregates for alkali-aggregate reactivity.” *Ministry of Transportation of Ontario Report EM-92*, 162-180.

Berube, M.A., Duchesne, J., and Chouinard, D. (1995). “Evaluating the effectiveness of supplementary cementing materials in suppressing expansion due to alkali-silica reactivity.” *Cem. Concr. Aggr.*, 17(1), 26-34.

Berube, M.A., Fournier, B., Dupond, N., Mongeau, P., and Frenette, J. A. (1992). “Simple autoclave mortar bar method for assessing potential alkali-aggregate reactivity in concrete.” *Proc., 9th Int. Conf. on Alkali-Aggregate Reaction in Concrete*, Slough, 81-91.

Bleszynski, R.F. and Thomas, M.D.A. (1998). “Microstructural studies of alkali silica reaction in fly ash concrete immersed in alkali solutions.” *Adv. Cem. Bas. Mat.*, 7(2), 66-78.

Bleszynski, R.F. and Thomas, M.D.A. (2000). “The efficacy of ternary cementitious systems for controlling expansion due to alkali-silica reaction in concrete.” *Proc., 11th Int. Conf. on Alkali-Aggregate Reaction in Concrete*, Québec City, 583-592.

Bolt, G.H. (1957). “Determination of the charge density of silica sols.” *J. Phys. Chem.*, 61, 1166-1169.

Brandt, M.P. and Oberholster, R.E. (1983). “Study of Tygerberg formation aggregate for potential alkali-reactivity: implications of test methods and applications of the findings in practice.” *SCIR Research Report No. 580*, South Africa, 96.

CANMET. (1991). “Petrography and alkali-aggregate reactivity.” *Course Manual*, Ottawa, 12-14.

Carino, N.J. (1984). “Maturity method: Theory and application.” *Cem. Concr. Aggr.*, 6(2), 61-73.

Carino, N.J. and Lew, H.S. (2001). “The maturity method: from theory to application.” *Proc., the 2001 Structures Congress and Exposition*, Chang, P.C. ed., ASCE, Reston, VA., 19.

Carrasquillo, R.L. and Farbiaz, J. (1988). “Alkali-aggregate reaction in concrete containing fly ash: Final report.” *Research Report #450-3F*, Center of Transportation Research.

Chatterji, S. (1978). “An accelerated method for the detection of alkali aggregate reactivities of aggregates.” *Cem. Concr. Res.*, 8(5), 647-650.

Chatterji, S. (1979). “The role of $Ca(OH)_2$ in the breakdown of portland cement concrete due to alkali-silica reaction.” *Cem. Concr. Res.*, 9(2), 185-188.

Chatterji, S. (1989a). “A critical review of the recent Danish literature on alkali-silica reaction.” *Proc., 8th Int. Conf. on Alkali-Aggregate Reaction in Concrete*, Kyoto, 37-42.

Chatterji, S. (1989b). “Mechanisms of alkali-silica reaction and expansion.” *Proc., 8th Int. Conf. on Alkali-Aggregate Reaction in Concrete*, Kyoto, 101-105.

Chatterji, S. and Kawamura, M. (1992). “Electrical double layer ion transport and reaction in hardened cement paste.” *Cem. Concr. Res.*, 22(5), 774-782.

Chatterji, S. and Thaulow, N. (2000). “Some fundamental aspects of alkali-silica reaction.” *Proc., 11th Int. Conf. on Alkali-Aggregate Reaction in Concrete*, Québec City, 21-29.

Chatterji, S., Thaulow, N., and Jensen, A.D. (1987). “Studies of alkali-silica reaction. Part 4: Effect of different alkali salt solutions on expansion.” *Cem. Concr. Res.*, 17(5), 777-783.

Chatterji, S., Thaulow, N., Jensen, A.D., and Christensen, P. (1986). “Mechanisms of accelerating effects of NaCl and $Ca(OH)_2$ on alkali-silica reaction.” *Proc., 7th Int. Conf. on Alkali-Aggregate Reaction in Concrete*, Ottawa, 115-119.

Conrow, A.D. (1952). “Studies of abnormal expansion of portland cement concrete.” *Proc. Amer. Soc. Test. Mat.*, 52, 1205-1227.

Criaud, A., Vernet, C., and Defosse, C. (1990). “The microbar method, an accelerated expansion test for evaluating aggregates. Assessment of Canadian aggregates, Canadian developments in testing concrete aggregates for alkali-aggregates reactivity.” *Ministry of Transportation of Ontario Report EM-92*, 201-214.

Criaud, A., Vernet, C., and Defosse, C. (1992a). “Evaluation of the effectiveness of mineral admixtures: A quick mortar bar test at 150°C.” *Proc., 9th Int. Conf. on Alkali-Aggregate Reaction in Concrete*, Slough, 192-200.

Criaud, A., Vernet, C., and Defosse, C. (1992b). “A rapid test for detecting the reactivity of aggregates: The microbar method.” *Proc., 9th Int. Conf. on Alkali-Aggregate Reaction in Concrete*, Slough, 201-209.

Dent Glasser, L.S. (1979). “Osmotic pressure and the swelling of gels.” *Cem. Concr. Res.*, 9(4), 515-517.

Dent Glasser, L.S. and Kataoka, N. (1981). “The chemistry of alkali-aggregate.” *Cem Concr. Res.*, 11(1), 1-9.

Dent Glasser, L.S. and Kataoka, N. (1982). “On the role of calcium in the alkali-aggregate reaction.” *Cem Concr Res.*, 12(3), 321-331.

Diamond, S. (1976). “A review of alkali-silica and expansion mechanisms 2. Reactive aggregate.” *Cem Con Res*, 6(4), 549-560.

Diamond, S. (1981). “Effect of two Danish fly ashes on alkali contents of pore solutions of cement-fly ash pastes.” *Cem. Concr. Res*., 11 (3), 383-394.

Diamond, S. (1983). “Alkali reactions in concrete: Pore solution effects.” *Proc., 6th Int. Conf. on Alkalis in Concrete*, Copenhagen, 155-166.

Diamond, S. (1989). “ASR-another look at mechanisms.” *Proc., 8th Int. Conf. on Alkali-Aggregate Reaction in Concrete*, Kyoto, 83-94.

Diamond, S. (1999). “Unique response of $LiNO_3$ as an alkali-silica reaction-prevention admixture.” *Cem. Concr. Res.*, 29, 1271-1275.

Diamond, S. and Penko, M. (1992). “Alkali silica reaction processes: The conversion of cement alkalis to alkali hydroxide”, *Int. Symp. on Durability of Concrete*, ACI SP-131, Detroit, 153-169.

Diamond, S, Barneyback, R.S., and Struble, L.J. (1981). “On the physics and chemistry of alkali-silica reaction.” *Proc., 5th Int. Conf. on Alkali-Aggregate Reaction in Concrete*, Cape Town, S252-22, 1-11.

Duchesne, J. and Berube, M.A. (1994). “Available alkalis from supplementary cementing materials.” *ACI Mater. J.*, 91, 289-299.

Folliard, K.J., Thomas, M.D.A., and Kurtis, K.E. (2002). “Guideline for the use of lithium to mitigate or prevent ASR.” *FHWA-RD-03-047*, Federal Highway Administration, Georgetown Pike, VA.

Fournier, B. (1997). “Management of concrete structures affected by alkali-aggregate reactions-a review.” *CEA Worksh. on Repair of Ageing Concrete Structures*, Montreal, 34.

Fournier, B. and Berube, M.A. (1991). “Application of the NBRI accelerated mortar bar test to siliceous carbonate aggregates produced in the St. Lawrence Lowlands

(Quebec, Canada). Part I: Influence of various parameters on the test results." *Cem. Concr. Res.*, 21,853-862.

Fournier, B. and Berube, M.A. (1993). "Recent applications of a modified gel pat test to determine the potential alkali-silica reactivity of carbonate aggregates." *Cem. Concr. Comp.*, 15, 49-73.

Fournier, B. , Berube, M.A., and Bergaron, G.A. (1991). "A rapid autoclave mortar bar method to determine the potential alkali silica reactivity of St. Lawrence Lowlands carbonate aggregates." *Cem.,Concr. Aggr.*, 13(1), 58-71.

Fournier, B., Berube, M.A., and Rogers, C.A. (2000). "Canadian Standards Association (CSA) standard practice to evaluate potential alkali-aggregate reactivity of aggregates and to select preventive measures against AAR in new concrete structures." *Proc., 11th Int. Conf. on Alkali-Aggregate Reaction in Concrete*, Quebec City, 633-642.

Fournier, B., Nkinamubanzi, P.C., Chevrier, R., and Ferro. (2006). "Evaluation of the effectiveness of high-calcium fly ash in expansion due to alkali-silica reaction (ASR) in concrete." *Rep. No. 1010383*, Electric Power Research Institute (EPRI), Palo Alto, CA.

Gaze, M.E. and Nixon, P.J. (1995). "Effect of PFA upon alkali-aggregate reaction." *Mag. Concr. Res.*, 35(123), 107-110.

German Committee for Reinforced Concrete. (1986). "Guidelines for alkali-aggregate reactions in concrete." *German Building Standards Committee of the Deutches Institute for Normungee*, Subject Specialty VII.

Glauz, D.L., Roberts, D., Jain, V., Moussavi, H., Llewellen, R., and Lenz, B. (1996). "Evaluate the use of mineral admixtures in concrete to mitigate alkali-silica reactivity." *Rep. No. FHWA/CA/OR-97-01*, Office of Materials Engineering and Testing Services, California Department of Transportation, 85.

Grattan-Bellew, P.E. (1989). "Test methods and criteria for evaluating the potential reactivity of aggregates." *Proc., 8th Int. Conf. on Alkali-Aggregate Reaction in Concrete*, Kyoto, 279-294.

Grattan-Bellew, P.E. (1997). "A critical review of ultra-accelerated tests for alkali-silica reactivity." *Cem. Conc. Comp.*, 19, 403-414.

Gress, D.L. and Kozikowski, R.L. (2000). "Accelerated ASR testing of concrete prisms incorporating recycled concrete aggregates." *Proc., 11th Int. Conf. on Alkali-Aggregate Reaction in Concrete*, Quebec City, 1139-1147.

Grosbois, M.D. and Fontaine, E. (2000). "Evaluation of the potential alkali reactivity of concrete aggregate: Performance of testing methods and a procedure's point of view." *Proc., 11th Int. Conf. on Alkali-Aggregate Reaction in Concrete*, Quebec City, 267-276.

Hansen, W.C. (1944). "Studies relating to the mechanism by which the alkali-aggregate reaction proceeds in concrete." *J. Amer. Conc. Inst*. 15(3), 213-227.

Hearne, T.M. Jr., Cowsert, J.E., and Cordle, V.O. (1992). "Monitoring mortar bar alkali-aggregate reactivity." *Trans. Res. Rec. 1362*, Transportation Research Board, National Research Council, Washington, DC, 44-50.

Helmuth, R., Stark, D., Diamond, S., and Moranville-regourd, M. (1993). "Alkali-silica reactivity: An overview of research." *Report SHRP-C-342*, Strategic Highway Research Program, National Research Council, Washington, DC.

Helster, J.A. and Smith, O.F. (1953). "Alkali-aggregate phase of chemical reactivity in concrete." *Highway Research Board Proceedings 32*, Highway Research Board, Washington, DC, 306-312.

Hobbs, D.W. (1988). *Alkali-silica reaction in concrete*, Thomas Telford, London.

Hooton, R.D. (1990). "Inter-laboratory study of the NBRI Rapid test method and CSA standardization status. Canadian developments in testing concrete aggregates for alkali-aggregate reactivity." *Engineering Materials Report 92*, Ontario Ministry of Transportation, 225-240.

Hooton, R.D. and Rogers, C.A. (1989). "Evaluation of rapid test methods for detecting alkali reactive aggregates." *Proc., 8th Int. Conf. on Alkali Aggregate Reaction in Concrete*, Kyoto, 439-444.

Hossain, M. and Zubery, M.H. (1995). "An evaluation of the SHRP alkali-silica reactivity (ASR) test." *Report No. KS U-EES-270*, Kansas Department of Transportation, 45.

Johnston, D.P. (1994a). "Interpretation of accelerated test method ASTM P 214 test results." *Trans. Res. Rec. 1458*, Transportation Research Board, National Research Council, Washington, DC, 129-134.

Johnston, D.P. (1994b). “Alkali-silica reactivity of fine aggregates in South Dakota.” *Report No. SD92-04-F*, South Dakota Department of Transportation, 60.

Johnston, D.P, Stokes, D., and Surdahl, R. (2000). “A kinetic-based method for interpreting ASTM C 1260.” *Cem. Concr. Aggr.*, 22(2), 142-149.

Jones, F.E. and Tarleton, R.D. (1958). “Recommended test procedures, Part IV: Alkali-aggregate reaction, experience with some forms of rapid and accelerated tests for alkali-aggregate reactivity.” *Research Paper No. 25*, DSIR National Building Studies, London, 64.

Kawamura, M., and Takemoto, K. (1986). “Effects of pozzolans and blast furnace slag on alkali hydroxide concentrations in pore solutions and expansion by the alkali-Silica reaction.” *Semento Gijutsu Nenpo*, 40, 328-331.

Kawamura, M., Takemoto, K., and Hasaba, S. (1993). “Application of quantitative EDXA analysis and microhardness measurements to the study of alkali-silica reaction mechanisms.” *Proc., 6th Int. Conf. on Alkali-Aggregate Reaction in Concrete*, Copenhagen, 167-174.

Kilgour, C.L. (1988). *Composition and properties of Indiana fly ashes*, Doctoral Thesis, Purdue University, Indiana.

Knudsen, T. A. (1987). “Continuous, quick chemical method for the characterization of the alkali-silica reactivity of aggregates.” *Proc., 7th Int. Conf. on Alkali-Aggregate Reaction in Concrete*, Ottawa, 289-293.

Knudsen, T.A. (1992). “The chemical shrinkage test: some corollaries.” *Proc., 7th Int. Conf. on Alkali-Aggregate Reaction in Concrete*, London, 543-549.

Knudsen, T.A. and Thaulow, N. (1975). “Quantitative microanalyses of alkali silica gel in concrete.” *Cem. Concr. Res.*, 5(5), 443-454.

Kolleck J.J., Varma, S.P., and Zaris, C. (1986). “Measurement of OH^- concentrations of pore fluids and expansion due to alkali-silica reaction in composite chemistry of cement mortars.” *Proc., 8th Int. Conf. on Chemistry of Cement*, Rio De Janeiro, 183-189.

Kurihara, T. and Katawaki, K. (1989). “Effect of moisture control and inhibition on alkali silica reaction.” *Proc., 8th Int. Conf. on Alkali Aggregate Reaction in Concrete*, Kyoto, Japan, 629-634.

Lane, D.S. (1993). “Experience with ASTM P 214 in testing Virginia aggregates for alkali-silica reactivity.” *Trans. Res. Rec. 1418*, Transportation Research Board, National Research Council, Washington, DC, 8-11.

Lane, D.S. and Ozyildirim, H.C. (1995). “Use of fly ash, slag or silica fume to inhibit alkali-silica reactivity,” *Report No. FHWA/VA-95-R21*, Virginia Department of Transportation, 41.

Larive, C., Laplaud, A., and Coussy, O. (2000). “The role of water in alkali-silica reaction.” *Proc., 11th Int. Conf. on Alkali-Aggregate Reaction in Concrete*, Québec City, 61-69.

Ludwig, U. (1989). “Effects of environmental conditions on alkali-aggregate reaction and preventive measures.” *Proc., 8th Int. Conf. on Alkali-Aggregate Reaction in Concrete*, Kyoto, 583-596.

Marks, V.J. (1996). “Characteristics of Iowa fine aggregate.” *Report, No. MLR-92-6*, Iowa Department of Transportation, 57.

McGowan, J.K. and Vivian, H.E. (1952). “Studies in cement-aggregate reaction: Correlation between crack development and expansion of mortar.” *Australian J. Appl. Sc.*, 3. 228-232.

Metha, P.K. (2004). “High-performance, high-volume fly ash concrete for sustainable development.” *Proc., Int. Workshop on Sustainable Development and Concrete Technology*, Beijing, 3-14.

Mehta, P.K. and Monteiro, P.J.M. (1992). *Concrete: Structure, Properties, and Materials (2nd Ed.)*. Prentice Hall, Upper Saddle River, NJ.

Mindess, S., Young, J.F., and Darwin, D. (2002). *Concrete (2nd Ed.)*, Prentice Hall, Upper Saddle River, NJ, 142-154.

Mukhopadhyay, A.K., Neekhra, S., and Zollinger, D.G. (2004). “Preliminary characterization of aggregate coefficient of thermal expansion and gradation for paving concrete.” *Research report FHWA/TX-04/0-1700-5*, Texas Transportation Institute, TX.

Mukhopadhyay, A.K., Shon, C.-S., and Zollinger, D.G. (2006). “Activation energy of alkali silica reaction and dilatometer method,” *Trans. Res. Rec. 1979*, Transportation Research Board, National Research Council, Washington, DC, 1-11.

Munowitz, M. (2000). *Principles of chemistry*, Norton & Company, London.

Nishibayashi, S, Yamura, K., and Matsuhita, H. A. (1987). "Rapid methods of determining the alkali aggregate reaction in concrete by autoclave," *Proc., 7th Int. Conf. on Alkali-Aggregate Reaction in Concrete*, Ottawa, 299-303.

Nixon, P.J. and Sims, I. (1992). "RILEM TC 106 alkali aggregate reaction-accelerated tests interim report and summary of national specifications." *Proc., 9th Int. Conf. on Alkali-Aggregate Reaction in Concrete*, Slough, 731-738.

Nixon, P.J., Canham, I., Page, C., and Bollinghaus, R. (1987). "Sodium chloride and alkali-aggregate reaction, concrete alkali-aggregate reactions." *Proc., 7th Int. Conf. on Alkali-Aggregate Reaction*, Ottawa, 110.

Oberholster, R.E. (1992). "The effect of different outdoor exposure conditions on the expansion due to alkali-silica reaction." *Proc., 9th Int. Conf. on Alkali-Aggregate Reaction in Concrete*, Slough, 623-628.

Oberholster, R.E. (1994). "Alkali-silica reaction." *In Fulton's concrete technology*, Portland Cement Institute, Midrand.

Oberholster, R.E. and Davies, G. (1986), "An accelerated method for testing the potential alkali reactivity of siliceous aggregates," *Cem.Conc.Res.*, 16 (2), pp. 181-189.

Olafsson, H. (1986). "The effect of relative humidity and temperature on alkali expansion of mortar bars." *Proc., 7th Int. Conf. on Alkali Aggregate Reaction in Concrete*, Ottawa, 461-465.

Pedneault, A. (1996). *Development of testing and analytical procedures for the evaluation of the residual potential of reaction, expansion, and deterioration of concrete affected by ASR*. M.Sc. Memoir, Laval Univeristy, Québec City, 133.

Pike, R. and Hubbard, D. (1957). "Miscellaneous observations on the alkali aggregate reaction and the ionic charge on hydrated cement." *36th Ann. Meeting of Highway Research Board*, Washington, DC, 16-33.

Poulsen, E., Hansen, T., and Sørensen, H. (2000). "Release of alkalies from feldspar in concrete and mortar." *Proc., 5th Int. Conf. on Durability of Concrete*, Barcelona, 807-824.

Power, T.C. and Steinour, H.H. (1995). “An investigation of some published researches on alkali-aggregate reaction. The chemical reactions and mechanism of expansion.” *J. Amer. Conc. Inst.,* 26(6), 497-512.

Rangaraju, P.R. and Sompura, K.R. (2005). “Influence of cement composition on expansions observed in standard and modified astm c 1260 test procedures.” *Trans. Res. Rec. 1914*, Transportation Research Board, National Research Council, Washington, DC, 53-60.

Rasheeduzzafar, M.G. (1993). “Cathodic protection current accelerates alkali-silica reaction.” *ACI Mat. J.*, 90, 247-252.

Regourd-Moranville, M. (1989). “Products of reaction and petrographic examination.” *Proc., 8th Int. Conf. on Alkali-Aggregate Reaction in Concrete*, Kyoto, 445-456.

Rodrigues, F.A., Monteiro, P.J.M., and Sposito, G. (1999). “The alkali-silica reaction: The surface charge density of silica and its effect on expansive pressure.” *Cem. Concr. Res.*, 29(4), 527-530.

Rogers, C.A. and Hooton, R.D. (1989). “Leaching of alkalies in alkali-aggregate reaction testing.” *Proc., 5th Int. Conf. on Alkali-Aggregate Reaction in Concrete*, Kyoto, 327-332.

Roy, S.K., Beng, P.K., and Northwood, D.O. (1997). “Identifying alkali reactivity of concrete aggregates-tests on autoclaved concrete samples.” *Proc., 3rd CANMET/ACI Conf. on High-Performance Concrete, Kuala Lumpur*, 193-207.

Saouma, V. and Perotti, L. (2006). “Constitutive model for alkali-aggregate reactions.” *ACI Mat. J.*, 103(3), 194-202.

Sarkar, S.L., Zollinger, D.G., Mukhopadhyay, A.K., Lim, S., and Shon, C.-S. (2004). “Handbook for identification of alkali-silica reactivity in airfield pavements.” *Advisory circular, AC No. 150/5380-8,* U.S. Department of Transportation Federal Aviation Administration.

Schmitt, J.W. and Stark, D.C. (1989). “Recent progress in development of the osmotic cell to determine potential for alkali-silica reactivity of aggregates.” *Proc., 8th Int. Conf. on Alkali-Aggregate Reaction in Concrete*, Kyoto, 423-431.

Sergi, G. (1992). “The effects of cathodic protection on alkali-silica reaction in reinforced concrete, stage 2.” *TRRL Contractor Report CR310*, Transportation and Road Research Laboratory, Crowthorne, 22.

Shayan, A., Diggins, R.G. , Ivanusec, L., and Westgate, P.L. (1988). “Accelerated testing of some Australian and overseas aggregates for alkali aggregate reactivity.” *Cem. Concr. Res.*, 18, 843-851.

Shehata, M.H. and Thomas, M.D.A. (2000). “The effect of fly ash composition on the expansion of concrete due to alkali silica reaction.” *Cem. Conr. Res.*, 30(7), 1063-1072.

Shehata, M.H., Thomas, M.D.A., and Bleszynski, R.F. (1999). “The effect of fly ash composition on the chemistry of pore solution in hydrated cement paste.” *Cem. Conc. Res*., 29(12), 1915-1920.

Shon, C.-S., Sarkar, S.L., Zollinger, D.G. (2004). “Testing the effectiveness of class c and class f fly ash in controlling expansion due to alkali-silica reaction using modified astm c 1260 test method,” *J. Mat. in Civ. Eng.*, 16 (1), 20-27.

Shon, C.-S., Zollinger, D.G., and Sarkar, L.S. (2003). “Application of modified ASTM C 1260 test for fly ash-cement mixtures.” *Trans. Res. Rec. 1834*, Transportation Research Board, National Research Council, Washington, DC, 93-106.

Sorrentino, D., Clement, J. Y., and Golberg, J. M. (1992). “A new approach to characterize the chemical reactivity of the aggregates.” *Proc., 9th Int. Conf. on Alkali-Aggregate Reaction in Concrete*, Slough, 1009-1016.

Stanton, T.E. (1940). “Expansion of concrete through reaction between cement and aggregate.” *Proc., Amer. Soc. Civ. Eng.*, 66, 1781-1811.

Stanton, T.E. (1943). “Studies to develop an accelerated test procedure for the detection of adversely reactive cement-aggregate combinations.” *ASTM Proc.*, 43, 875-905.

Stanton, T.E., Portep, O.J., Meder, L.C., and Nicol A. (1942). “California experience with the expansion of concrete through reaction between cement and aggregates.” *ACI J.*, 13(3), 209-235.

Stark, D. (1983). “Osmotic cell test to identify potential for alkali-aggregate reactivity.” *Proc., 6th Int. Conf. on Alkali-Aggregate Reaction in Concrete*, Copenhagen, 351-357.

Stark, D. (1992). “Lithium salt admixture-An alternative method to prevent expansion alkali-silica reactivity.” *Proc., 9th Int. Conf. on Alkali-Aggregate Reaction in Concrete*, Slough, 1017-1025.

Stark, D. (1993). “Alkali-silica reactivity: An overview of research.” *Strategic Highway Research Program SHRP-C-342*, National Research Council, Washington DC.

Stark, D. and Bhatty, M.S.Y. (1986). “Alkali-silica reactivity: Effect of alkali on aggregate expansion in alkalies in concrete.” *ASTM STP 930*, American Society for Testing and Materials, Philadelphia, PA., 16-30.

Stark, D., Morgan, B., and Okamoto, P. (1993). “Eliminating or minimizing alkali-silica reactivity.” *SHRP-C-343, Strategic Highway Research Program*, National Research Council, Washington, DC.

Steffens, A., Li, K., and Coussy, O. (2003). “Aging approach to water effect on alkali-silica reaction degradation of structures.” *J. Eng. Mech*., 129(1), 50-59.

Struble, L.J. and Diamond, S. (1981a). “Swelling properties of synthetic alkali silica gels.” *J. Amer. Cer. Soc.*, 64(11), 652-656.

Struble, L.J. and Diamond, S. (1981b). “Unstable swelling behavior of alkali silica gels.” *Cem. Concr. Res.*, 11(4) 611-617.

Strunge, H. and Chatterji, S. (1991). “Studies of alkali silica reaction: Part 8. Correlation between mortar-bar expansion and values.” *Cem. Conc. Res.*, 21, 61-65.

Swamy, R.N. (1992). *Testing for alkali-silica reaction, the alkali silica reaction in Concrete*, Blackie &Sons, Glasgow, 54-95.

Tamura, H. (1987). “A test method on rapid identification of alkali reactivity aggregate (GBRC rapid method).” *Proc., 7th Int. Conf. on Alkali-Aggregate Reaction*, Ottawa, 304-308.

Tamura, H., Hoshino, Y., and Saito, H. (1984). “An experiment on rapid identification of alkali reactivity of aggregates.” *CAJ Review*, 100-103.

Tang, M.S. and Han, S.F. (1983b). “Rapid method for determining the preventive effect of mineral admixtures on alkali-silica reaction.” *Proc., 6th Int. Conf. on Alkali-Aggregate Reaction in Concrete*, Copenhagen, 383-386.

Tang, M.S., Han, S.F., and Zhen, S.H. (1983a). “A rapid method for identification of alkali-reactivity of aggregate.” *Cem. Concr. Res.*, 13, 417-422.

Tatematsu, H. and Sasaki, T. (1989). “Proposal of a new index for a modified chemical method.” *Proc., 8th Int. Conf. on Alkali-Aggregate Reaction in Concrete*, Kyoto, 333-338.

Thaulow, N. and Olafsson, H. (1983). “Alkali-silica reactivity of sands comparison of various test methods-Nordtest project.” *Proc., 6th Int. Conf. on Alkali-Aggregate Reaction in Concrete*, Copenhagen, 359-365.

Thomas, M.D.A. (1994). *The effect of fly ash on alkali-aggregate reaction in concrete*, Building Research Establishment, Garston.

Thomas, M.D.A. (2000). “The role of calcium hydroxide in alkali recycling in concrete.” *Workshop on the Role of Calcium Hydroxide in Concrete*, Anna Maria, 225-236.

Thomas, M.D.A. (2001). “The role of calcium hydroxide in alkali recycling in concrete.” *In Material Science of Concrete: Calcium Hydroxide in Concrete*, The American Ceramic Society, Westerville, OH, 225-236.

Thomas, M.D.A. and Bleszynski, R.F. (2001). “The use of silica fume to control expansion due to alkali-aggregate reactivity in concrete.” *Material Science of Concrete VI*, American Ceramics Society, PA, 350-371.

Thomas, M.D.A. and Innis, F.A. (1998). “Effect of slag on expansion due to alkali-silica reaction in concrete.” *ACI Mat. J.*, 95(6), 716-724.

Thomas, M.D.A., Blackwell, B.Q., and Pettifer, K. (1992). “Suppression of damage from alkali silica reaction by fly ash in concrete dams.” *Proc., 9th Int. Conf. on Alkali-Aggregate Reaction in Concrete*, 2, Slough, 1059-1066.

Thomas, M.D.A., Nixon, P.J., and Pettifer, K. (1991). “The effect of pulverized fuel ash with a high total alkali content on alkali silica reaction in concrete containing natural U.K. aggregate.” *Proc. 2nd Int. Conf. on Durability of Concrete*, 2, Detroit, 919-940.

Thompson, M. (2000). “Field installation in Pennsylvania to assess SHRP recommendations for ASR control: Part 2-Laboratory testing of job material.” *Proc., 11th Int. Conf. on Alkali-Aggregate Reaction in Concrete*, Québec City, 1215-1224.

Tomosawa, F., Tamura, K., and Abe, M. (1989). “Influence of water content of concrete on alkali-aggregate reaction.” *Proc. 8th Int. Conf. on Alkali Aggregate Reaction in Concrete*, Kyoto, 881-885.

Turriziani, R. (1986). “Internal degradation of concrete: Alkali aggregate reaction, reinforcement steel corrosion.” *Proc., 8th Int. Cong. on Chemistry of Cement*, Rio De Janeiro, 388-441.

Uomoto, T., Furusawa, Y. and Ohga, H. (1992). “A simple kinetics based model for predicting alkali-silica reaction.” *Proc., 9th Int. Conf. on Alkali-Aggregate Reaction in Concrete*, Slough, 2, 1077-1084.

Verbeck, G.J. and Gramlich, C. (1955). “Osmotic studies and hypotheses concerning alkali-aggregate reaction.” *Proc., the American Society for Testing and Materials*, 55, 1110-1128.

Vivian, H.E. (1981). “The effect of drying on reactive aggregate and mortar expansions.” *Proc., 5th Int. Conf. on Alkali Aggregate Reaction in Concrete*, Cape Town, , 252-28.

Wang, H. and Gillot, J.E. (1991). “Mechanisms of alkali-silica reaction and the significance of calcium hydroxide.” *Cem. Con. Res.*, 21(4), 647-654.

West, G. (1991). “A note on undulatory extinction of quartz in granite.” *J. Eng. Geol.*, 24(1), 159-165.

Zhang, X., Blackwell, B.Q., and Groves, G.W. (1990). “The microstructure of reactive aggregate.” *Brit. Cer. Trans. J.*, 89, 89-92.

APPENDIX A

UNIT CONVERSION FACTORS

Quantity	In.-lb unit	SI unit*	Conversion factor (Ratio: in.-lb/SI)
Length	Inch (in.)	Millimeter (mm)	25.40
Volume	Cubic foot (ft^3)	Cubic meter (m^3)	0.02832
	Cubic yard (yd^3)	Cubic meter (m^3)	0.7646
Mass	Pound (lb)	Kilogram (kg)	0.4536
Stress	Pounds per square inch (psi)	Megapascal (MPa)	$6.895x10^{-2}$
Density	Pounds per cubic foot (lb/ft^3)	Kilograms per cubic meter (kg/m^3)	16.02
	Pounds per cubic yard (lb/ft^3)	Kilograms per cubic meter (kg/m^3)	0.5933
Temperature	Degree Fahrenheit (°F)	Degree Celsius (°C)	9/5(°C+32°)

* International System of Unit

APPENDIX B

SAMPLING, PREPARATION, AND CALCULATION OF AMOUNT OF AGGREGATE SAMPLES FOR DILATOMETER TESTING

1. SCOPE

This section covers the procedure for the sampling and preparation of aggregate samples for dilatometer testing by means of splitting or quartering, sieving, and volume calculation of aggregates.

2. SAMPLING AND PREPARATION OF AGGREGATE

2.1 Obtain test portions from the field sample.

2.2 Obtain a suitable size of aggregate samples by splitting (Fig. B-1) or quartering (Fig. B-2) according to ASTM C 702-71T. Splitting is for fine aggregate samples that are drier than the saturated surface-dry condition and for coarse aggregates, whereas quartering is for fine aggregate samples having free moisture on the particle surface.

2.3 Determine maximum aggregate size.

2.4 Select sieve size according to Tables B-1 and B-2 (ASTM C 33 and C 136) and the number of sieve size used in calculation of fineness modulus (FM). In general, the sieve sizes used for fine aggregate and intermediate aggregate are 75 μm (No. 200), 150 μm (No. 100), 300 μm (No.50), 600 μm (No.30), 1.18 mm (No.16), 2.36 mm (No.8), 4.75 mm (No.4), 9.5 mm (3/8 in.), and 19 mm (3/4 in.). For coarse aggregate, the sieve sizes are 2.36 mm (No.8), 4.75 mm (No.4), 9.5 mm (3/8 in.), 19 mm (3/4 in.), 25 mm (1 in.), and

37.5 mm (1 ½ in.).

(a) (b)

Fig. B–1. Riffle sampler for the reduction of the size of aggregate sample by splitting: (a) Small riffle sampler for fine aggregates. (b) Large riffle samplers for coarse aggregate

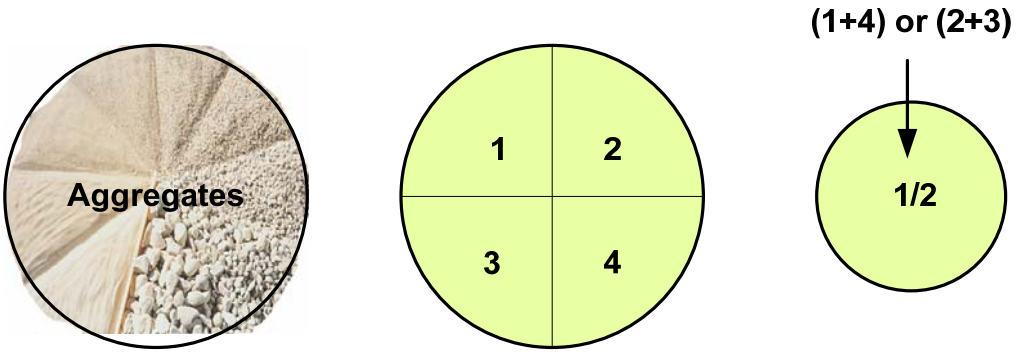

Fig. B–2. Reduction of the size of aggregate sample by quartering. (a) Mix and form cone new cone. (b) Sample divided into quarters. (c) Retain opposite quarters; reject the other two quarters

Table B–1. Grading Requirements for Fine Aggregate

Sieve No.	Sieve Size (mm)	% of passing
10	9.5	100
4	4.75	95~100
8	2.36	80~100
16	1.18	50~85
30	0.60	25~60
50	0.30	10~30
100	0.15	2~10

Table B–2. Grading Requirements for Coarse Aggregate

Sieve size (mm)	Size of coarse aggregate									
	90~40	**65~40**	**50~25**	**50~5**	**40~20**	**40~5**	**25~5**	**20~5**	**15~5**	**10~2.5**
100	100									
90	90~100									
75		100								
63	25~60	90~100	100	100						
50		35~70	90~100	95~100	100	100				
37.7	0~15	0~15	35~70		90~100	95~100	100			
25			0~15	35~70	20~55		95~100	100		
19				0~15	35~70	20~55		95~100	100	
12.5			0~5	10~30			25~60		90~100	100
9.5					0~5	10~30		20~55	40~70	85~100
4.75				0~5		0~5	0~10	0~10	0~15	10~80
2.36							0~5	0~5	0~5	0~10
1.18										0~5

*When maximum aggregate size is selected to 25 mm (1 in.).

2.5 Perform sieving, determine percentage of passing or portions retained on the various sieves, find fineness modulus (FM), and plot gradation curve. Because the 80 percent of aggregate out of 100 percent total volume of cylindrical container of dilatometer is used for

dilatometer test, actual weight retention on the selected sieves obtained from sieve analysis is used in order to fix the aggregate quantity for all the tests.

3. DETERMINATION OF ACTUAL WEIGHT OF AGGREGATE FOR AGGREGATE TEST

3.1 The cylindrical container is able to accommodate aggregates with size as large as 75 mm (3 in.). Furthermore, concrete / mortar cylindrical specimens (4 in. diameter x 5.5 in. height) can also be tested in this device.

3.2 Use the 80 percent of aggregate (by volume) of total volume of cylindrical container.

3.3 Follow the same aggregate gradation, i.e., weight percent retention on each sieve remains fixed for all the tested aggregates.

3.4 Prepare the oven-dry (overnight) aggregate sample before testing.

3.5 Weigh the empty unit weight cylinder (dilatometer) and record it as $Wt_{cylinder}$.

3.6 Fill the cylinder in three layers: Rod each layer 25 times.

3.7 After filling in 3 layers up to the top, level the surface with the tamping rod.

3.8 Weigh the cylinder with the aggregate and record it as $Wt_{cylinder+aggr.}$

3.9 Find the inside volume of the cylinder, $V_{cylinder}$.

3.10 Dry-Rodded Unit Weight (DRUW) is given by

$$DRUW = \gamma_d = \frac{Wt_{cylinder+aggr.} - Wt_{cylinder}}{V_{cylinder}}$$

3.11 The actual weight of aggregate for aggregate test is calculated using the following

equation.

$$Wt_{80\%\ aggregate} = 0.8 \cdot \gamma_d \cdot V_{cylinder} = 0.8 \cdot \gamma_d \cdot \frac{\pi \cdot d^2 \cdot h}{4}$$

3.12 Use this formula to calculate the weight of the aggregates necessary to make 80% of the total volume of the cylindrical container. This way allows that we can keep constant volume for all the tested aggregates (Fig. B-3).

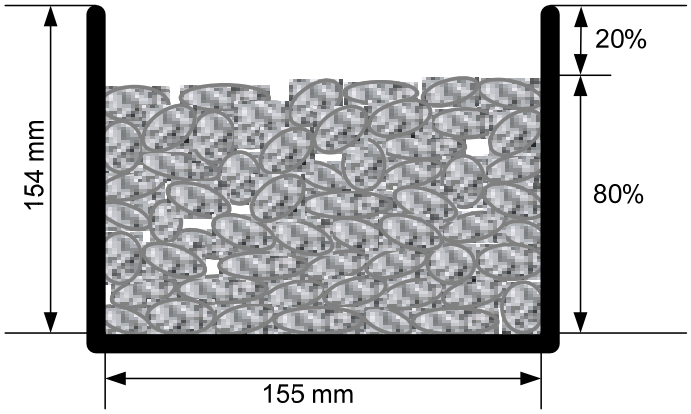

Fig. B–3. Calculation of amount of aggregate used in the test

4. EXAMPLE

In general, the reactivity of an aggregate increases as the size of aggregate decreases. The reactivity of an aggregate in a crushed condition with a higher specific surface, which is a common practice in some existing test methods (e.g. ASTM C 289, C 411, and C 1260), may not represent the reactivity under field conditions. Therefore, aggregate in the dilatometer method is tested in uncrushed condition (an as-received condition). However, the amount of passing on each selected sieve is kept constant for tested aggregate to make

the particle size distribution a common denominator.

After sampling by quartering method, New Mexico rhyolite (NMR) aggregate was oven-dried overnight, and then dry rodded unit weight (DRUW) test of aggregate sample in dilatometer was performed. Table B-3 shows the calculation of DRUW of NMR aggregate.

The maximum size of NMR aggregate was decided as 25mm (1 in.). In accordance with Table B-2, six different sieves which are 2.36 mm (No.8), 4.75 mm (No.4), 9.5 mm (3/8in.), 19 mm (3/4in.), 25 mm (1in.), and 37.5 mm (1 1/2in.), were selected. NMR aggregate had the following percentage passing the coarse sieves (Table B-4) and plotted the grading curves (Fig. B-4) with the grading limits of coarse aggregates given in Table B-2.

NMR aggregates used in this study were satisfied with ASTM limitation. Therefore, the portions retained on the selected various sieves are used to aggregate dilatometer test and casting mortar or concrete specimen.

Table B–3. Dry Rodded Unit Weight (DRUW) of New Mexico Rhyolite Aggregate in Dilatometer

		NMR Aggregate			Average
		Trial 1	Trial 2	Trial 3	
Weight $_{cylinder+aggregate}$ (g)		9875.5	9910.8	9900.5	9895.6
Weight $_{cylinder}$ (g)		5305.5	5305.5	5305.5	5305.5
Weight $_{aggregate}$ (g)		4572.5	4680.6	4670.6	4641.2
Weight $_{cylinder+water}$ (g)		8218.6	8218.6	8218.6	8218.6
Volume $_{cylinder\ (by\ water)}$		2913.1	2913.1	2913.1	2913.1
DRUW	Kg/m^3	1569.3	1606.7	1593.2	1593.2
	lb/ft^3	98.0	100.3	100.1	99.5
Weight $_{80\%\ aggregate}$					3712.99

Table B–4. Sieve Analyses for New Mexico Rhyolite Aggregate

Sieve Size (mm)	Cumulative amount passing (%)	Amount Retained (wt. %)	Actual weight retention (g)
75 (3 in.)	100	0	0
37.5 (1 1/2 in.)	100	0	0
25 (1 in.)	4.7	4.7	175.3
19 (3/4 in.)	63.1	58.3	2166.9
9.5 (3/8 in.)	95.0	31.9	1186.0
4.75 (No. 4)	99.2	4.2	154.7
2.36 (No. 8)	100.0	0.8	31.0
Total weight of sample			3713.0

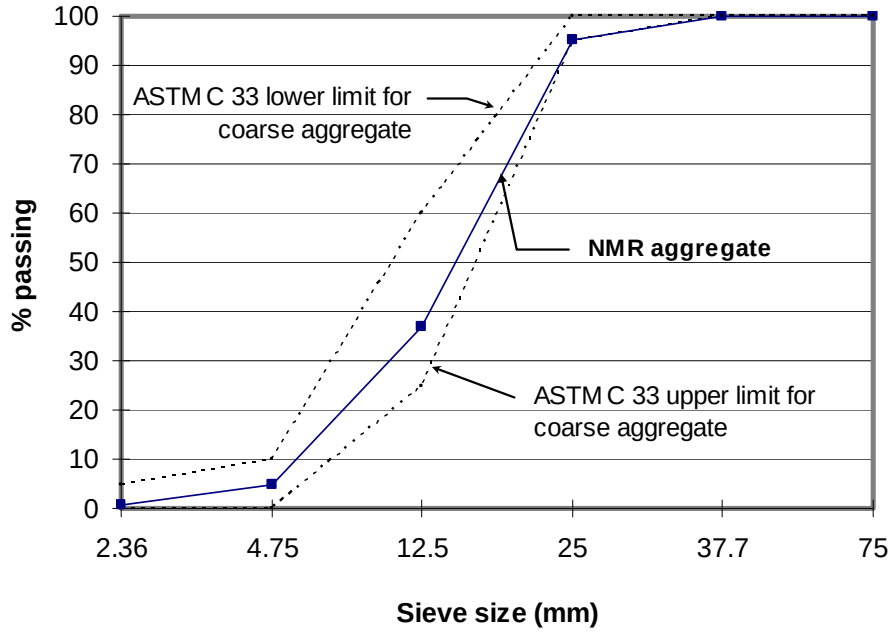

Fig. B–4. Gradation curve of NMR aggregate

APPENDIX C

TEST PROTOCOL FOR DETERMINATION OF ALKALI-SILICA REACTIVITY EXPANSION OF AGGREGATE, MORTAR, AND CONCRETE USING DILATOMETER

1. SCOPE

This section covers determination of the alkali-silica reactivity (ASR) expansion of coarse and fine aggregates by using the dilatometer. It can also be used to determine the ASR expansion of mortar and concrete specimens

2. APPARATUS

The apparatus developed to measure the ASR expansion of aggregate, referred to as dilatometer, is illustrated in Fig. C-1. It basically consists of a stainless steel cylindrical container, a lid, a hollowed tower standing on the lid and a float. The inner surface of the lid is configured at 15 degree angle so that the entrapped air bubbles can move readily along the surface. On the side of the tower, there are three access holes with three screws. These screws are used to adjust the initial sodium hydroxide (NaOH) solution surface level to the desired height.

When the dilatometer is in use, the aggregate sample and NaOH solution are filled in the container. The float moves freely along with the NaOH solution surface. A linear variable differential transducer (LVDT) is installed and its core is connected to the float to measure the rise of the NaOH solution surface. Electrical signals from the LVDT are generated as the core moves. The signals are acquired and amplified by a signal conditioner and then recorded by a computer data acquisition system. The LVDT used is SCHAEVITZ Model 1000 HCA, which provides a displacement of 2 inches (± 1 in.). This provides a sufficiently high accuracy in the measurement of a certain volume change in the small area of the NaOH solution surface in the tower. A thermocouple is immersed in the NaOH solution to monitor the temperature inside the container. The temperature is recorded along with the LVDT signal by the same computer data acquisition system. In operation, the container is placed in the water bath and heated by the water surrounding it.

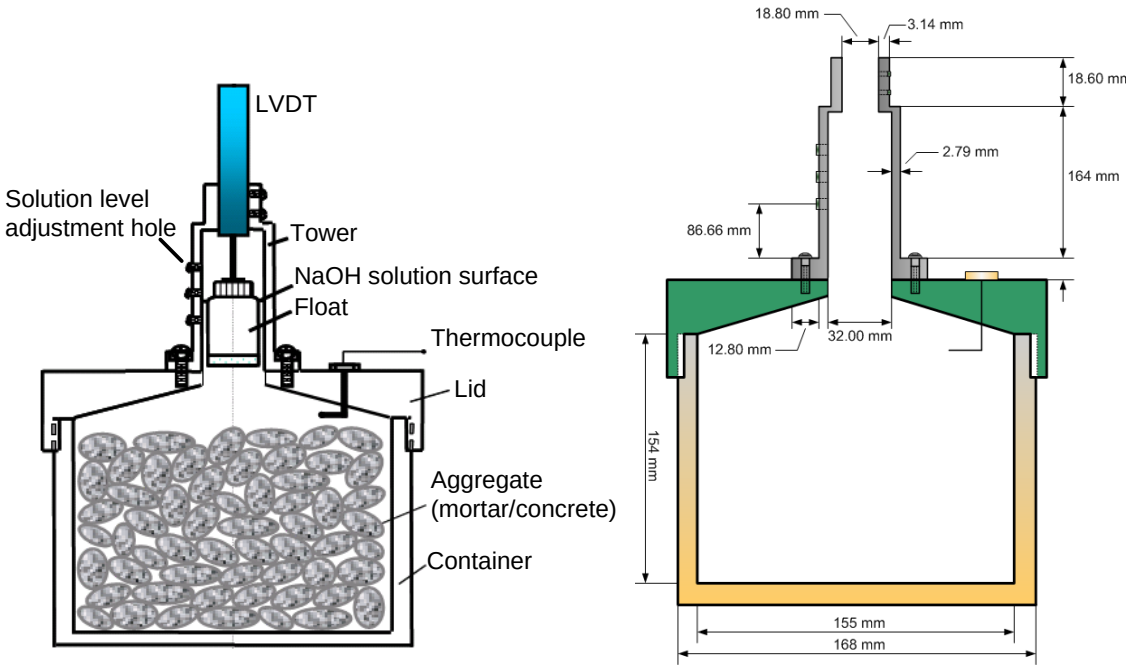

(a) Cross-section of the testing apparatus (b) Dilatometer dimension

Fig. C–1. The dilatometer device

3. PREPARATION OF TEST SOLUTION

4.1 The test solution is prepared from 40 g of sodium hydroxide (NaOH) dissolved in 900 mL of water, diluted with additional distilled water to obtain 1.0 L of solution. A 1.0 ± 0.01N NaOH solution is prepared and standardized to ± 0.001N. Similarly, 0.5N and 0.25N NaOH solutions are also prepared.

4. PROCEDURE

4.1 Measure the weight of oven-dried aggregate (W_{od}) according to the procedure described in Appendix B.

4.2 Mix the aggregates, fill the flask with aggregates, and then make surface of aggregate smooth by shacking the container.

4.3 Fill the flask with NaOH solution and immerse the aggregate for at least 1 day before starting actual test (Fig. C-2).

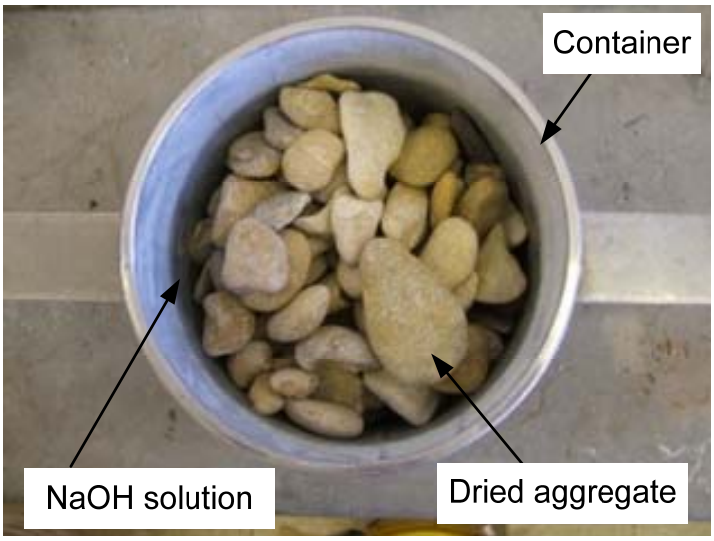

Fig. C–2. Filled aggregates and NaOH solution in the container at room temperature

4.4 Insert the float into the tower. Screw the lid on the flask and ensure against leaks. Use the clip to hold the float system when the lid is securely screwed to close the container (Fig. C-3).

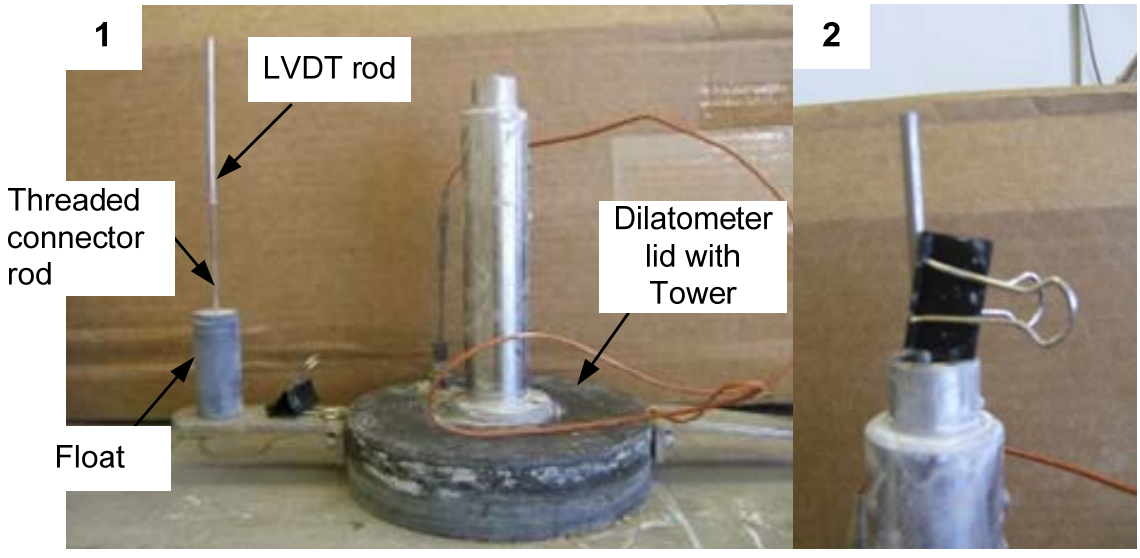

Fig. C–3. Filled aggregates and NaOH solution in the container at room temperature

4.5 Unscrew the selected screw on the side of the tower and fill in additional NaOH solution. Check the float has proper buoyancy, and then put back the screw (Fig. C-4).

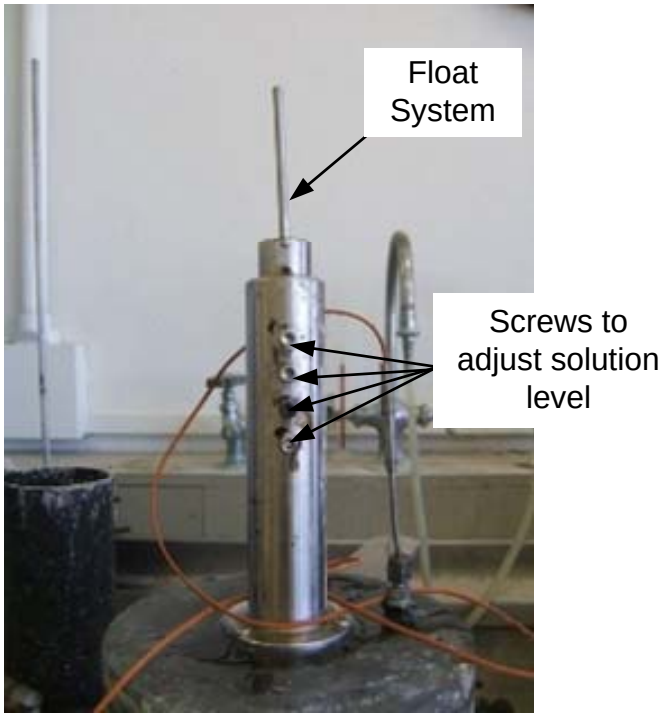

Fig. C–4. Filled aggregates and NaOH solution in the container at room temperature

4.6 Apply a vacuum (35 mm Hg) for 45 minutes through the top opening of the tower by means of a de-airing system shown in Fig. C-5. A-C Motor pump of 1725 rpm (GE-MOD 5KC36LN83X) is used for the vacuum. Apply vibration while vacuuming to facilitate removal of entrapped air efficiently.

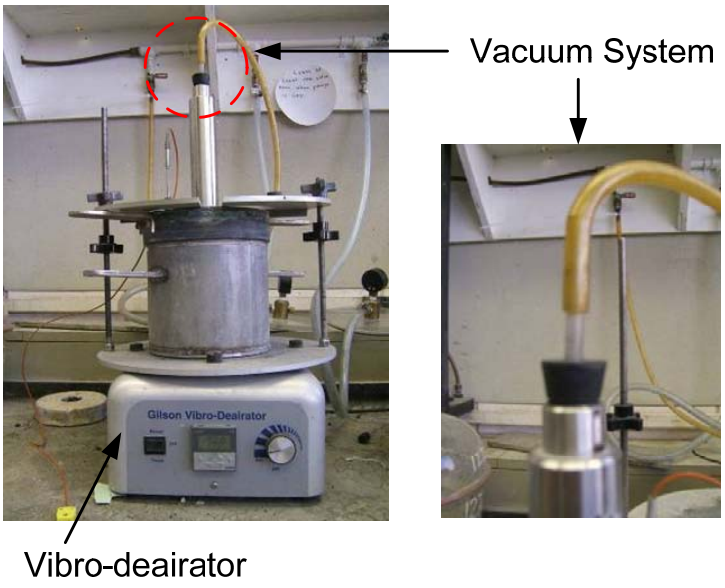

Fig. C–5. A vacuum to remove entrapped air between aggregate particles

4.7 Move the dilatometer device to the water bath. Let it equilibrate for about an hour at the room temperature. Unscrew the selected screw on the side of the tower and let NaOH solution come out freely. When there is no more NaOH solution flowing out, put back the screw. Check the float buoyancy again (Fig. C-6).

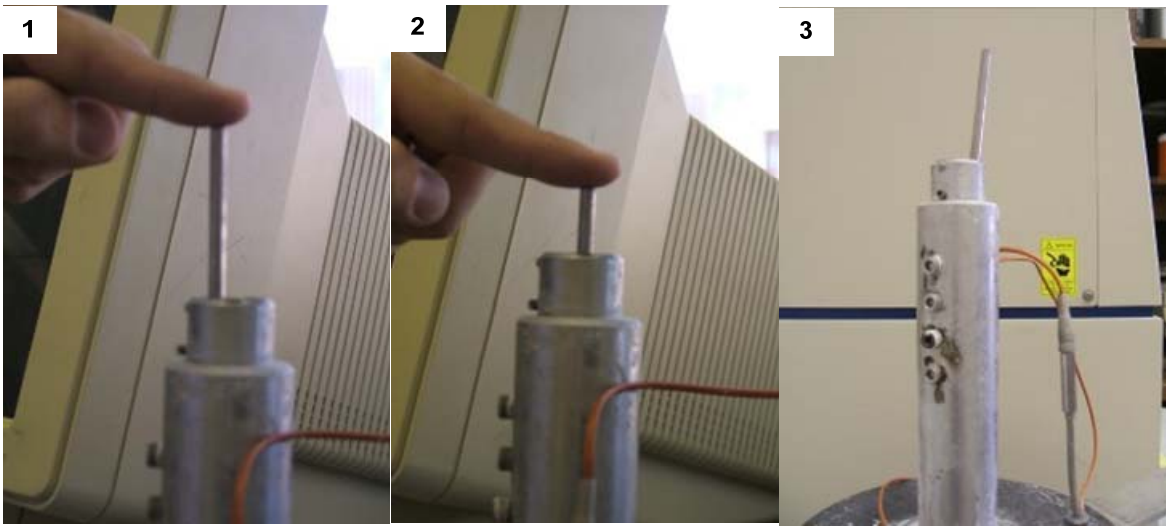

Fig. C–6. Float buoyancy: A reasonably good uplift force after releasing the float in step 3 is an indication for sufficient buoyancy.

4.8 Install LVDT in the tower with its core connected to the float to measure the rise of the test solution surface (Fig. C-7). If necessary, add more solution in the cavity of the tower until the float is positioned properly.

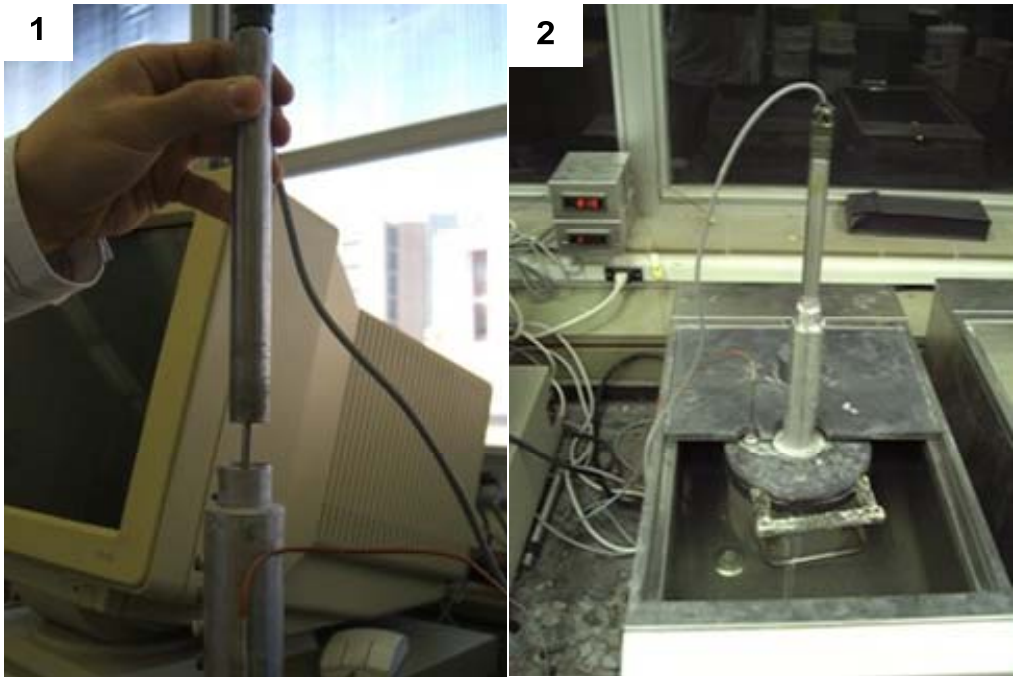

Fig. C–7. Float buoyancy: A reasonably good uplift force after releasing the float in step 3

4.9 Heat the water in the water bath with (rate of heating) to the desired temperature (e.g., 60 / 70 / 80 °C). It takes around 1 hour to reach 80 °C. It takes additional 4 hours for NaOH solution temperature inside dilatometer to be equilibrated with the water bath temperature. This additional time can be considered as a stabilization time to reach target temperature. Recorded temperature and LVDT readings by the computer data acquisition system at this stage represent the initial LVDT reading at stabilized target temperature (Fig. C-8).

4.10 LVDT readings after the specified period of testing (e.g., 48 hours) represent the final readings.

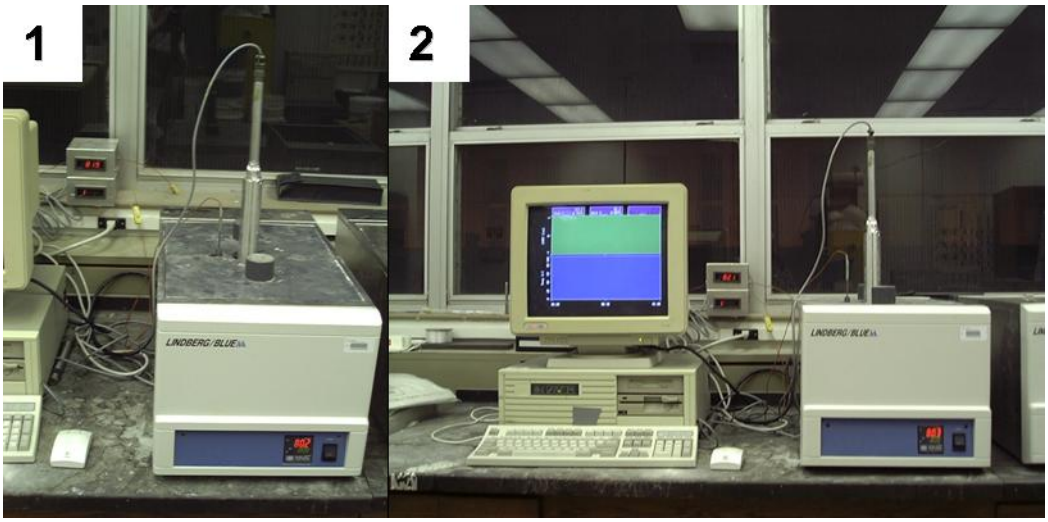

Fig. C–8. Setup of dilatometer system

5. Calculation

5.1 The volume of change of aggregate, mortar, and concrete specimen is generally considered as the most sensitive index of internal micro-cracking due to ASR. For dilatometer tests, Fig. C-9 shows measuring volume change. The volume change is calculated as follows:

$$\varepsilon_n = \frac{\Delta V_{ASR}}{V_{aggregate}} \times 100$$

Where, ε_n = percent expansion at n hours; $V_{aggregate}$ = initial aggregate volume; ΔV_{ASR} = the volume changes due to ASR at n hours at a given normality of NaOH solution and target temperature.

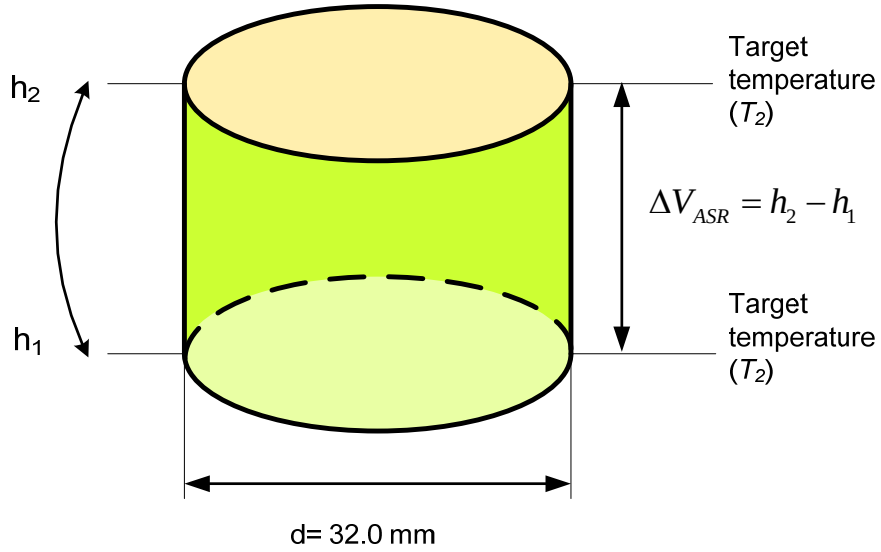

Fig. C–9. Diagram of specimen volume change due to ASR of aggregate or concrete

5.2 It should be noted that ASR expansion is calculated from only volume changes on and after the dilatometer is reached to the target temperature (e.g., 80 °C), where it is held constant. Therefore, the volume changes due to thermal expansion caused by increase in temperature from room to the desired temperatures are not considered to ASR expansion calculation.

Fig. C-10 shows the thermal expansion result of New Mexico rhyolite aggregate (actual data readings for temperature and NaOH solution surface displacement). NaOH solution surface moves up with the increase of temperature simultaneously. However, the displacement is constant when the dilatometer reaches the target temperature 70 °C. The temperature and LVDT readings at this stage represent the initial LVDT reading used in calculation of ASR expansion. The final ASR volume expansion after the specified period of testing (e.g. 48 hours) is calculated.

5.3 Calculate volume change values for each sample to the nearest 0.001% and report average to the nearest 0.01%.

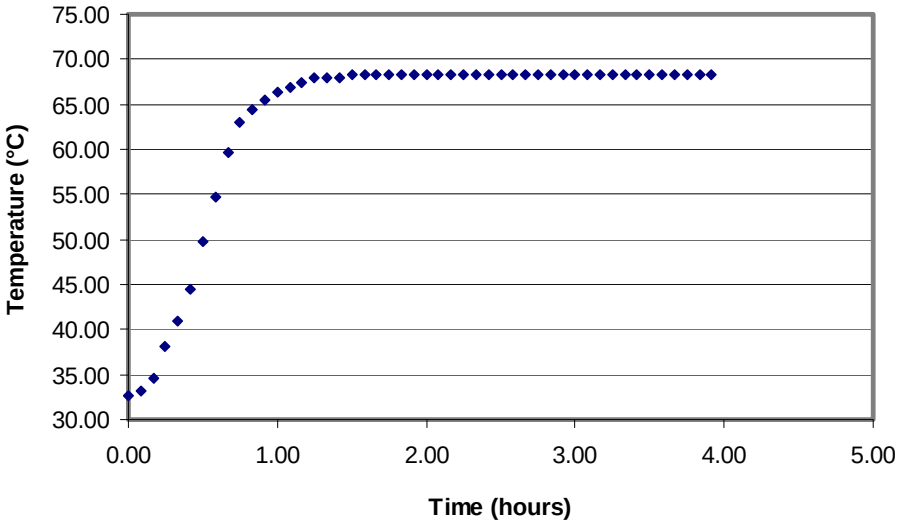

(a) Temperature measurement

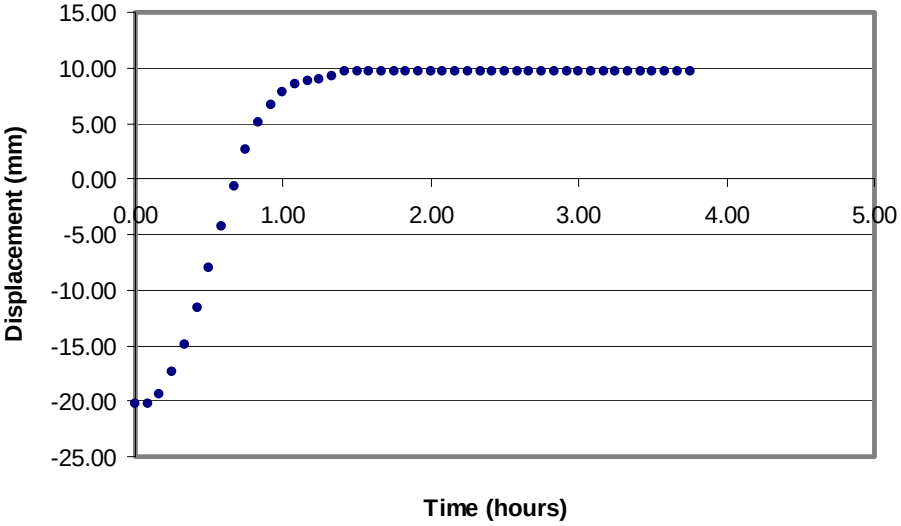

(b) Corresponding displacement of the NaOH solution surface level at the tower of dilatometer

Fig. C–10. Thermal expansion of New Mexico rhyolite aggregate measured by dilatometer at 1N NaOH solution

APPENDIX D

NATURAL LOGARITHM OF REACTION RATE PARAMETER VERSUS THE INVERSE OF THE ABSOLUTE TEMPERATURE PLOTS

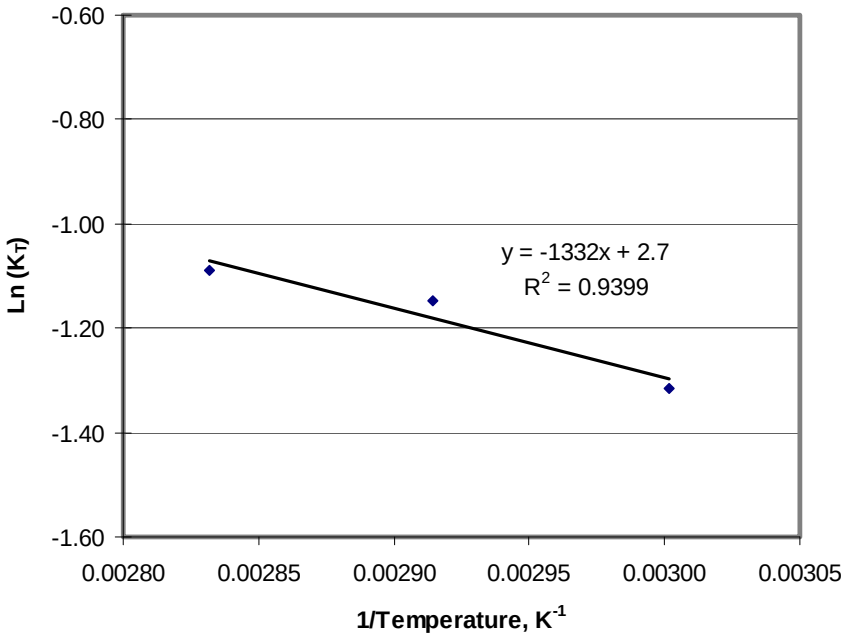

Fig. D-1. Natural logarithm of reaction rate parameter vs. the inverse of the absolute temperature (opal)

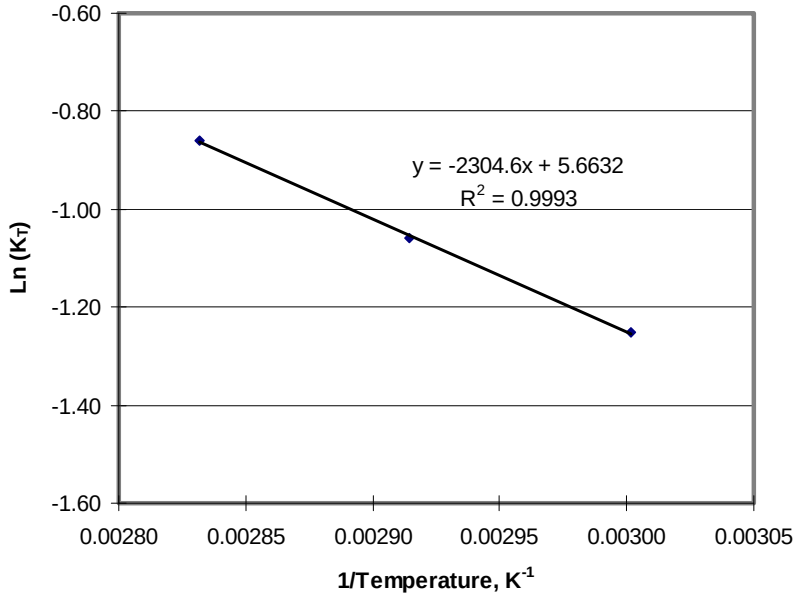

Fig. D-2. Natural logarithm of reaction rate parameter vs. the inverse of the absolute temperature (jasper)

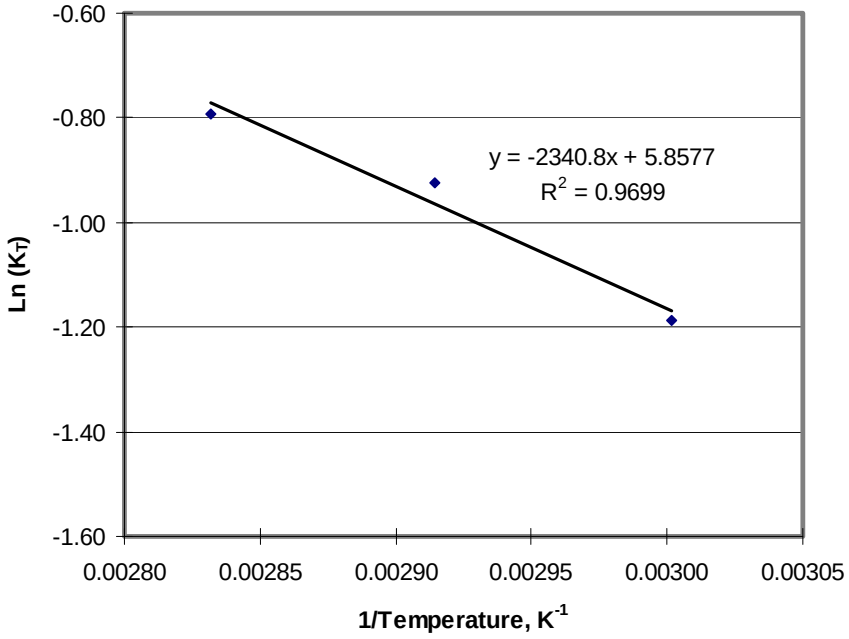

Fig. D-3. Natural logarithm of reaction rate parameter vs. the inverse of the absolute temperature (chalcedony)

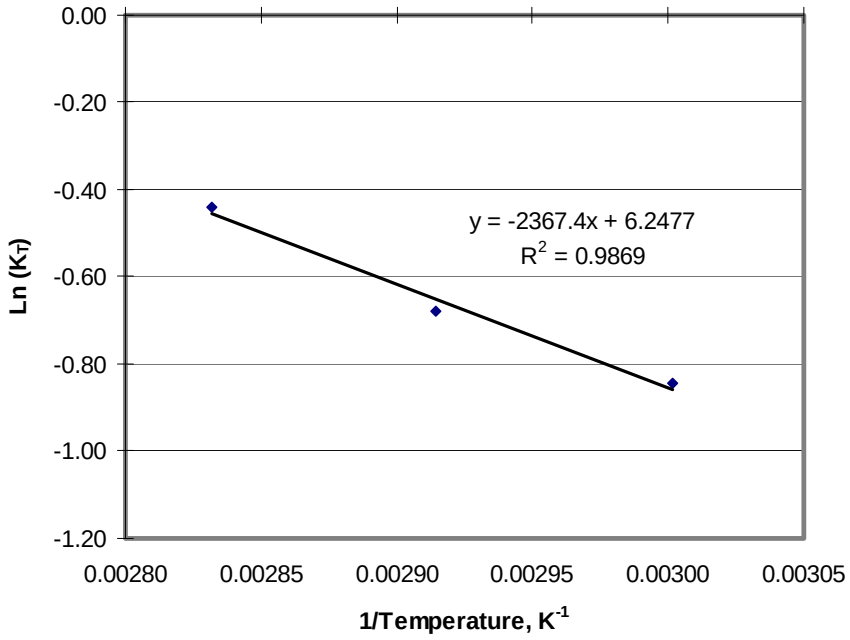

Fig. D-4. Natural logarithm of reaction rate parameter vs. the inverse of the absolute temperature (Flint)

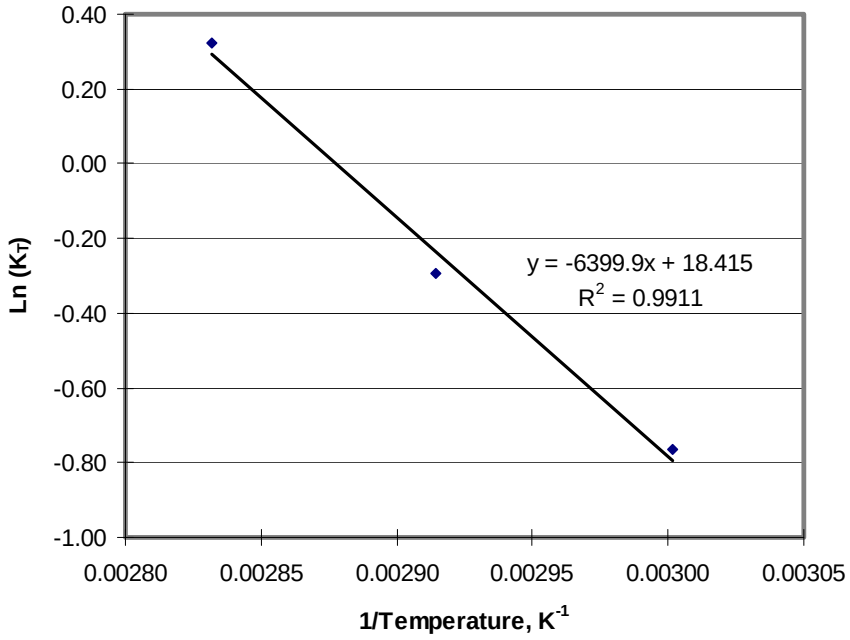

Fig. D-5. Natural logarithm of reaction rate parameter vs. the inverse of the absolute temperature (reactive gravel)

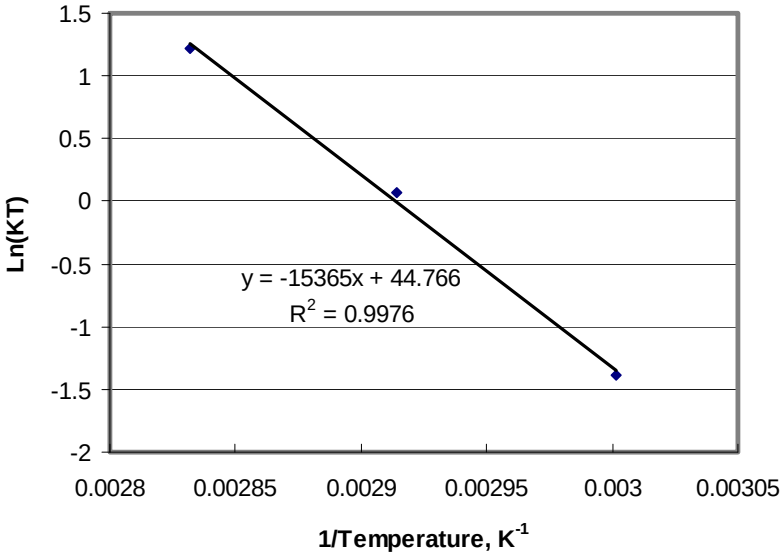

Fig. D-6. Natural logarithm of reaction rate parameter vs. the inverse of the absolute temperature (non-reactive gravel)

VITA

Chang Seon Shon was born in Pusan, Korea on July 17, 1970. He received a degree of Bachelor of Science in Architectural Engineering in 1997. In March 1997, he went to Pusan National University, and obtained a degree of Master of Science in Architectural Engineering in 1999. Afterward, he gained admission to Department of Civil Engineering, Texas A&M University, to study for his Ph.D. in June 2000 and received a Ph.D. degree in Civil Engineering in May, 2008.

His contact information is:
Zachry Department of Civil Engineering
Texas A&M University
College Station, Texas 77843-3136
Phone: (979) 862-9348
E-mail address: shons70@yahoo.com